CHEMICAL WEATHERING ON SELECTED NUNATAKS IN WESTERN DRONNING MAUD LAND, ANTARCTICA

A thesis submitted in fulfilment of the requirements for the degree

of

MASTER OF SCIENCE

of

Rhodes University

By

JENNA TRACY KNOX

November 2017

Supervisor

Professor K.I. Meiklejohn (Department of Geography, Rhodes University)

Co-Supervisor

Professor S. Büttner (Department of Geology, Rhodes University)

RHODES UNIVERSITY
Where leaders learn

GEOGRAPHY
RHODES UNIVERSITY

1. Abstract

High latitude areas are sensitive to the impacts of climate change, and it is expected that the impact of greenhouse warming will be much higher in the polar regions than in any other climatic zones, with the most highly affected area being that of the Antarctic rim (Barsch, 1993). Weathering and pedogenic processes respond to variations in climate, with models predicting that chemical weathering may increase synchronously with global carbon dioxide levels increase, due to dissolution rates and the erosional impact of hydrological cycles in warming climates (Anderson & Anderson, 2010). As liquid water becomes more available in Antarctica the potential for chemical weathering, due to a less moisture-limited environment and increased temperatures, increases (Convey *et al.*, 2009). Weathering processes are important for soil formation and the production of fine-grained material, with chemical weathering being an active constituent of this. Increased rates of soil formation are likely to occur, with global climate changes resulting in greater chemical weathering occurring in Antarctica.

Opportunistic sampling was conducted during the Austral summer of 2016/2017, whereby rock, snow and meltwater samples were taken at various sites within the western portion of Dronning Maud Land of Antarctica. Rock samples were placed in resin, and cut with a diamond saw to create thin sections. Optical microscopy and scanning transmission electron microscopy (STEM) were used to analyse mineral weight percentage with depth. Twelve soil samples were dried and weighed, sieved and statistically represented according to particle size. Inductively coupled plasma mass spectrometry (ICP-MS) determined the geochemical analysis for 10 water and snow samples. Rock hardness was inferred through the use of an Equotip, with rebound values recorded for multiple rock faces and samples. Thermal regimes of rock temperature was further recorded using a FLIR infrared camera, and documented for each rock face over a 24 hour period at 2 hourly intervals.

The products of increased chemical weathering were evident from particle size analysis; samples were very poorly sorted in nature, and undergo *in situ* weathering, whereby products were not removed by erosional processes. Weathering rinds were found to be siliceous and ferric, depending on parent lithology. Ferric ratios increased in wt.% from the substrate rock to the external surface, creating the red, iron rich crusts noted on the hand specimens. The observable chemical weathering was found adjacent to intrusions through Precambrian dolerites. Geochemical analysis revealed thin, carbonaceous features, with impurity-rich layers, characteristic of speleothem formation. Carbonaceous layers did not follow underlying substrate features, rather deposited at the external surface, upon which, further precipitation growth could occur, creating karst features. Extensive

gypsum coatings (>2mm) under BSE imagery were identified, with the abundance of gypsum salts (below surface level) and rock coatings indicating active sulphuric acid weathering, in western Dronning Maud Land, Antarctica.

Were mechanical processes faster than chemical, weathering rinds and solution features on silicate rocks would be uncommon in the Antarctic, periglacial landscape. However, this is not the case as the existence of these landforms implies that chemical weathering may occur faster than mechanical weathering processes (Pope *et al.*, 1995). In a changing world, one needs to monitor these processes at a micro-scale in order to fully understand how periglacial environments react to global climatic changes, and the subsequent impacts on these sensitive environments.

2. Acknowledgements

I would like to take this opportunity to thank the National Research Foundation (NRF), through the South African National Antarctic Program (SANAP) and Department of Environmental Affairs for logistical support. Without the funding for my masters, I would never have been able to pursue my interest in Antarctic geomorphology nor be able to participate in scientific research in such a remote, breath-taking environment.

Secondly, I would like to thank my superior Prof. Ian Meiklejohn for his continued support and effort in helping me achieve my MSc in Geography. His contribution in terms of fieldwork navigation, data collection and conceptualisation of my thesis topic is highly valued and appreciated. I would also like to thank my co-supervisor Prof. Steffen Büttner in the Geology department for his enthusiastic help in interpreting my samples for various minerals, and teaching me the necessary analysis techniques. The Geology department at Rhodes University played an integral role in the production of thin sections with Ms Andrea King, being an invaluable asset. Without her knowledge and expertise, large quantities of the external weathering rind and soluble salts would have been lost in the process.

Finally, I would like to thank my family for their support throughout my academic career at Rhodes University; without their emotional and financial assistance, this thesis would not have been possible. Special thanks goes to my mom, who sacrificed a great deal to help me achieve this level of education; the first university graduate in my family. Honourable mention to my friends who have kept me sane, and provided comedic, motivational and emotional support throughout this thesis.

These past two years have been an adventure into visiting places I never thought possible, learning new skills, making lifelong friends, and have been part of a journey of self-discovery and affirmation. This thesis is a testament to personal growth, perseverance, education and independence. The following statement by Mark Anthony sums up this experience and speaks true to my future endeavours;

> *'and one day she discovered that she was fierce, and strong, and full of fire, and that not even she could hold herself back because her passion burned brighter than her fears'.*

Table of Contents

Figures:

Tables:

3. Introduction

High latitude areas are sensitive to the impacts of climate change, evident by observed relationships between environmental components of terrestrial ecosystems; for example, the active layer, permafrost, vegetation and the interactions between them (Guglielmin *et al.*, 2014). These areas are characterised by surface snow being buried by new snowfall, compressed and eventually forming ice (Convey *et al.*, 2009). A chemical record of past climate and environments is effectively preserved, acting as a paleo-environmental indicator (Convey *et al.*, 2009). Antarctica, thus, provides the potential to study climate change and the interactions of biological responses, as climate change is estimated to occur in polar regions at faster rates than elsewhere (Convey *et al.*, 2009).

It is expected that the impact of greenhouse warming will be much higher in the polar regions than in any other climatic zones, with the most highly affected area being that of the Antarctic rim (adjacent to the continents of South America and Australia), (Barsch, 1993). The predicted zonal warming in periglacial areas, such as Antarctica, will be altered by several factors that have a local influence (Barsch, 1993). These factors include, but are not limited to, changes in temperature, net radiation, snow cover and other surface conditions which cause local variations to the permafrost table (Barsch, 1993). Changes in permafrost depth are related to local climatic variations and other environmental factors, such as regional differences (Barsch, 1993). Examples of this are the differences between maritime Antarctica and continental Antarctica, which have influences on high latitude and high altitude permafrost, influencing its degradation or aggradation, through the local effects of global warming (Barsch, 1993). Although changes in the permafrost table have been identified, one needs to also take into consideration the effect which predicted greenhouse warming will have on active periglacial landforms, which are likely to experience a marked change in environmental contributing processes as well as movement rates and formation (Barsch, 1993).

Antarctica plays a vital role in the global climate system, with global circulation being driven by the equator-to-pole temperature differences and Earth's rotation on its axis, through which heat is transported poleward (Convey *et al.*, 2009). Low latitude areas are, hence, the heat source and high latitude areas are the heat sink (Convey *et al.*, 2009). The Antarctic continent is especially important for establishing the links between long and short term climatic change and evolution as, they are the least understood processes (Convey *et al.*, 2009). Antarctica provides examples for study as it is a near pristine environment with little human involvement, allowing for the understanding of the impacts of past, current, and future changes on biodiversity (Convey *et al.*, 2009). Studying biodiversity change allows for the creation of benchmarks which decision makers are able to work with, unto which future changes can be assessed (Convey *et al.*, 2009).

During the Pliocene (5-3 Ma) mean global air temperatures were 2-3°C above pre-industrial values and carbon dioxide values were approximately 400 parts per million, on par with today's carbon dioxide levels, with sea level 15m-25m higher than currently (Convey *et al.*, 2009). Studying the history of Antarctic climate and environments, thus, provides the context for the current issues of climate change facing humanity (Convey *et al.*, 2009). At the same time it allows for the study of processes which led to the development of the present interglacial period and the characterization of ranges of natural climate and environmental variability (Convey *et al.*, 2009).

For the above reasons, amongst others, Antarctica has been deemed a continent for science, as per the Antarctic Treaty of 1959 (Secretariat of The Antarctic Treaty, 2011). As part of its role as scientific custodian for the Antarctic Treaty Organisation, the Scientific Committee for Antarctic Research (SCAR), identified six priorities for Antarctic research over the next two decades (Kennicutt *et al.*, 2015; Kennicutt *et al.*, 2014). These research priorities were developed using an Antarctic and Southern Oceans Horizon Scan to narrow down identified research questions into six overarching themes (Kennicutt *et al.*, 2014). One of the priorities was titled "Dynamic Earth-probing beneath Antarctic ice", which encompasses both research questions 39 and 42 (Kennicutt *et al.*, 2015: 9). These being "*what are and have been the rates of geomorphic change in different Antarctic regions, and what are the ages of preserved landscape*?" and "*how will permafrost, the active layer and water availability in Antarctic soils and marine sediments change in a warming climate, and what are the effects on ecosystems and biogeochemical cycles?*" respectively (Kennicutt *et al.*, 2014). Attempting to answer the questions is important as it has the potential to reveal Antarctica's history and the products of weathering, with implications for the current climate change issue facing humankind (Kennicutt *et al.*, 2014).

Exposed land in the interior of the Antarctic continent and surrounding oceans has been sparsely probed, inhibiting the study of historical interactions between ice and solid Earth, thus, more studies are needed (Kennicutt *et al.*, 2014). Specific studies into the rock and sediment records of the Continent are important to determine if similar historical climatic changes are likely to occur again (Kennicutt *et al.*, 2014). Another important theme when investigating rocks and sediments in Antarctica is the impact of understanding erosional processes and rates of geomorphic and surficial change in subglacial terrains (Kennicutt *et al.*, 2014). These changes are often linked to feedbacks between global climate, tectonic surface displacement and the evolution and decay of ice sheets (Kennicutt *et al.*, 2014).

Feedbacks between global climate and the rock weathering processes are connected through extensive timescales, where carbon is transferred between the atmosphere and lithosphere through the precipitation of elements, chemical weathering and metamorphic outgassing (Anderson & Anderson, 2010). Weathering and pedogenic processes respond to variations in climate, with climate models predicting that chemical weathering may increase as global carbon dioxide levels increase, due to dissolution rates and the erosional impact of hydrological cycles increasing in warmer climates (Anderson & Anderson, 2010). As liquid water becomes more available, the potential for chemical weathering increases, due to a less moisture limited environment and increased temperatures to facilitate it (Convey *et al.*, 2009). Chemical weathering, in particular, has the ability to alter the physical nature of rocks, through decreasing the strength of rock, increased porosity, and the formation of weak clay minerals, thereby leaving them susceptible to erosion (Anderson & Anderson, 2010). Alternatively, chemical weathering can alter the precipitation of minerals, creating cement horizons in soils which are resistant to physical weathering, impeding water and root penetration (Anderson & Anderson, 2010).

Chemical weathering processes have been sparsely documented in the literature, with these processes needing further study (Hall *et al.*, 2002). For instance, it has been suggested that chemical processes may have helped create a particular landforms under different climatic conditions in the party, which have yet to be modified in current conditions (Hall *et al.*, 2002). However, it has also been suggested that the landform controls the character of weathering and hence, maintains itself (Pope *et al.*, 1995; Hall *et al.*, 2002). These contradicting thoughts, although possibly true in each regard, may impact present-day weathering and resultant forms in cold regions (Hall *et al.*, 2002). Thus, one needs to determine chemical weathering processes and how they impact landforms (Hall *et al.*, 2002; Hall, 2013).

Climatic geomorphology dictates that due to the cold temperatures experienced in Antarctica, chemical weathering is limited (Hall, 2013). “Cold” in this sense is related to air temperatures and not rock temperatures, which are seen to fluctuate on a diurnal basis and show similar thermal oscillations to rocks found in hot desert and wet alpine areas (Hall, 2013). Antarctic literature has provided inadequate detail on other processes of weathering, such as chemical change due to a historical predisposition that favoured mechanical weathering processes in cold environments (Hall & André, 2001). Recent studies, however, have brought to light the role of moisture in water limited environments and high rock temperatures, which may actually increase the potential for chemical weathering (Hall & André, 2001).

New data in relation to the potential for chemical weathering to occur in cold polar deserts, thus, provides the foundation for investigating chemical weathering in Western Dronning Maud Land, Antarctica. Not only will this study provide new information and literature into a sparsely studied field, but it will also provide a baseline from which other weathering studies may occur in the future.

3.1 Aim

To document chemical weathering on selected nunataks in western Dronning Maud Land, Antarctica.

3.2 Objectives

1. To undertake a chemical analysis of rock composition at different depths beneath the surface.
2. Determine the chemical composition of the input and outputs of chemical weathering.
3. Document and compare chemical weathering processes and forms at different sites.
4. To determine the type and extent of rock coatings and weathering rinds.

4. Literature Review

4.1 Contested issues in Geomorphology that impact Antarctic studies

The following subsections intend to note and address the common issues found in Antarctic geomorphic literature. Varieties of topics have been covered, often extensively researched yet; a lack of clarity still exists. Three contested concepts are discussed below, such as, but not limited to, issues of scale, terminology and the differentiation between weathering and erosion. Literature often carries a historical legacy from which concepts are built; however, a noticeable trend within the literature is the acceptance of weathering studies without critique.

Throughout the years, issues with geomorphological concepts have become apparent, one of these being scale (Hall & Thorn, 2011). Scale concepts vary spatially and temporally, from scale defined terminology, to the scale of processes and landforms, all encompassed within a broad scientific context (Hall & Thorn, 2011). Essentially, all geomorphic processes are contained by scale, with these scale linkages having challenges in terms of timescales and mismatches between spatial representation and the spatial capacity of current instrumentation (Dixon & Thorn, 2005).

Hall and Thorn (2011), state that there is no reason why the scale of a geomorphic process controls the scale of the product (landform), as opposed to the materials inherent characteristics. This leads to two premises, if a landform is the product of the interaction between existing material and a geomorphic process, then there is no reason to believe that (Hall & Thorn, 2011):

i) the same driving force (process) will lead to the same resulting landform, and

ii) any form will always result from the same process.

As a result of the above premises, the nature of the formative process remains unknown, or is misunderstood, in regards to the products of these landforms or landform elements (Hall & Thorn, 2011). Spatial scale issues, especially when looking at nano-scale processes, thus, become critical (Hall & Thorn, 2011). For example, how metre-scale landforms are resultant from nano-scale processes (Hall & Thorn, 2011). An illustration of this is seen as a scale-process disjunction in the classification of chemically weathered landscapes; the question being, are these landscapes inherited from the past, or are they the products of climatic changes and landscape stability (Pope *et al.*, 1995)? This is of importance as, weathering inherited from past climates allows for the current weathering processes to be amplified, as previous pathways for water transport are able to be taken advantage of (Pope *et al.*, 1995).

The spatial applicability of creating a process-scale-linkage system, where the parameters and process operations are unknown, or are unknown in relation to other processes, leads to relevancy issues for future studies in this field (Hall & Thorn, 2011). It is clear that in understanding weathering processes, issues of scale underpin all the discussions and understanding in this field (Viles, 2013). An example of this, is noted in variability of the types and rates of weathering at the short term, which are unable to be extrapolated to weathering measurements in the long term, due to rates of change varying over timescales and weathering system nonlinearity (Viles, 2013).

A secondary issue raised in published literature, is a historical legacy within the broader discipline of the terminology that is used (Hall & Thorn, 2011). Existing terminology is linked to the origin of Periglacial Geomorphology (the study of periglacial processes and landform development) and Climatic Geomorphology (the role of climate in shaping landforms and near surface processes) (Hall & Thorn, 2011). Onto which modern Process Geomorphology (the process dynamics which are involved in the origin of landforms and their evolution), has been superimposed (Hall & Thorn, 2011). An example of this is seen in the terms: macro-, meso-, and micro-, which are widely used in geomorphology but, are relative and often variable in meaning (Hall & Thorn, 2011). These issues are apparent when a term from one branch of Geomorphology (for example Climatic) is adopted by another (such as Process Geomorphology), as it leads to the confusion of processes and terms (Hall & Thorn, 2011). The main consequence of this inherent issue, is the misunderstanding and misinterpretation of evidence and, thus, weak experimental approaches (Hall & Thorn, 2011).

In mechanical weathering literature, terms such as “soft” and “hard” rocks are sometimes used, which are erroneous substitutions for the terms weak and strong (Hall & Thorn, 2011). This further creates substantial problems with terminology (Hall & Thorn, 2011). The issue is that hardness is a property related to erosion, while strength typically relates to fracture (Hall & Thorn, 2011). The use of the word “strength” can be associated with resistance to failure by many stresses, while “hardness” is related to a purely compressive stress situation (Hall & Thorn, 2011). Furthermore, the use of “soft” to describe a rock susceptible to frost and “hard” for rock which is not susceptible to frost (Matsuoka and Murton, 2008), should rather be termed permeable and impermeable respectively (Hall & Thorn, 2011). From the above example, it can be seen that the use of various terminology adds to the confusion and unnecessary complexity to situations or experiments (Hall & Thorn, 2011).

A third issue in geomorphological studies is the differentiation between weathering and erosion, and if they can be separated from one another (Viles, 2013). Within literature there has been confusion in the relationship between weathering and erosion, essentially the question is asked where does one stop and the other begin (Pope *et al.*, 1995; Viles, 2013). In reality, there is an overlap between both concepts; for example, sometimes a process is identified as erosional in one environment, and weathering in another (Viles, 2013). There is a blurring of boundaries when looking at weathering and erosional studies as, one may lead to the other or prepare the other (Viles, 2013). It is for this reason, that weathering needs to be recognised as a non-linear, non-equilibrium system, because the processes which control weathering are constantly changing in both timescales and geographic locations (Viles, 2013).

4.1.1 The dominance of mechanical weathering in Antarctic literature

Cold regions weathering has been described by three basic principles (Pope *et al.*, 1995; Hall *et al.*, 2002):

i) it is dominated by mechanical processes,

ii) the dominant mechanical process is free-thaw weathering, and

iii) chemical weathering is not a significant influence in cold regions due to low temperatures.

Freeze-thaw weathering is a concept based off the broad belief that alternating freezing and thawing cycles of hydrated materials at multiple scales have the potential to break up a rock (Hall & Thorn, 2011). For many years the angularity of coarse debris was emphasised as an indicator of freeze-thaw weathering, with causality being the proof of these weathering systems dominance in cold regions (Sumner *et al.*, 2004; Hall & Thorn, 2011). Thus, freeze thaw weathering was assumed to be the dominant cause of bedrock landform production (Hall *et al.*, 2002). The use of angularity as a means of determining the dominant weathering process is inherently flawed, however, as hot desert weathering produces angular clasts which are comparable to those in cold regions (Hall *et al.*, 2002). The discovery of these landforms, thus, undermines the cause-and-effect relationship noticed between angularity and frost action, disproving the notion that angularity is proof of mechanical dominance in periglacial environments (Hall *et al.*, 2002). Recent literature has further reiterated the disproval of block production as the outcome of frost action, especially in the case of Boelhouwers (2004), who stated that mechanisms of block production appear to be increasingly linked to chemical weathering and thermal stress fatigue, with bedrock fractures being prerequisites rather than final products.

An issue found when correlating observations with theory, is the qualitative nature, whereas quantitative data is now favoured within the discipline and is often a core component of modern Geomorphology (Hall & Thorn, 2011). Within this issue is the fact that weathering processes in cold environments were inferred, rather than proved (Hall & André, 2001). Previous literature suggested that products are an indicator of the originating process (Hall & Thorn, 2011). This, however, this is no longer viewed as a valid argument (Hall & Thorn, 2011). One of the reasons for the lack of validity, is due to the poor understanding of these processes, and the fact that their operation on a specific scale is predicated upon and based off assumptions rather than facts (Hall & Thorn, 2011).

Another reason validity is questioned is in that viewing a geomorphic process through its products fuses two scale issues together; the processes and products, reiterating why freeze-thaw weathering became dominant in these environments (Hall & Thorn, 2011). For example, attempts which have been made to validate two scales of weathering have been found to cause the acceptance of assumptions, one of which being that there are only two weathering scales (Hall & Thorn, 2011). This has the potential to result in misdirection and poor experimental evaluation approaches in the field, as seen in mechanical weathering dominance (Hall & Thorn, 2011).

A terminological implication that helped reinforce the idea of freeze thaw dominance in cold regions, is that of zonality (Hall *et al.*, 2002). It must be mentioned that classifying weathering as "cold region" or "hot desert region" specific had an influence on how processes were viewed (Hall *et al.*, 2002). The issue with this is that these weathering processes may occur in any climate. For example, hot desert texts indicate that freeze-thaw weathering is an important component of these weathering suites, but zonality does not allow for this to be accepted (Hall *et al.*, 2002). This is also noticed in cold region texts where thermal stresses are vaguely mentioned while in hot region texts they are explicitly studied (Hall *et al.*, 2002). Thermal stresses are ideally suited to cold region studies and may be more plentiful than in hot regions but, the preconceived importance of notions about "cold" and "hot" controls the classification (Hall *et al.*, 2002). The similarity in products between "hot" and "cold" regions and the potential for similar thermal regimes in terms of thermal changes challenges the zonality theory (Sumner *et al.*, 2004). In relation to this, absolute temperatures may be applicable to specific processes, but, this needs to be incorporated into the apparent influence of rock moisture conditions (Sumner *et al.*, 2004). Due to these misleading terms or classifications one should critically investigate how frequency, magnitude and intensity act synergistically to produce these mechanical weathering suites, rather than the influence of zonality (Hall *et al.*, 2002; Sumner *et al.*, 2004).

The influence of "hot" or "cold" climate prefixes needs to be removed from literature as the primary means of determining the type of weathering which occurs (Hall, 2013). This is increasingly seen in recent texts, where weathering processes are now viewed as azonal in nature rather than being under the influence of zonality, for example, thermal stress or thermal fatigue (Hall, 2013). Climate, can be seen as having an indirect role in erosion, mediating boundary-layer temperatures, providing weathering agents (Pope *et al.*, 1995). It must now be noted, however, that new studies into the climatic influence on weathering have found that climate is no longer linked as the determinant of the process, but rather, should be viewed as an influence on process timing, efficiency and extent of weathering (Hall, 2013).

4.1.2 New insights and theories of weathering in periglacial environments

Traditional conceptual models (Fig. 4.1.1) for Periglacial Geomorphology overestimated the importance of temperature ranges and underestimated the role of moisture in cold environments (Hall *et al.*, 2002). While they also placed too much importance on the air climate of these regions rather than ground climates, which are of significant importance when studying weathering processes (Hall *et al.*, 2002). Air climates are not an acceptable metric to geomorphologists, as this does not account for ground climates, which are more related to rock weathering (Hall *et al.*, 2002).

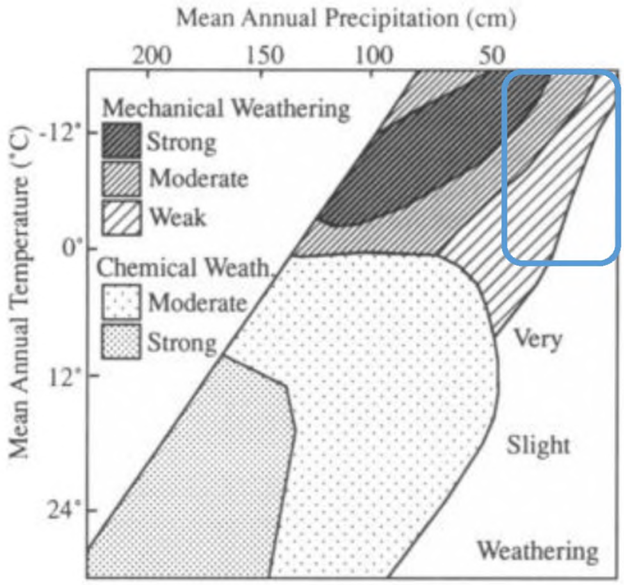

Note the box in Fig. 4.1.1, *indicating the missing action of chemical weathering in cold environments, such as Antarctica. Mechanical weathering processes dominate in the area under the box outline. Chemical weathering processes are attributed to high air temperatures and high precipitation. Please note that this diagram is concerned with purely air temperature and does not consider rock temperatures.*

Figure 4.1.1: Diagram illustrating a model of dryland weathering and climate interactions, showing the relative importance of weathering types in relation to mean annual precipitation and temperature, (directly copied from Pope *et al.*, 1995)

An example that illustrates the above concept, is in Antarctica where it has been found that summer rock temperatures are able to facilitate chemical weathering, provided that water is available (Hall *et al.*, 2002). According to Hall *et al.* (2002), rock temperatures are frequently above 0°C even when air temperatures are -10°C, or lower. It has also been found that during a period from mid-January to mid-March air temperatures were recorded as being sub-zero, while, at the same time rocks in Antarctica experienced diurnal fluctuations across the 0°C level, often exceeding 20°C (Hall *et al.*, 2002). In terms of a thermal process perspective, weathering thus, has a potential to occur from October to March (six months) with water availability being found to be the limiting factor rather than temperature (Hall *et al.*, 2002). From these observations water-based weathering processes (including chemical) occur for a larger portion of time than previously thought, with rock temperatures above 20°C greatly facilitating chemical weathering, wetting and drying, and salt weathering processes where moisture is present (Hall *et al.*, 2002). At a fundamental level, it is a lack of data in regards to chemical weathering in polar environments, which has prompted the undertaking of this thesis.

4.2 An overview of weathering

Although this is a discussion in regards to weathering, one frequently needs to take the intimate relationship with erosion into account. This includes, but is not limited to, the products of weathering, the three types of weathering and the processes that either influence weathering or are a result of them. This chapter intends to further broaden the traditional views of weathering and conceptualise chemical weathering in relation to this, while incorporating the synergistic system processes apparent in weathering studies.

Traditionally, erosional processes are controlled through weathering, whereby slopes are defined by the removal of material with soils being a direct result of these interactions (Pope, 2013). Weathering plays an important role in biogeochemical cycles, which have direct impacts on the surrounding landscape and subsequent erosional types which occur in these areas (Pope, 2013). It is important to note, however, that weathering and soil interactions are interactive, synergistic systems which are increasingly complex (Pope, 2013). For example, mechanical erosional processes operate in a synergistic manner with chemical processes in either being constructive, where transportation is required to the landform (*e.g.*: screes) or a destructive, where transportation is required from the landform (*e.g.*: tafoni); subsequently influencing landform evolution (Hall, 2013). While exogenic factors are of importance in weathering, they should not be examined in isolation (reductionist approach) but, rather need to be viewed holistically (Pope, 2013; Hall, 2013). From this reasoning, the concept of weathering suites has been created, which looks at how landform production cannot be attributed to only one type of weathering mechanism (Hall, 2013).

In periglacial and permafrost environments, such as Antarctica, it has been suggested that mechanical, chemical and biological weathering contribute significantly to rock weathering (Murton, 2007). When studying rock weathering in particular, three factors need to be taken into consideration: rock temperature, rock properties and rock moisture as they have an influence on the degree, rate and type of weathering which is likely to occur (Hall & André, 2001). In cold climates, the influence of heat is often disregarded in favour of mechanical processes and a dominance of freeze-thaw weathering (Hall & André, 2001). Cold region processes, however, are driven by warmth rather than cold, the input of heat initiates weathering processes and the removal of material (Hall *et al.*, 2002). Temperature changes are inherent in weathering of cold regions and are a prerequisite for weathering, without which weathering would not occur (Hall *et al.*, 2002). It is for this reason, the effect of summer in high latitudes and the influence of rock warming in these environments needs to be documented rock surface temperatures are, thus, critical in understanding both spatial and temporal rock weathering (Hall & André, 2001).

Although collecting rock temperature data is important, the frequency used to collect the data is often insufficient to evaluate the rate of change of temperature (Hall & André, 2001). In collecting these data, there needs to be an acknowledgement of albedo, which effects the warming of rock surfaces or thermal fluctuations, due to the insulating effect of snow cover, as well as the effect of wind speed (Hall & André, 2001). In terms of albedo, Antarctic literature suggests that large magnitude temperature changes occur, regardless of rock colour (André *et al.*, 2004). High frequency rock temperature data from western Antarctica supports this finding, indicating changes in excess of 2°C per minute experienced by both light and dark coloured rock surfaces (André *et al.*, 2004). It can, thus, be said that rock heterogeneity prevails over rock colour as a controlling factor on thermal rock behaviour (André *et al.*, 2004). Rock translucence relates to the influence of rock mineral colour, in that it supplies an additive effect on local conditions rather than acting as a controlling factor (André *et al.*, 2004). In Antarctic regions, the subsequent influence of wind is a prevailing factor on large magnitude temperature changes, as opposed to radiation, as previously thought (André *et al.*, 2004). It can, consequently, be said that in terms of rock temperatures there are four main factors that need to be acknowledged (Hall & André, 2001):

i) Air temperatures are not a proxy for rock temperatures,

ii) rock surface temperatures need to be measured,

iii) rock temperatures at various depths need to be measured, and the thermal gradient should thereby be calculated, and

iv) the values of the rate of change are required.

Rock properties are known to change under the weathering regime. For example, it has been stated that compressive and tensile stresses of rocks tend to decline in the early stage of weathering, with decreased rock strength being a resultant outcome (Oguchi, 2013). These changes in rock strength are of vital importance when considering how weathering influences geomorphic processes. However, the number of studies which consider the changing rates of physical, chemical, mineralogical and mechanical properties are limited (Oguchi, 2013).

With an increased likelihood of azonal processes occurring, as opposed to zonal processes, the importance of rock properties becomes critical (Hall, 2013). Future studies in rock weathering need to account for the influence which rock properties have, especially in areas whereby climate is a control on the timing and efficiency of weathering processes, and where weathering is facilitated by the rock itself (Hall, 2013). Essentially, there needs to be increased recognition of the role that the underlying rock properties play in the control of weathering processes (Hall, 2013). How rock properties react to external stressors of weathering needs to be fully understood and rock fracture mechanics for weathering need to be developed and used in conjunction with physical weathering studies (Hall, 2013).

4.2.1 Products of weathering

Weathering products vary over various scales and in their nature of production. At a microscale, silt sized particles are produced, such as quartz (Murton, 2007). Small sized particles contribute as a means of silt to riverine systems and eolian systems (Murton, 2007). Within periglacial soils, sand to pebble sized particles are the remains of disaggregated bedrock material, with reddish colours indicating oxidisation (Murton, 2007). This reddish-brown colouring of bed rock surfaces is noted as ever-present features in parts of Antarctica which are devoid of glacial shielding; this colouration is interestingly observed on rocks with iron and on those devoid of iron such as granites and gneisses (Mergelov *et al.*, 2012). Lithological differences influence the style of weathering, such as the production of pebble to boulder sized angular or rounded clasts, found in hillslopes and rocky periglacial regions (Murton, 2007). This variation is noticed in weathering forms like rounded pits, tafoni, grooves and angular rock walls (Murton, 2007). In terms of fracturing, parallel fractures are associated with ice segregation, while perpendicular fracturing is associated with thermal shock or hydro-fracture events (Murton, 2007).

Soil formation (pedogenesis), is one of the main products of weathering which is essential for landscape formation and other physical and biological processes. In cold climates, soil formation is derived from regolith associated with periglacial, glacial and colluvial landforms (Dixon, 2013). Alpine soils are characterised by limited profile development, limited organic matter, little chemical weathering and frozen subsoils (Dixon, 2013). Arctic soils on the other hand, are characterised by limited chemical weathering and a dominant cryogenic process (Dixon, 2013).

In the moraine-covered and bare ground of Antarctica, weathering and subsequent soil formation on exposed rocks and glacial deposits has begun (Claridge & Campbell, 1985). Although many Antarctic glacial deposits lack an identifiable biological component, nonetheless, the products of weathering in this environment have been regarded as soils, in which the influence of living organisms is negligible (Claridge, 1965). The development and properties of these soils are influenced by physical and chemical processes, identical to those found in soils of temperate regions (Claridge & Campbell, 1985).

4.2.2 Mechanical weathering

Mechanical weathering is defined as a process which alters the physical attributes of a rock such as crack propagation, often leading to a decrease in strength and is commonly described to act *in situ* (Hall, 2013). Some movement needs to occur, however, which makes it incredibly difficult to define where mass movement and mechanical weathering start or end (Hall, 2013). Mechanical weathering processes are dominantly driven by climatic conditions, with the spatial and temporal patterns of an area being the distinctive determinant of the process which occurs (Hall, 2013). Although mechanical weathering plays an important role in landform development, it only does so through preparing material for transport by either gravitational or erosional processes, while allowing for chemical and biological weathering to occur (Hall, 2013). Mechanical weathering research has been documented in depth by academics such as Bockheim and Hall (2002), Hall *et al.* (2002), Hall and Andre (2003), Murton (2007) and Hall (2013), among many others. In lieu of this, a basic overview of each type of mechanical weathering process and a diagram has been produced (Fig. 4.2.1).

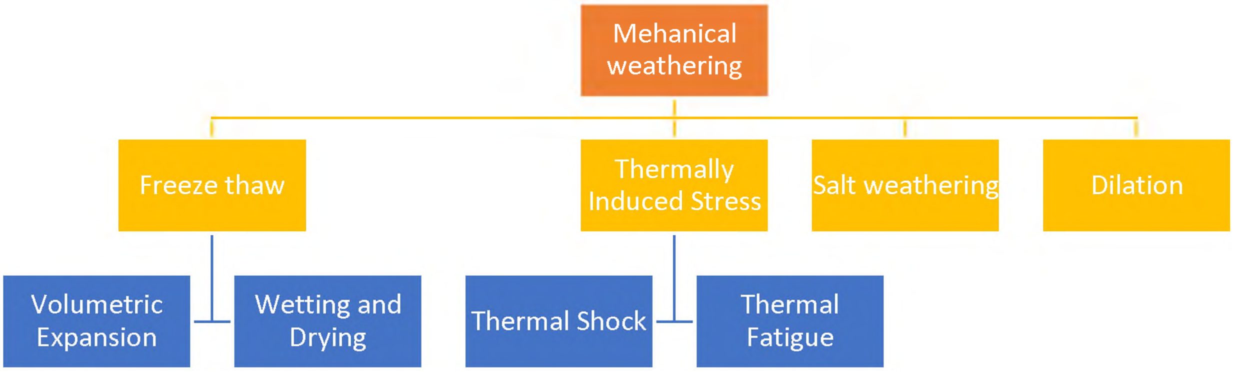

Figure 4.2.1: A breakdown of mechanical weathering processes (based on data from Hall *et al.*, 2002; Murton, 2007; Hall, 2013)

Mechanical weathering encompasses a wide variety of physical processes and mechanisms, often these are vaguely described and confusing to the reader. The following paragraphs intend to deconstruct each type of mechanical weathering process and the resulting landforms, allowing for a broader understanding of each process and providing relevant examples where necessary.

a) Freeze Thaw Weathering

Freeze thaw weathering is concerned with frost action and is often used as a reference point for secondary concepts such as nivation and cryoplanation (Hall, 2013). Essentially the processes are based on many mechanisms that result in the mechanical weakening and failure of rock, through alternating phases of freezing and thawing of water within a rock at different scales (Hall, 2013). An example of this is noted by Hall (2013), where an ultrasonic evaluation of freeze thaw events of rock in Antarctica, showed a change in pulse velocity simultaneous with exotherm data, validating the signal of a phase change within the rock (water to ice).

An issue relative to the freeze thaw weathering concept is that frozen water found within the pore spaces of rocks may be protective rather than destructive, as it prevents the penetration of liquid water (Hall, 2013). While the laboratory analysis of a singular process of freeze thaw is flawed in that synergistic feedbacks are ignored, data used to model simulations are often inadequately quantified (Hall, 2013). This, thus, has implications for spatial variability and leads to flawed findings, such as the dominance of freeze thaw weathering in cold environments or exaggerate the process (Hall, 2013).

The following two paragraphs are related to the overarching process of freeze thaw weathering and are resultant from this type of weathering. The two sub-processes namely being volumetric expansion, and wetting and drying. Each has fundamental roots in freeze thaw weathering and often they are only available to occur once freeze thaw weathering has provided sufficient surface area for initiation.

Volumetric Expansion

Water, upon freezing, expands by approximately 9% in volume, which is great enough to theoretically fracture a porous rock, granted the rock is thoroughly filled with water and that it freezes *in situ* (Murton, 2007). It can be calculated that this stress exceeds the tensile strength of the rock, thus, causing the rock to fracture (Murton, 2007). Other conditions need to be present for volumetric expansion to occur, although it is relatively seldom that they all occur simultaneously (Murton, 2007). This is especially interesting when considering that these experiments and subsequent 9% volume change only occur within a closed system, such as in laboratory conditions. These conditions include: a high degree of rock saturation, rapid cooling rates for *in situ* freezing and freezing temperatures below -5°C (Murton, 2007). Subsequently, since such conditions are seldom all present within the natural environment, the validity of volumetric expansion is questionable, as is the scale factor (Murton, 2007). Volumetric expansion is said to operate at the uppermost centimetre surface level of rocks, whereby pores/cracks are sufficiently filled with water, but how does one determine where the upper most surface begins and ends (Murton, 2007)? On a small scale, volumetric expansion is attributed to rock flaking and individual mineral flacking while, on a large scale, joint widening and bedrock heave (Murton, 2007).

Wetting and Drying

The presence of water has a known influence on rock hardness, rock strength and compressibility (Murton, 2007). Wetting and drying of rock such as basalt and granite among many others, can increase the shrinkage and swelling of each type in accordance with their individual rock properties (Murton, 2007). In places where nivation has been noted, water released from melting snow patches and where the surrounding areas are relatively snow free, wetting and drying processes may be enhanced (Murton, 2007). Episodic melting in summer, facilitates mechanical weathering due to wetting and drying, however, this has only been investigated in a limited manner and needs further study (Murton, 2007). Most importantly wetting and drying contributes in a synergistic manner to other weathering processes, furthering granular disintegration (Murton, 2007).

b) Thermally Induced Stress

Rock expands upon warming and contracts on cooling, to what degree is determined by the thermal co-efficient of linear expansion, according to the properties of the minerals (Murton, 2007). Thermally induced stress is documented to have a considerable effect on rock breakdown in cold environments (Hall *et al.*, 2002). Tensile stresses during a cooling event are often twice as destructive as opposed to a warming event (Hall *et al.*, 2002). Rock fracture may result according to either the magnitude or frequency of the thermally induced stress, creating either the process of thermal shock or thermal fatigue (Murton, 2007). Thermal shock occurs from a single, high magnitude event initiated by a rapid temperature change (>2°C min^{-1}), whereby, the inelastic properties of the rock material fails to respond to a thermally driven expansion or contraction, causing rock fracture (Murton, 2007; Boelhouwers & Jonsson, 2013). Thermal fatigue on the other hand, is caused from a repetitive, gradual, low magnitude stress which causes rock failure over time, often attributed to the expansion-contraction process, whereby the stress is lower than the amount required for immediate rock failure (Murton, 2007; Boelhouwers & Jonsson, 2013).

Thermally induced stresses rely closely on changing temperatures, the most favourable of these being found in high altitude, high latitude regions which receive high amounts of solar radiation; while maintaining an air temperature below freezing (Murton, 2007). Extreme solar radiation varies according to the season, thus, impacting factors such as; aspect, slope angle and rock temperatures at a different scale (Hall, 2013). Frequent and rapid changes in temperature regimes of rock surfaces, affect their thermal gradients, which favour thermally induced stresses (Murton, 2007). An example of this is seen in Antarctica, whereby polygonal crack patterns in ice free areas are observed, often attributed to limited surface temperature waves which decrease with depth (Murton, 2007).

A variety of papers mentioned in Boelhouwers & Jonsson (2013), argue for the acceptance of the 2°C min^{-1} rate of change as being relevant to produce a substantial, permanent amount of strain irrespective of rock type. Especially in cold regions, whereby high frequency temperature monitoring (<1 minute intervals), demonstrates the 2°C min^{-1} rate of change occurring at the rock surface, although limited to the grain scale at the rock surface (Boelhouwers & Jonsson, 2013). The use, however, of a single temperature value in controlling rock breakdown, without incorporating other factors into the process is a weak scientific approach to base a hypothesis on. Interestingly, the history behind the formation of the 2°C min^{-1} rate is based off Todd (1973), a PhD thesis laboratory study, whereby the value was used as a safe limit in documenting crack changes in rocks exposed to temperatures in excess of 150°C (Boelhouwers & Jonsson, 2013). According to this thesis, when investigating the effect of thermal gradients of *in situ* rocks, one needs to interpret the thermal gradient with reference to distance (Boelhouwers & Jonsson, 2013). Published papers over the following decade, created the impression that the 2°C min^{-1} is a generally valid value in thermal cracking, however, this is erroneous in that it has been reiterated to the point of common acceptance and disconnection from the original literature (Boelhouwers & Jonsson, 2013).

c) Salt Weathering

Characterised as an azonal process, salt weathering is primarily linked to evaporative environments or ice free coasts which have a direct input of salts on the land (Hall, 2013). In cold, arid environments, such as Antarctica, salts portray a similar role to hot arid environments, this is due to high evaporation in both areas in relation to precipitation (Summerfield, 1991; Hall, 2013). Salt once in a rock can either undergo thermal contraction, expansion, hydration or dehydration, with the cold environment determining the timing of the process and controlling the extent (Hall, 2013).

When saline solutions within rock pores become saturated as a result of temperature change, or evaporation, salt crystals form and pressure is generated (Summerfield, 1991). The results of the increased pressure depend on the stressed produced by crystal growth and tensile stress of the rock (Summerfield, 1991). The specificity of conditions required for salt weathering leads to the weathering being highly variable spatially (Summerfield, 1991).

Weathering can either be enhanced or decreased according to the salt combinations; for example, certain salts can inhibit weathering by forming a crust, while others facilitate chemical weathering and form new salts (Hall, 2013). The nature of the salt, either inhibiting or encouraging weathering, is based on the salts efficiency as a weathering in agent, one of the most significantly active salts is that of sodium sulphate (Summerfield, 1991). This efficiency is due to the various physical characteristics, one of these being the increase in volume as it is hydrated and the second being the high equilibrium solubility allowing for large amounts to be precipitated out of a given volume of solution (Summerfield, 1991). Third, the equilibrium solubility is influenced by temperature (32.3°C), which is reached in many arid environments daily, resulting in precipitation as the temperature changes over this gradient (Summerfield, 1991). It is in this manner that salt weathering has the ability to interact with other weathering types and significantly contribute to rock fracture, either independently or synergistically.

d) Dilation

Dilation, like salt weathering, is also an azonal process, whereby stress release or pressure release results in the fracture of rock (Hall, 2013). Although commonly associated with deglaciation, dilation processes are suggested to provide a surface area for frost action, whereby previous rock fractures are exploited, resulting in rock failure (Hall, 2013). This association is due to stress relief of the removal of overburden material as well as glacial unloading or erosion thorough which, fracturing or micro fractioning occurs (Hall, 2013). Pressure release and the resultant dilation thus, requires a driver (Hall, 2013). In the case of micro fractures, however, once present they provide a surface area exploitable by other weathering processes (Hall, 2013). This raises the question of whether the creation and exploitation of micro fractures can be attributed to dilation, or rather if this process is linked to other weathering processes on smaller scales, such as micro-dilation (Hall, 2013).

4.2.3 Chemical weathering

Chemical weathering is defined as “the chemical and mineralogical alteration of rocks and minerals of the Earth’s crust to secondary minerals more stable at the Earth’s surface” (Dixon, 2013). Chemical weathering has been considered to be an insignificant geomorphic process in cold environments, due to the lack of vegetation, low temperatures, desiccation, permafrost and limited moisture (Pope *et al.*, 1995; Dixon, 2013). Chemical reaction rates are seen to be temperature driven, even though chemical reactions are not inhibited by cold climates, but, rather can proceed at temperatures below freezing (Dixon, 2013). Older texts use the colder temperatures as justification that, as air temperatures decrease, chemical weathering will become less significant in cold environments (Dixon, 2013). These texts also suggest that the presence of angular debris demonstrate a dominant attributed of mechanical weathering in cold regions, with chemical weathering being seen as a “weak” process in these areas; ultimately leading to the dismissal of chemical weathering studies in periglacial regions (Hall, 2013). According to Hall (2013), however, biological or chemical weathering, rather than mechanical weathering, may dominate cold environments. This theory is based off previous work which, suggested that given the presence of water, chemical weathering could occur throughout summer and into winter despite air temperatures below -40°C (Hall, 2013). Thus, it can be stated that the key determinant of chemical weathering is the presence of water, combined with a high (>10°C) rock temperature (Meiklejohn & Hall, 1997; Hall, 2013).

Chemical weathering processes in cold environments have been suggested to have a significant impact on denudation rates and landscape change (Dixon, 2013). With chemical weathering assigned the role of an important precursor to the creation of bedrock glacial landforms (Pope *et al.*, 1995). This is especially noted through soil formation and chemical weathering resulting from denudation, which have been documented as widespread in Antarctica, despite the low temperatures and limited moisture availability (Dixon, 2013). Analysis of soil solutes, have demonstrated the presence of iron oxidation products and products derived from rock weathering (Dixon, 2013). The transport of these products is thus, inherently related to the process of chemical weathering. The main of contribution chemical weathering in these environments is the ability to transport solutes efficiently, especially runoff water from snowmelt and glaciers (Dixon, 2013). In contextualising chemical weathering and its agents, the relation between water and minerals/bedrock needs to be understandable and can be found diagrammatised below (Fig. 4.2.2).

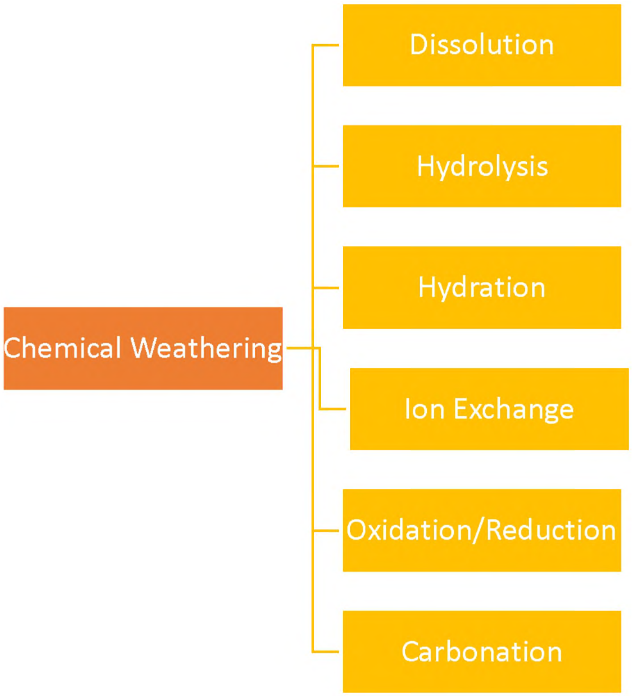

Figure 4.2.2: Categories of chemical weathering (based on data from Dixon, 2013)

a) Dissolution

Dissolution or congruent dissolution, is concerned with the dissolving of minerals by water and the subsequent removal of constituent atoms from the mineral surface (Dixon, 2013). One needs to reiterate, however, that weathering occurs *in situ*, with movement occurring within the processes. Material that is transported through the weathering process (such as material in solution), facilitates weathering to be on going, rather than self-limiting in nature. An example of this is the removal of material, such as caves in karst features or the deposition of material, such as stalactites.

It is important to note, however, that the occurrence of dissolution is based on two pretexts; solubility and rate of movement of water (transportation) within the environment (Summerfield, 1991). The throughput of water influences and controls the rate of dissolution; for example, as a mineral surface which is in contact with water becomes more saturated with solutes, it hinders further dissolution (Summerfield, 1991). As a consequence of this, the saturated zone needs to be constantly flushed with under-saturated water, in order for dissolution to be an effective mechanism of chemical weathering (Summerfield, 1991).

Dissolution is, however, controlled by pH dependence, which is seen through proton-promoted dissolution mechanisms, whereby the bonds between cations and the crystal lattice are weakened, accelerating the release of cations into solution; proportional to the concentration of protons (H^+) or hydroxyl ions (OH^-) (Anderson & Anderson, 2010). Most silicate minerals dissolve at greater rates, including high and low pH, with relatively low dissolution rates in the neutral pH ranges (Anderson & Anderson, 2010). Table 4.2.1, displays how the rate constants for pH change per unit increase according to the pH level. Overall the slopes of pH-rate constant relationship and the pH range of independence differ from one mineral to another, most silicate minerals tend to show the same pattern of dissolution (Anderson & Anderson, 2010).

Table 4.2.1: Relationship between pH and rate constant per unit increase in pH, (modified from Anderson & Anderson, 2010)

pH Value	**pH Range**	**Rate Constant Per Unit**
Low pH	< 3	Increase by $10^{0.5}$ (about 3)
Middle pH	4 - 8	Independent of pH
High pH	> 8	Increase by $10^{0.3}$ (about 2)

In alpine periglacial regions, for example, the dissolution of minerals occurs once fresh bedrock has been exposed to the surface or near-surface environments (Murton, 2007). In cold environments dissolution results in dissolved mineral surfaces and increased porosity, an example being weathering pits (Dixon, 2013). Increases in porosity, thus, facilitate a feedback which increases weathering rates and eventually results in rock disintegration and facilitates continual weathering through other processes (Dixon, 2013).

b) Hydrolysis

Hydrolysis, or incongruent dissolution, involves a reaction between water and a mineral, resulting in the production of either a weak acid or base (Dixon, 2013). When the mineral surface and water interact, the water splits into hydrogen ions and hydroxyl anions (Dixon, 2013). H^+ replaces the initial cations of the mineral disrupting the structural bonds, weakening the mineral structure, while the displaced cations react with the hydroxyl anions forming secondary clay minerals (Dixon, 2013).

c) Hydration

Hydration involves the addition of water to a mineral surface; however, it does not react with the mineral rather it is added to the structure of the mineral (Dixon, 2013). Hydration is also dependant on the crystal structure of the mineral, in that some minerals have the ability to absorb water into their relevant crystal structures (Summerfield, 1991). An example of this is seen in Summerfield (1991), through the hydration of iron oxide:

$$2Fe_2O_3 + 3H_2O \leftrightharpoons 2Fe_2O_3 . 3H_2O$$

The above reaction is of significance in terms of chemical weathering, due to it being able to aid other processes through the introduction of water molecules deep into the internal crystal structure (Summerfield, 1991). Hydration, although principally an expansive process rather than chemical, does in some instances result in the formation of secondary minerals, an example being hydrobiotite (Dixon, 2013).

d) Ion Exchange

Ion exchange is most common in clay minerals as, they have loosely bonded ions on the surfaces, which can be readily exchanged for ions in solution (Summerfield, 1991). Clay minerals are hence, significantly affected by this process, as they contain a strong capacity for ion exchange, either between interlays of a mineral or on surface layers (Dixon, 2013). During the exchange of ions the basic structure of a clay mineral remains unchanged, but the interlayer spacing changes depending on the size of the new ions entering the new positions (Dixon, 2013). For example, in cold environments biotite is weathered into vermiculite or montmorillonite through the loss of interlayer potassium and absorption of sodium and calcium (Dixon, 2013).

e) Oxidation/Reduction

This chemical weathering process involves the transfer of electrons between atoms, oxidation refers to the loss of electrons while reduction is the gain of electrons (Dixon, 2013). Oxidation is primarily involved in the reaction of minerals with oxygen in the presence of water, while the most common redox reactions being those of iron and sulphur (Dixon, 2013). For example in Summerfield (1991), iron can be oxidised to form iron oxide:

$$4Fe^{2+} + 3O_2 \longrightarrow 2Fe_2O_3$$

Iron usually exists as a bivalent ferrous state (Fe^{2+}) in most rock forming minerals, with oxidation however, it can be converted into the trivalent ferric form (Fe^{3+}), upsetting the neutral charge of the crystal structure, which can only be regained by the loss of other cations (Summerfield, 1991). Through this mechanism, the collapse of the mineral lattice occurs allowing other weathering processes to colonise the weakened rock (Summerfield, 1991).

In periglacial regions, oxidation of sulphides and solution of carbonates occurs as a response to increased water availability in soils, due to ice melting in the summer months (Murton, 2007). The oxidation of iron rich minerals produces a red to reddish brown rind on bedrock or on clast surfaces, commonly called a weathering rind (Murton, 2007).

f) Carbonation

Carbonation involves carbon dioxide dissolved in water with minerals, involving the acid hydrolysis of carbonates and silicates (Dixon, 2013). In humid environments with high organic activity, the dissolution of carbon dioxide in precipitation creates an additional source of bicarbonate ions, and thus, a contribution to weak carbonic acid solutions found in surface waters (Summerfield, 1991). The subsequent leaching of metal cations from silicate minerals is controlled by acid supply, including sulphuric, carbonic and organic acids (Summerfield, 1991).

Carbonation is important in the weathering of calcareous rocks (*e.g.* limestone), with the reaction involving carbonate acid and calcium (Dixon, 2013). The weathering of these rocks, involves reversible chemical reactions (Fig. 4.2.3) with carbon dioxide in the subterranean atmosphere or soil (Summerfield, 1991). In polar environments, temperature plays an important role in the process of creating carbonic acid (Summerfield, 1991). The equilibrium solubility of carbon dioxide decreases with increasing temperature, resulting in large amounts of carbonic acid build up in cold regions, even though the rate of carbon dioxide production by organic activity is low (Summerfield, 1991). Carbonation is thus, an important initial weathering process for calcium rich minerals, with it being widely reported in cold environments for the above reasons (Dixon, 2013).

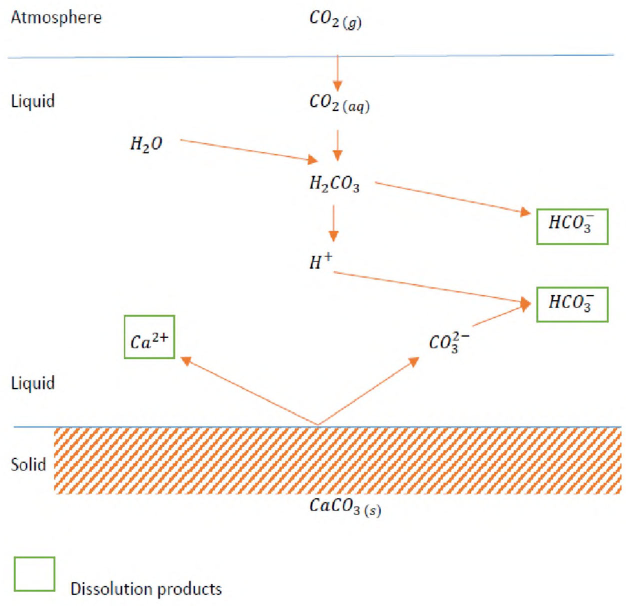

Figure 4.2.3: General scheme of the reactions involved in the chemical weathering of calcium carbonate (modified from Trudgill, 1985)

4.2.3.1 Rates of chemical weathering

The rates at which minerals weather and release ions is determined by five factors: pH, temperature, moisture availability, biological action and surface morphology (Dixon, 2013). Silicate materials dissolve significantly at higher and lower pH rates, with a neutral pH maintaining a low solubility (Dixon, 2013). At a lower pH, the H^+ proton promotes dissolution, increasing the hydrogen ion concentration increasing dissolution (Dixon, 2013). At higher pH values (>8), hydroxyl anions promote dissolution, which increases exponentially as pH does (Dixon, 2013). Weathering reactions are, hence, the result of multiple elementary reactions occurring from the smallest chemical step to a complex mechanism, typically involving two or at most three chemical species (Anderson & Anderson, 2010).

Temperature is a function in the Arrhenius equation, which states that the higher the temperature, or the lower the activation energy, the faster the reaction (Dixon, 2013). Exothermic reactions are possibly more dominant in cold environments, as the chemical equilibrium results in a more effective reaction between solutes depending on temperature. Linked to this, moisture availability is of great importance, with the prevalence of water the limiting factor in chemical weathering. High rock temperatures provide the heat for ice to melt, releasing the moisture required for dissolution and for subsequent chemical weathering to occur in these cold environments.

On a morphological scale, organisms such as plants, lichen and other micro-organisms interact with a rock surface and have the ability to influence rock breakdown and subsequent weathering rates. This is due to the production of acids, which provide hydrogen ions that replace cations on mineral surfaces, facilitating and accelerating mineral disintegration (Dixon, 2013). Not only do organisms and plants produce acids but, they are able to inadvertently retard chemical weathering processes, through the reverse feedbacks in the accumulation of soils (Pope *et al.*, 1995). For example, in humid environments with rapidly forming soils, the dense tropical vegetation acts as a shield to chemical weathering on bedrock (Pope *et al.*, 1995). Essentially thick soil horizons lead to decreased chemical weathering processes, especially in areas where bedrock is covered by soil, protecting the bedrock from weathering. This is of interest, particularly when in "weathering limited", periglacial environments such as Antarctica, the rate of weathering remains high (Pope *et al.*, 1995). Consequently, in relation with this high rate of weathering one must question whether this is it due to the transport limiting environment that Antarctica is characterised by, hence higher production values, or is the rate of weathering higher than other areas?

The surface morphology of a crystal controls the rate of dissolution of silicate minerals, the rate and type of dissolution is dependent on the location of the crystal imperfection (highly energetic atoms), and the prevalence of any surface coatings (Anderson & Anderson, 2010; Dixon, 2013). Kinks are most favoured dissolution sites (Dixon, 2013). Kinks are crystals which have three sides exposed, while steps have two exposed sides, planar crystals have one exposed side (Dixon, 2013). They are favoured as dissolution sites as, they contain atoms with the highest energy and fastest detachment rates, allowing for the rapid exchange of ions (Dixon, 2013).

4.2.3.2 Rock coatings and weathering rinds

Rock coatings are defined as the visual representation of the accumulation of transported solutes (Dixon, 2013). They are of importance as they have the ability to alter weathering rates, help to facilitate case hardening of surfaces, while they can also be used for understanding environmental change and provide chronometric insight into the underlying rock surface (Dorn, 2013).

Rock coatings represent the accumulation of chemical precipitates derived from the internal structure of the rock to the external rock surface, but ultimately they are derived from bedrock weathering (Dixon & Thorn, 2005). The growth of rock coatings, or rock varnish, is not limited to precipitates from internal rock structure, but, can also be derived from the deposition of air particles onto the rock surface, such as in coastal areas (Mergelov *et al.*, 2012). These rock coatings are essentially layers of sediment glued onto one another, with the main source of phyllosilicates being attributed to dust, which is supplied from northern desert sources and transported to Antarctica (Mergelov *et al.*, 2012). These observed coatings (Table 4.2.2) are often diverse in their chemical composition, with the most common coatings attributed to iron, silicon, aluminium, potassium and calcium (Mergelov *et al.*, 2012; Dixon, 2013). The chemical composition of such coatings are unique to rock morphology and dynamics, but they are also determined by microscale environmental interactions (Pope, 2013).

Table 4.2.2: Major types of rock coatings observed in Western Dronning Maud Land, Antarctica (adapted from Dorn (2013)

Coating Type	Description	Co-related terminology
Case Hardening	The addition of a cementing agent (Mg, SO_4, Fe, organisms or anthropogenic) to a rock matrix	Rock coating
Rock Varnish	A surface layer (trace elements, clay minerals, Mn and Fe oxides) which is attributed to a colour change due to variable concentrations of manganese and iron oxides	Patina, desert varnish
Iron Film	Rock coating which is comprised of primarily oxy-hydroxides or iron oxides	Iron staining, ferric oxide
Silica Glaze	Rock coating which is composed of primarily silica and aluminium (often with iron), which produces a shiny surface layer (clear white, orange shiny lustre, sometimes dark in appearance)	Desert glaze, silica skins/coatings/crusts, turtle skin patina

In order to classify rock coatings, such as those noted in Table 4.2.2, landscape geochemistry created a systematic manner in which to analyse and predict which types of rock coatings would develop in different locations (Dorn, 2013). The geography of rock coatings is subdivided into five main groupings (hierarchy system) whose individual factors are seen to have a control on the development of rock coatings (Dorn, 2013). This hierarchy system (Fig. 4.2.4), details the controls and their characteristics in relation to rock coating development.

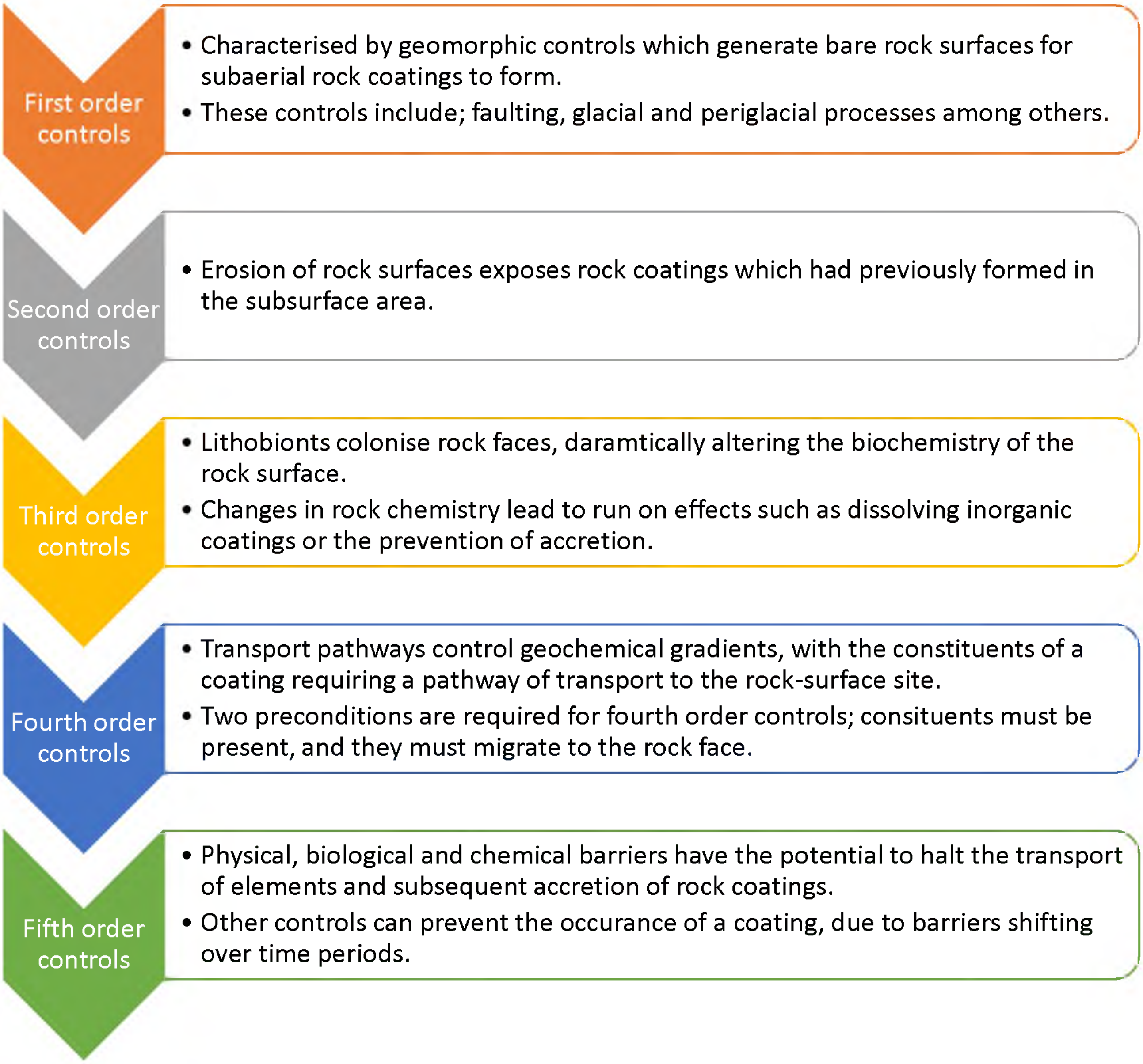

First order controls
- Characterised by geomorphic controls which generate bare rock surfaces for subaerial rock coatings to form.
- These controls include; faulting, glacial and periglacial processes among others.

Second order controls
- Erosion of rock surfaces exposes rock coatings which had previously formed in the subsurface area.

Third order controls
- Lithobionts colonise rock faces, daramtically altering the biochemistry of the rock surface.
- Changes in rock chemistry lead to run on effects such as dissolving inorganic coatings or the prevention of accretion.

Fourth order controls
- Transport pathways control geochemical gradients, with the constituents of a coating requiring a pathway of transport to the rock-surface site.
- Two preconditions are required for fourth order controls; consituents must be present, and they must migrate to the rock face.

Fifth order controls
- Physical, biological and chemical barriers have the potential to halt the transport of elements and subsequent accretion of rock coatings.
- Other controls can prevent the occurance of a coating, due to barriers shifting over time periods.

Figure 4.2.4: Hierarchy controls on rock coating development (adapted from Dorn, 2013)

Although Fig. 4.2.4 displays the basic processes which underpin the concepts of orders of control, it must be noted that rock coatings need to be considered as forming at a subsurface layer, rather than at the rock surface interface (Dorn, 2013). Assumptions in past studies have not taken subsurface weathering into account, but, rather infer that if a coating occurs at the rock surface interface, then it must have also originated at that location (Dorn, 2013). Fig. 4.2.4, thus attempts to overcome this assumption, especially with second and higher order controls.

When specifically considering fourth and fifth order controls, a more complex relationship exists, particularly when reflecting on case hardening and accretion. For rock coatings to occur, there is a prerequisite for constituent elements and subsequent transport to the accretion site (Dorn, 2013). In particular, the fourth order control on rock coatings relies on constituents having a pathway to the rock surface site (Dorn, 2013). Transport pathways, for example, may extend over kilometres, as in the case of dust which becomes rock varnish, or they can involve short distances such as in the case of iron and manganese, which are mobilised from rock varnish into pores for the case hardening of underlying rock (Dorn, 2013). The lack of transport pathways for key constituents has the potential to influence the type of rock coating which accretes, with this being essentially true in the case of rock varnish (Dorn, 2013).

Fifth order controls are the lowest ranked controls in terms of rock coatings, due to the prevalence of other controls exerting an influence on their formation, or rather the prevention of their formation (Dorn, 2013). For example, according to Dorn (2013), in warm deserts, dust coatings occur due to electrostatic forces holding the particles together. However, the lack of bare rock (first order), the exposure of a rock surface coating (second order), the growth of fungi/lithobionts (third order), or transport of materials through wind or water (fourth order), can interfere with the creation of a dust coating (Dorn, 2013). It is, thus, essential to recognise that chemical and physical barriers often work together to create inorganic rock coatings such as silica glaze, while a sequence of biological, physical and physiochemical barriers are needed for rock varnish formation (Dorn, 2013).

Following the documentation of chemical and physical barriers and unification in ideas relating to the creation of rock coatings, a polygenetic model of rock varnish formation was developed (Dorn, 2013). Rock varnish begins with the addition of dust particles to a subaerial surface, which are maintained in place by physical barriers of electrostatic or physical forces (Dorn, 2013). This is followed by biological actions, which concentrate elements, and the subsequent adjacent transport of these minerals to clay substrates occurs (Dorn, 2013). Physiochemical processes then cement the minerals to the rock surface prior to rock varnish formation (Dorn, 2013). Although it is noted that barriers vary, and that they are subject to higher order controls during rock coating processes, it must also be mentioned that elemental migration can shift over time and result in a change in the type of rock coating which is formed (Dorn, 2013). Due to these changes over millennia timescales, rock varnish can be used as a means of looking at climate change, as it effectively accretes evidence of past climates (Dorn, 2013). For example, shifting geochemical barriers over time periods can record changes in manganese barriers, with stronger manganese barriers attributed to wet intervals (Dorn, 2013).

In Antarctic regions, for example, rock varnish predominantly comprises iron oxides with little to no manganese oxides, with these coatings being less than 100 micrometres thick (Glasby *et al.*, 1981). Several studies of these coatings are linked to the possible influence of moisture in their formation, however, this theory has yet to be proved (Glasby *et al.*, 1981). Within the Dry Valley areas of Antarctica, fine grained dolerites display rock varnish with smooth surface coatings, due to wind action

(Glasby *et al.*, 1981). Similarly, in Beacon Supergroup sandstones, the upper surfaces show staining and varnish, even though sandstones are characteristically low in iron, these attributes have occurred due to the leaching of iron from overlying dolerite and the subsequent deposition of iron oxides (Glasby *et al.*, 1981; Mergelov *et al.*, 2012). While it must also be noted that in Antarctic regions, rock varnish is predominantly controlled by wind action (velocity) and the availability of moisture, which are characteristic features of these high altitude regions (Glasby *et al.*, 1981). It can, thus, be said that rock varnish is controlled to a lesser degree by aspect and acts like a shield, protecting rock surfaces from the ailments mentioned above (Glasby *et al.*, 1981).

Although the protection of rock surfaces and aspect influence the formation of rock varnish, it must also be mentioned that another control on the extent of rock varnish is the rock type in itself (Glasby *et al.*, 1981). For example, different rock lithologies facilitate rock varnish formation at different rates and influence the type of rock coating, an example being the colour of the rock coating (Glasby *et al.*, 1981; Mergelov *et al.*, 2012). Coarse granites, for example, produce very little/poor rock varnish as slower chemical weathering occurs, with a shorter period of time noted for accumulation to occur (Glasby *et al.*, 1981). This lack of rock varnish is attributed to salt and freeze thaw weathering, whereby, moisture and salt solutions move rapidly along predefined crystalline boundaries, using them as transportation pathways (Glasby *et al.*, 1981). This movement facilitates increased cavernous weathering (through increased transportation of minerals away from the site) on the leeward side, and increased physical weathering; resulting in shorter periods of time for the formation of rock varnish (Glasby *et al.*, 1981). Fine grained granites, on the other hand, display a reverse pattern of development, whereby rock varnish is well developed (Glasby *et al.*, 1981).

The time periods required for rock varnish to occur are protracted, while their formation is simultaneously controlled by predetermined characteristics (Glasby *et al.*, 1981). One of these characteristics is the presence of ice free areas (Glasby *et al.*, 1981). Typically, areas which have been ice free for longer have more developed rock varnish layers, in comparison to those which have recently been exposed through glacial recession (Glasby *et al.*, 1981).

In periglacial and glacial regions, for example in the Swedish Lapland, iron films are attributed to the oxidation of pyrite and the transport of iron over short distances (Dixon, 2013). In terms of subglacial meltwaters, iron films are a commonality and are noted in cold polar deserts such as Antarctica (Dixon, 2013). Rock coatings in Antarctica are either dominated by iron, silica or gypsum (Dixon, 2013). The precipitates of such coatings are particularly evident along bedding planes or joints in rocks, with iron oxide staining often found next to horizontal beds (Meiklejohn & Hall, 1997). While silica glazes are primarily due to the dissolution of airborne clay and quartz (Dixon, 2013).

Gypsum coatings, however, are linked to the redisposition of calcium found within the surrounding weathered carbonate dominated bedrock (Dixon, 2013). Gypsum deposits are sometimes substantial in Antarctica, often found in joints or close to ground level around bedrock (Meiklejohn & Hall, 1997). For example, the underside of the rocks in southern Victoria Land, Antarctica, displayed calcite ($CaCO_3$) and gypsum ($CaSO_4.2H_2O$) being the dominant constituents (Glasby *et al.*, 1981). It has been hypothesised that the accumulation of precipitates is linked to stagnant conditions, but it has also been hypothesised that precipitates may be a result of mobile solution (Meiklejohn & Hall, 1997). Although each hypothesis may be equally likely and occur in both cases, evidence for precipitates of mobile solute origin is suggested through the deposition of such precipitates at edges of water channels or areas where moisture is available (Meiklejohn & Hall, 1997).

Weathering rind or rock coating?

It is important to note that rock coatings and weathering rinds are not the same. Weathering rinds are developed at the top 0.5-45mm of a bedrock or coarse debris, while maintaining a reddish coloured outer surface, overlying a lighter bleached zone (Dixon & Thorn, 2005; Murton, 2007). Rock coatings often accompany weathering rinds and are a by-product of nano- and microscale weathering processes, which often interact synergistically with organically mediated weathering processes (Dixon & Thorn, 2005; Dixon, 2013; Pope, 2013). Weathering rinds frequently represent a coloured weathered zone near the rock surface, which is identified using visual observations rather than chemical analysis (Oguchi, 2013). There is difficulty in determining the weathering rind, mostly due to the fact that many rocks display more than one coloured zone throughout the profile (Oguchi, 2013). The observed change in rock colour is due to the oxidation of iron within the bedrock, which may be overlain with a rock coating, is often seen as a shiny surface layer (Gibson *et al.*, 1983; Murton, 2007).

Weathering rinds are often referred to as a form of desert varnish and may be intensely developed, possibly protecting the internal rock surface from disaggregation (Dixon & Thorn, 2005). Thus, rock coating material which is reprecipitated into weathering rinds, does more than just physically protect the rock through case hardening (Dorn, 2013). This is due to chemical weathering rates decreasing due to the role of clay-coated mineral surfaces; for example, silica glazes slow the rate of chemical weathering (Dorn, 2013). It can be seen that case hardening's essential function is to stabilise landform surfaces, due to the mobilisation and reprecipitation of rock coating materials inside pore spaces within the weathering rind (Dorn, 2013). Case hardening also has the additional property of making a rock less permeable, this is partially due to the localized mobilisation and reprecipitation of minerals on the rock surface, effectively strengthening it from the outside in (Summerfield, 1991). Areas less effectively case hardened would be susceptible to further weathering processes, noticed where weathering is found in the rock interior resulting in cavity formation (Summerfield, 1991).

Although weathering rinds are projected as landscape conserving processes, it must also be mentioned that landscape denudation processes also occur on rock surfaces, with certain rock coatings accelerating physical weathering processes (Dorn, 2013). Calcrete crusts and dust, for example, precipitate and accumulate inside the pores and fissures of rock, and hence, have the ability to wedge open these features over large time scales (Dorn, 2013).

In conclusion, rock coatings are controlled by four major factors: lithology, altitude, aspect and wind direction (Glasby *et al.*, 1981). It has been suggested that the dominant mode of rock varnish formation is based wind induced advection of moisture from the upper surface layers of rocks, especially in sandstones (Glasby *et al.*, 1981). In Antarctic regions, the high aridity and wind speeds permit increased rates of evaporation, leading to enhanced surface weathering as these processes are increased (Glasby *et al.*, 1981).

Although the Antarctic provides the basics for enhanced chemical weathering to occur, it must be noted that certain criteria must be met for this to occur (Glasby *et al.*, 1981). These criteria are linked to the above four controlling factors. The rock must be texturally and compositionally amenable to rock varnish formation, not eroding rapidly nor being resistant to chemical weathering (Glasby *et al.*, 1981). Wind velocities must not be so high as to increase the rate of abrasion to higher than the rate of rock varnish formation (Glasby *et al.*, 1981). While the iron content of the rock must be high enough for leaching to occur, or alternatively, the adjacent or surrounding rock must be of a low iron content for the transfer or iron to occur through an external source (Glasby *et al.*, 1981).

Chemical weathering processes can be seen as significant components of geomorphic and pedogenic processes in cold climates (Dixon, 2013). The only difference between these processes in cold environments and mild, temperate, environments is the rate at which they operate (slowed in colder environments) (Dixon, 2013). From the above argument, it is clear that chemical weathering processes are vital in denudation of bedrock and landscape formation (Dixon, 2013). With the prominence of geochemical denudation in cold environments exceeding mechanical denudation, there is a need to further understand chemical weathering processes in cold environments (Dixon, 2013). An unresolved problem linked to this, is the nature and impact of chemical weathering, and the effect on landscape formation (Meiklejohn & Hall, 1997).

It is increasingly obvious that throughout chemical weathering studies, there has been a tendency to isolate individual weathering processes (Hall *et al.*, 2002). This isolation has resulted in the understanding of weathering from one perspective (isolation), rather than holistically or as a suite of processes (Hall *et al.*, 2002). Future studies, thus, need to both challenge current theory and need to investigate periglacial weathering regimes with an open mind (Hall *et al.*, 2002).

4.2.4 Biological weathering

Biological weathering in cold climate environments is documented as occurring extensively in a variety of regions, but in comparison to tropical studies, it has yet to receive as much recognition (Hall *et al.*, 2002). Biological weathering, in conjunction with chemical weathering, is important for the production of inorganic and organic acids (Etienne, 2002). However, the true impact of microorganisms in weathering suites remains understudied (Etienne, 2002). This is due in part to their manifestations being masked by the prevalence of higher vegetation and the activity of pedogenetic and weathering processes (Mergelov *et al.*, 2012). Antarctica, and desert regions, allow for the study of endolithic colonisation as, many of the masking factors in tropical regions are absent and reddish-brown colourations of rock varnish are straightforward to identify (Mergelov *et al.*, 2012). With the development of this varnish is argued as a prerequisite for rock surface stabilisation and, thus, further colonisation by endolithic organisms (Mergelov *et al.*, 2012).

Biological weathering involves a variety of organisms including lichen, mosses, and bacteria, as well as rock colonising fungi and even trees (warm environments), which either induce chemical reactions (oxidation/reduction/chelation), or exert physical stresses on a rock surface/subsurface (Hall *et al.*, 2002; Murton, 2007). In extreme cold environments, such as Antarctica, organisms use subsurface areas of rock as a form of environmental protection from wind, UV radiation, desiccation, high rock surface temperatures, and negative air temperatures (Hall *et al.*, 2002). Micro-organisms that live in or beneath rocks in polar deserts, have the ability to facilitate chemical weathering at the rock surface horizon through the precipitation of minerals or removal of minerals from the interior (Hall *et al.*, 2002). Organisms can affect weathering, especially in deriving inorganic nutrients from the rock subsurface, however, this is controlled through spatial variability such as aspect, moisture availability and light transmissivity (Hall *et al.*, 2002). This can seen in previous work conducted by Dwight (2015) and Ayers (2017), which investigated the geomorphic and ambient environmental impacts on lichen distribution and the influences of the natural environment on habitat preference for lichen in western Dronning Maud Land respectively.

Cryptoendolithic microbial communities are found within the interstitial spacing or subsurface hollows of favourable translucent sandstones, extending up to 10mm below the rock surface (Blackhurst *et al.*, 2003; Mergelov *et al.*, 2012). These communities are primarily consistent of microbial symbiotic, or free-living lichen (Blackhurst *et al.*, 2003). Polar habitats are ideal environments for these organisms, as they survive in extreme environments where water availability is scarce, temperatures are low, high winds are prevalent, and large variations in solar radiation input occur (Omelon *et al.*, 2006). Cryptoendoliths are common in Beacon Supergroup and Devonian Quartzite geologies in Antarctica, and enhance the weathering rates of sandstones through acidification (Blackhurst *et al.*, 2003; Budel *et al.*, 2004). Cryptoendoliths alter rock through the production of distinct biotic zones; these are restricted to zones of sufficient light, often indicated by colour changes, which change rock properties as a result (Blackhurst *et al.*, 2003; Budel *et al.*, 2004). Surface mineral formation is determined by the chemical and physical characteristics of the cell envelope, which are either indirect (pH, redox changes) or direct (sorption of metals to cell surface binding sites), resulting in mineral precipitation (Omelon *et al.*, 2006). In the case of cryptoendoliths, the alteration of rock properties has a direct result on weathering processes, which act on these surfaces such as mechanical and chemical weathering.

Lichens, in particular, have the ability to cause exfoliation of the rock surface through a mechanical process, where the permeation of their hyphae into a rock creates cleavage planes/fractures and thorough the solubilisation of cement (Guglielmin *et al.*, 2005; Murton, 2007; Hansen *et al.*, 2013). Endolithic lichens, however, can assist in the expansion and contraction of rock surfaces through freeze-thaw induced processes that interact with the endolithic lichen's thallus (Murton, 2007). Lichens do not only provide physical stresses, but they also allow for the mobilisation of minerals such as phosphorus, iron and silicates (Guglielmin *et al.*, 2005; Hansen *et al.*, 2013). Hence, lichens allow for both precipitation, solubilisation and removal of materials, effectively changing the rock properties (Hall *et al.*, 2002; Guglielmin *et al.*, 2005; Hansen *et al.*, 2013).

Within the discipline of biological weathering, there is a similar apparent trend to that noticed in mechanical weathering, whereby freeze thaw processes were favoured in the literature. This trend is also related to a specific mechanism of weathering, namely biological weathering by lichen (Etienne, 2002). In cold region texts on biological weathering there is a focus on studying lichen (Etienne, 2002). While other micro-organisms such as bacteria and fungi are often sparsely studied or only studied in a rudimentary manner (Etienne, 2002). The exclusion of certain organisms in polar region weathering studies has in impact on modern weathering studied as, the complex role of biological weathering through micro-organisms in cold environments has yet to be incorporated (Hall *et al.*, 2002). In the future, the effects of rock breakdown by these organisms needs to be considered as a conventional process, with more study being required in cold polar regions (Hall *et al.*, 2002).

4.3 Soluble geochemistry

Water serves various multiscale functions in weathering processes, it acts as an agent for transport, as a medium through which reactions diffuse at reaction sites, exerts partial pressure, increases surface area, as a chemical solvent and buffer, as a needed part of chemical reactions and a constituent as a product of weathering (Pope *et al.*, 1995). An example of the role of water in weathering is that of capillary water, where the amount of weathering depends on hydrodynamic flow, size and connectivity of capillary pores and in turn, volume of water, which is dependent on the texture or lithology of the weathering materials (Pope *et al.*, 1995).

Solute concentrations of flowing water, or of lakes, is of importance in an Antarctic context, due to the influence that these factors have on chemical weathering in two perspectives, rate and kind (Dixon & Thorn, 2005). In alpine regions particularly, deglaciation in a warming environment is increasing the quantities of water from glaciers, ice melt and snow packs (Dixon & Thorn, 2005). While deglaciation in a warming environment is expected, the mean rise in temperatures of Antarctica is predicted to be between 5°C and 7°C , with greater areas of mountainous areas (nunataks) being prone to the melting of permafrost (Barsch, 1993). The increased water availability, thus, has the potential to increase the amount of chemical weathering and erosion in the area, due to increased moisture availability (Dixon & Thorn, 2005). It is important to note, however, that the predictions of models, especially in regards to seasonal changes and future precipitation are coarse at best and more than likely unreliable at the current time (Barsch, 1993).

Previous research in partially glaciated drainage basins revealed that cation denudation rates increase with discharge across both glaciated and non-glaciated basins (Dixon & Thorn, 2005). For example, in alpine areas such as the Colorado Rocky Mountains Front Range, inorganic loads are dominated by Ca^{2+} and Si loads, while Na^{+}, K^{+} and Mg^{2+} were found in smaller quantities, while in this case the anions were dominated by bicarbonate and sulphate (Dixon & Thorn, 2005). From studies as the above, solute contents were generally found to exceed that of the incoming precipitation, effectively suggesting that stream loads are functions of atmospheric additions (wet/dry deposition), and the chemical weathering of regolith and bedrock (Dixon & Thorn, 2005).

In the case of waters from glacial catchments, however, it was found that they are typically enriched with K^{+} and Ca^{2+} in comparison to those of non-glacial catchments (Dixon & Thorn, 2005). The reasoning for this is the combined effects of dissolution of soluble trace phases exposed by glacial abrasion and dissolution of biotite, which releases potassium (Dixon & Thorn, 2005). It can, thus, be stated that lower solute yields from alpine basins are the result of the lack of regolith coverings in these areas and the subsequent domination of exposed bedrock (Dixon & Thorn, 2005). The above statement can be seen to relate to periglacial environments such as Antarctica, as similar enhancement of chemical species dissolution is expected to occur where glaciers are present in headwater areas, this theory, however, is still to be tested in Antarctica (Dixon & Thorn, 2005).

5. Study Area

5.1 Overview

Antarctica has been divided into four main biogeographic regions; Southern Cold Temperate, Sub-Antarctic, Maritime Antarctic and Continental Antarctic (Terauds *et al.*, 2012). This classification, however, has shortcomings and is regarded as both simplistic in nature and ignorant of the connections between regions and their biotic and abiotic functions (Terauds *et al.*, 2012). A new classification has, thus, been developed which groups Antarctica into 15 conservational bioregions, with Dronning Maud Land identified as one of them (Fig. 5.1.1, black box) (Terauds *et al.*, 2012). These bioregions are supported through phylogeographic analysis, indicating differences between them, such as the distribution of taxa (Terauds *et al.*, 2012).

The implications of the classification of 15 bioregions is mainly linked to the implementation of policies and guidelines for conservation within each distinct area (Terauds *et al.*, 2012). Essentially, each of the 15 bioregions should be represented by at least one designated, protected area unto which appropriate quarantine practices should occur (Terauds *et al.*, 2012). The creation of these bioregions is linked to the conservation of pristine Antarctic ecosystems and is vital for the relevance of scientific study and future research on the continent.

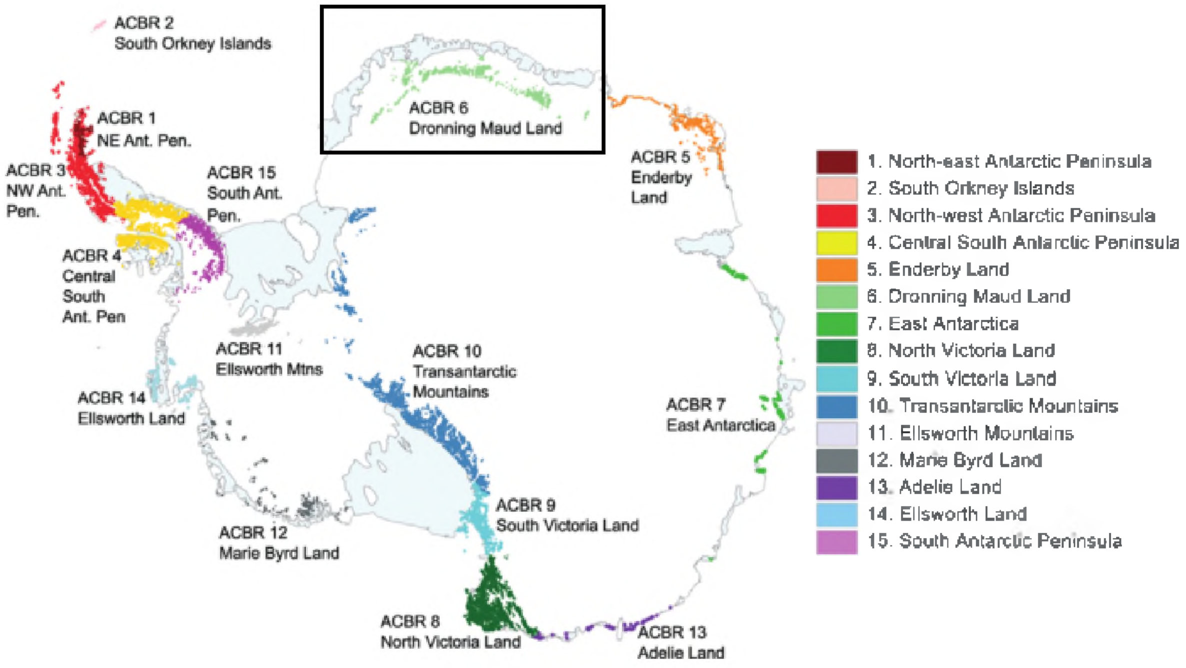

Figure 5.1.1: The 15 Antarctic Conservation Biogeographic Regions (directly copied from Terauds *et al.*, 2012)

Antarctica is the coldest and driest continent on Earth, receiving very little precipitation throughout the year (Claridge & Campbell, 1985; Hansen *et al.*, 2013). It is covered in ice and snow, with an approximation of only 2% of the underlying bedrock being accessible; the current overlying ice sheet, is attributed to the Last Interglacial Transition (8000 years before present), following the Last Glacial Maximum (18000 years before present) (Hansen *et al.*, 2013). The continent has an approximate area of 14 x 10^6 km^2, roughly one tenth of the earth's surface, with 90% of the world's ice and 70% of its fresh water being stored either around or on the continent itself (Convey *et al.*, 2009; Kennicutt *et al.*, 2014). The ice sheet over Antarctica consists of three glaciological zones, the East Antarctic, West Antarctic and Antarctic Peninsula (Convey *et al.*, 2009). East Antarctica includes the high Polar Plateau, and is separated from Western Antarctica by the Transantarctic Mountains which has the highest peak on the continent of 4528m above sea level (Convey *et al.*, 2009).

Antarctic soils are classified as gelisoils, soils with permafrost within 100cm of the surface, or soils with gelic material within 100cm of the surface and permafrost within 200cm of the surface (Bockheim & Hall, 2002). The most common types of soil found in Antarctica are turbels (mineral soils which have one or more horizons showing cryoturbation) or orthels (other soils) (Bockheim & Hall, 2002). Soils of the Transantarctic Mountains are, however, classified as anhydrous (exceptionally dry), dominated by anhyturbels and anhyorthels (Bockheim & Hall, 2002).

Western Dronning Maud Land is one of the biogeographic regions within Eastern Antarctica (Table 5.1.1). On average western Dronnning Maud Land receives 55-88mm of precipitation (Hansen *et al.*, 2013). Research into humidity in this area of the Continent has found that the relative humidity is 63%, increasing to 66% during the Austral summer (Hansen *et al.*, 2013). Dominant wind speeds for this region are on average 11 $m.s^{-1}$ while the dominant direction is easterly (Hansen *et al.*, 2013). The average minimum air temperature from previous studies is -27.8°C with the average maximum -2.2°C (Hansen *et al.*, 2013). Ambient average daily air temperature is -8.3°C for Austral summer and -21.8°C for Austral winter months (Hansen *et al.*, 2013).

Scattered throughout western Dronning Maud Land are sections of ice-free rock called nunataks. These nunataks are a part of the Ahlmannryggen and Borgmassivet Mountain ranges, and are primarily of intrusive geology of the Jutulstraumen Group which is of Mesoproterozoic origin (Hansen *et al.*, 2013). Eight study sites within the Ahlmannryggen Borgmassivet Mountain range were selected in western Dronning Maud Land (Fig. 5.1.2). These sites span a range of latitudes and longitudes, from 3°11'31,208"W, 71°26'48,97"S (Robertskollen) to 3°31'16,19"W, 72°39'34,549"S at the furthermost point (Borgmassivet). Most of the geology in the study area is dolerite, cut by younger intrusive rock exhibiting case hardening and rock coatings (Hansen *et al.*, 2013). While exposed nunataks are characterised by continuous permafrost, and a shallow active layer (10-20cm) (Meiklejohn & Hall, 1997; Hansen *et al.*, 2013).

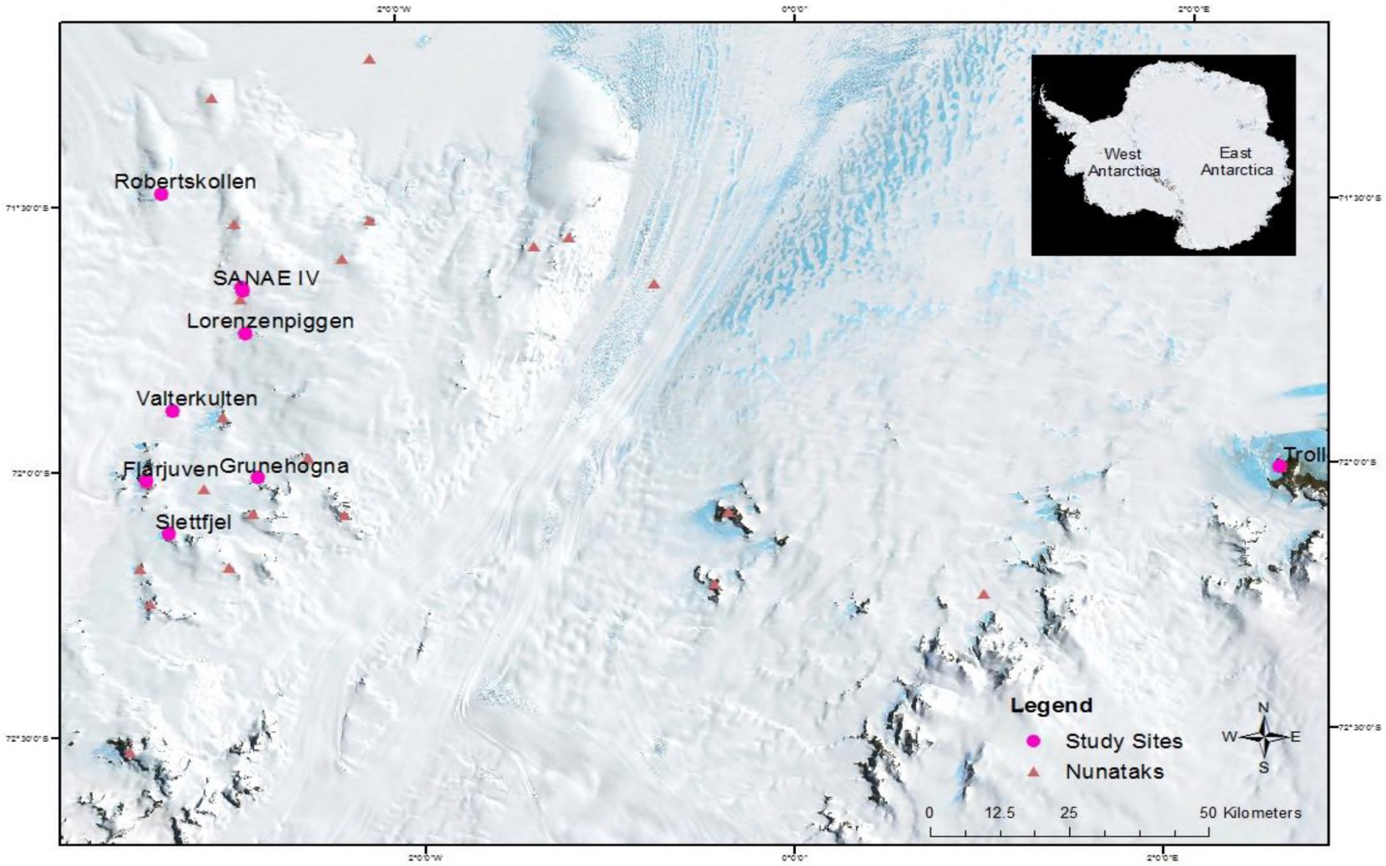

Figure 5.1.2: Map of the study sites in western Dronning Maud Land, Antarctica

5.2 Geology

Ahlmann Ridge (Fig. 5.2.1), upon which the majority of the sample sites fall lies 160 km south of the South African National Antarctic Expedition (SANAE IV) base, wedged between the polar plateau and the Fimbul Ice Shelf (Neethling, 1969). The general ice surface is at an altitude of between 1500-2000 m at the foot of the mountain range, which runs approximately 150-200 km inland (Roots, 1969). The nunataks form blocky, disconnected lines with groups of highly dissected horns, arêtes and glacially scoured massifs which become smaller and more scattered in the northern regions, towards the coast (Neethling, 1969; Roots, 1969). Western Dronning Maud Land consists of two distinct geological regions:

a) Metamorphic rock complexes – banded gneiss, schist, amphibolite and pegmatite, and

b) flat-lying clastic sediment sedimentary rocks and andesitic volcanics, with large sills and dykes of dolerite and diorite (Neethling, 1969).

The sedimentary-volcanic region is separated from older metamorphic complexes by north flowing glaciers such as the Jutulstraumen (to the east) and Schytt glaciers (to the west) (Neethling, 1969). The Ahlmannryggen Mountain range formation is characterised by slightly metamorphosed rock, with the lower part consisting of interbedded, dark, siliceous siltstone and arkose, conformably overlain by arenaceous beds, minor black shale and clastic rock beds (Neethling, 1969). Although the texture and metamorphic minerals found within these rocks is greatly developed, it is important to note that this may be due to the relative impurity of the rocks, as opposed to the higher degree of metamorphism (Roots, 1969). All exposed sedimentary rocks in the Borg Massif and on Ahlmann Ridge, have been assigned to the Ahlmannryggen Group of stratified rocks (Roots, 1969). Which are composed of clastic strata, barren or extremely poor in organic remains, with repetitive, well banded, grey, green and buff coloured quartzite, mudstone, siltstone and mudstone-fragment conglomerates without distinctive horizon markers (Roots, 1969). The sills of the Borg intrusions have invaded the Ahlmannryggen Group of sedimentary rocks throughout the extent of the range, they are resistant to erosion at a higher rate than the latter and, as such, these sills form most of the cliffs and nunataks of the Ahlmann Ridge (Roots, 1969).

The ages of the Borg intrusions are comparatively younger than the strata found in the Ahlmannryggen Group (Roots, 1969). The relationship between the two strata is found to be similar to that of the Jurassic Ferrar dolerites and the Beacon Group in the Transantarctic Mountains (Reece, 1958). These relationships, however, are also similar to those of pre-Devonian diabase found in the Pensacola Mountains and the Patuxent Formation that it intrudes (Schmidt *et al.*, 1964).

The majority of the Ahlmannryggen Range is characterised by low grade metamorphosed sheets of dolerite to quartz dolerite, being noted on a regional scale throughout the nunataks in the area (Neethling, 1969). The emplacement pattern of dioritic intrusions is commonly transgressive, shifting from one stratigraphic horizon to another in many places (Neethling, 1969; Roots, 1969). These sill formations may have a thickness of over 350m in some areas, being composed of a differentiated syenodioritic upper part and a more mafic lower part (Neethling, 1969; Roots, 1969). Basaltic selvages, sharp contacts and minor assimilation of rock wall strata are common (Neethling, 1969). Granophyric zones in the metamafics may represent transformed sedimentary rocks, the final stages of metasomatism in terms of rheomorphic phenomena is possibly responsible for the felsic veins present in poorly exposed outcrops (Neethling, 1969). Petrographic examination of these altered mafic rocks (although not representative as a unit) indicates a composition of 43-50% plagioclase, 30-50% augite, pigeonite, enstatite, hornblende, olivine and biotite with 0.8-3.5% quartz, ore and myrmekite (Neethling, 1969). Characteristic of these features is the intense sericitization of feldspar and serpentinization of pyroxene and olivine (Neethling, 1969).

The Ahlmann Ridge therefore “apparently represents a mountain range formed by progressive step-faulting along narrow north-easterly trending zones, with associated transverse dislocations, the former culminating in the major graben structures of the Schytt and Jutulstraumen Glaciers” (Neethling, 1969: Sheet 6). The strata of individual nunataks have been tilted in more than one direction, but the prevailing strike of the rocks tends to be parallel to the local joints and fault connections, noted particularly in the Ahlmann Ridge (Neethling, 1969). In terms of the structural history of the area, this is at present obscure, but, earth movements appear to be vertical, with rejuvenation of fault areas along weak zones (Neethling, 1969). Block faulting is thought to have preceded the emplacement of sills and eruption of the Precambrian volcanics; the present features indicate recent uplift along the old fault lines (Neethling, 1969).

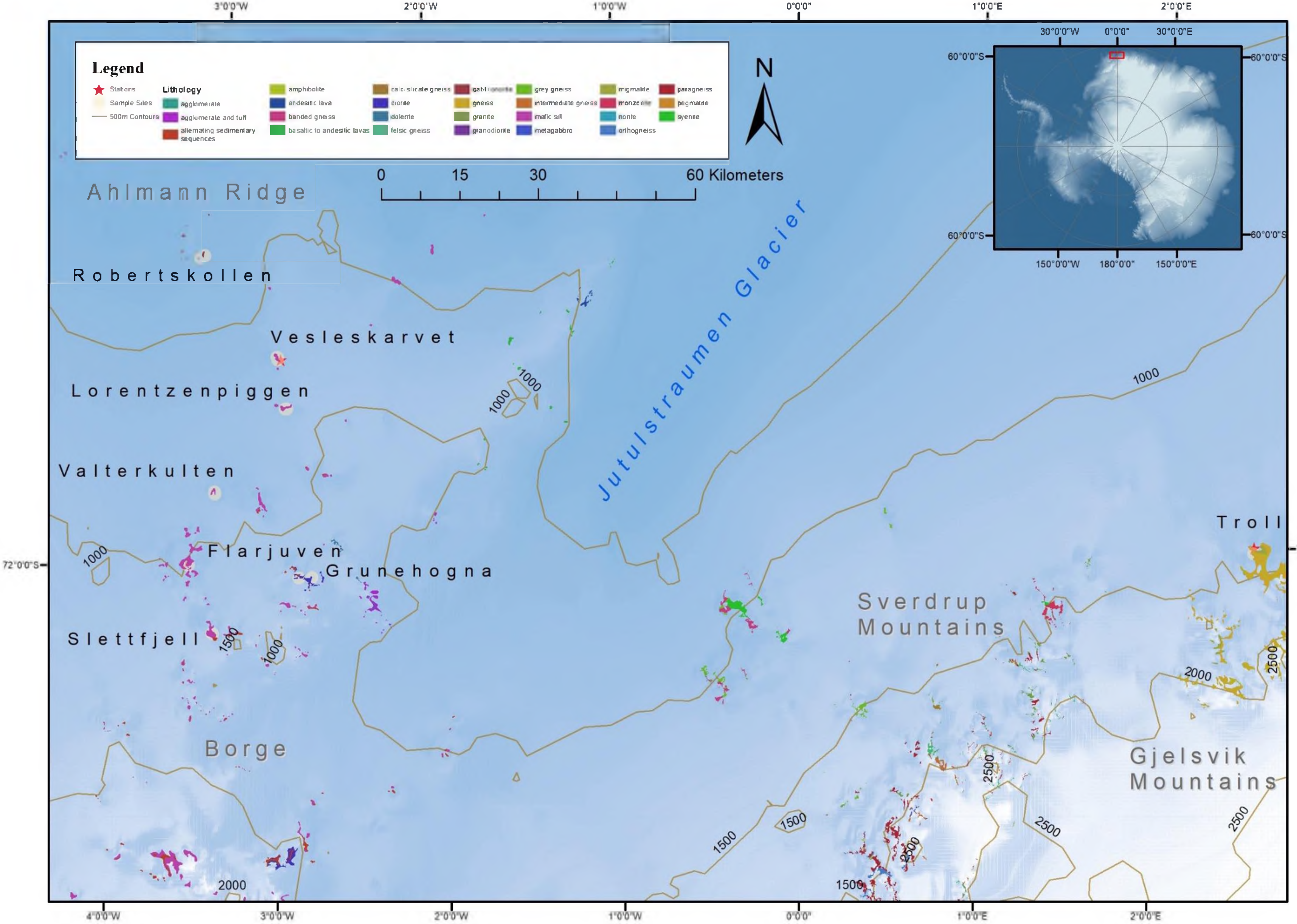

Figure 5.2.1: Lithology of exposed rock within the study area. Based on data from O'Kennedy (2016)

The northern most exposures of nunataks, such as Robertskollen and Vesleskarvet (Fig. 5.2.2), in the Boreas-Passat area consist of a lithology of uniform, medium grained dolerite intrusions of tholeiitic composition (Von Brunn, 1962; Neethling, 1969). The texture is ophitic to sub-ophitic with the grain size showing no variation in the outcrop area (Neethling, 1969). Average modal composition is 54% plagioclase, 36% pyroxene, 5% micropegmatite and minor accessories including biotite, iron oxide, and rare apatite, with olivine absent (Von Brunn, 1962; Neethling, 1969). The degree of alteration is of a lower grade than the Borg metamafic intrusions, but varies on the extent of late deuteric and hydrothermal action (Von Brunn, 1962; Neethling, 1969).

It is important to note, however, that Robertskollen does display ultramafic rocks of peridotitic composition (Von Brunn, 1962; Neethling, 1969). The ultramafic rocks have a sharp contact, but no chilled borders, occurring below altered dolerite, tentatively classified as Borg metamafics (Von Brunn, 1962; Neethling, 1969). Veins of tremolite and serpentine are locally present, augite is subordinate to bronzite, while olivine is dominantly unserpentinized (Neethling, 1969). These ultramafics are considered genetically related to the overlying dolerite, while the relationship to the peridotitic dikes occurring in the sedimentary and mafic rocks is unknown (Neethling, 1969).

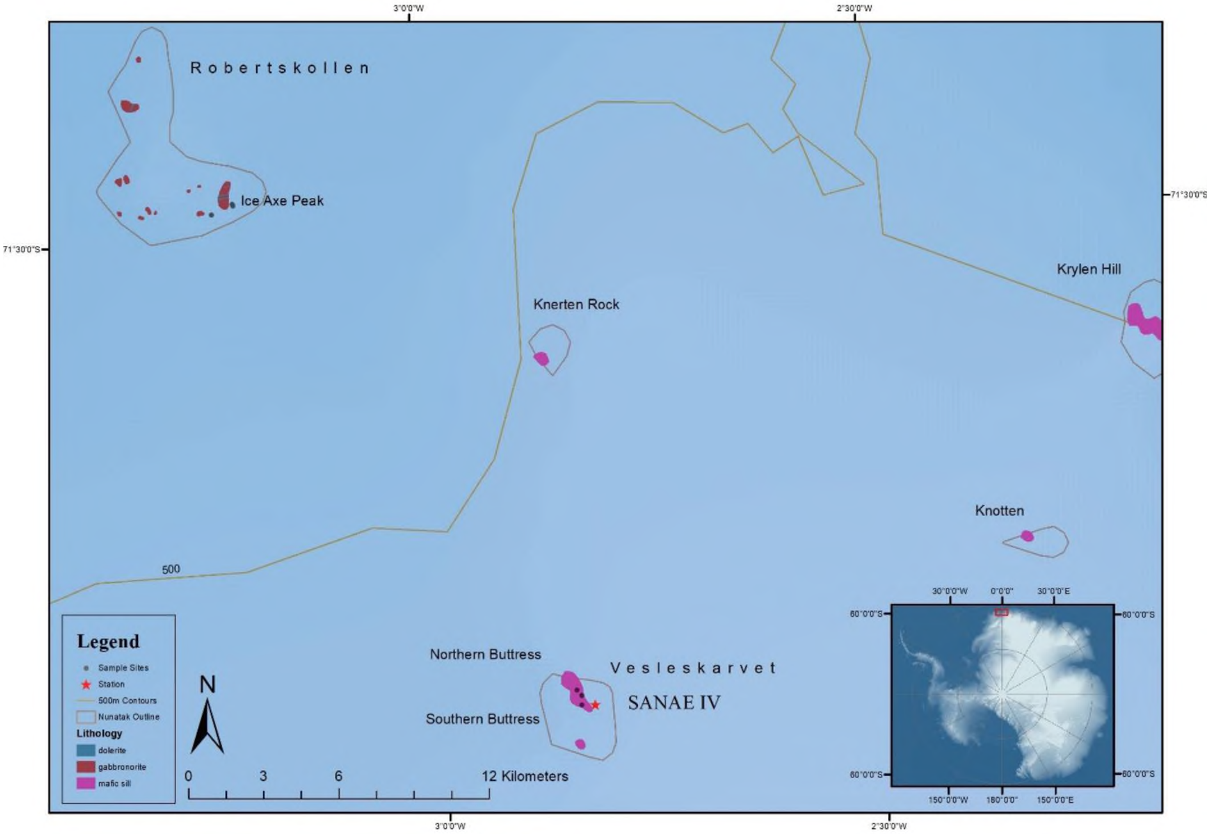

Figure 5.2.2: Lithology of study areas Robertskollen and Vesleskarvet. Based on data from O'Kennedy (2016)

Valterkulten and Lorentzenpiggen (Fig. 5.2.3) are dominated by Boreas dolerite and Borg metamafics (Neethling, 1969). These nunataks expose intrusions which are significantly different from the Borg intrusions (Roots, 1969). The Ahlmannryggen group on Nils Jorgennutane, Jekselen, Grunehogna and Schumacherfjellet are cut by small, irregular stock-like bodies and dikes of gabbro, syenite and diorite and named the Niles Syeno-diorite (Roots, 1969). Nunataks such as Grunehogna, Jekselen, Schumacherfjellet and Flårjuven display a formation called Nils red beds (Neethling, 1969). This formation is composed of red quartzo-feldspathic mudstone, separated by minor bands of pale sub-arkose (Neethling, 1964). The characteristics of this geology include intraformational mud-pebble conglomerates and rare marlstone being comprised of the lower 40m of the sedimentary sequence, especially on the Jekselen nunatak (Neethling, 1964).

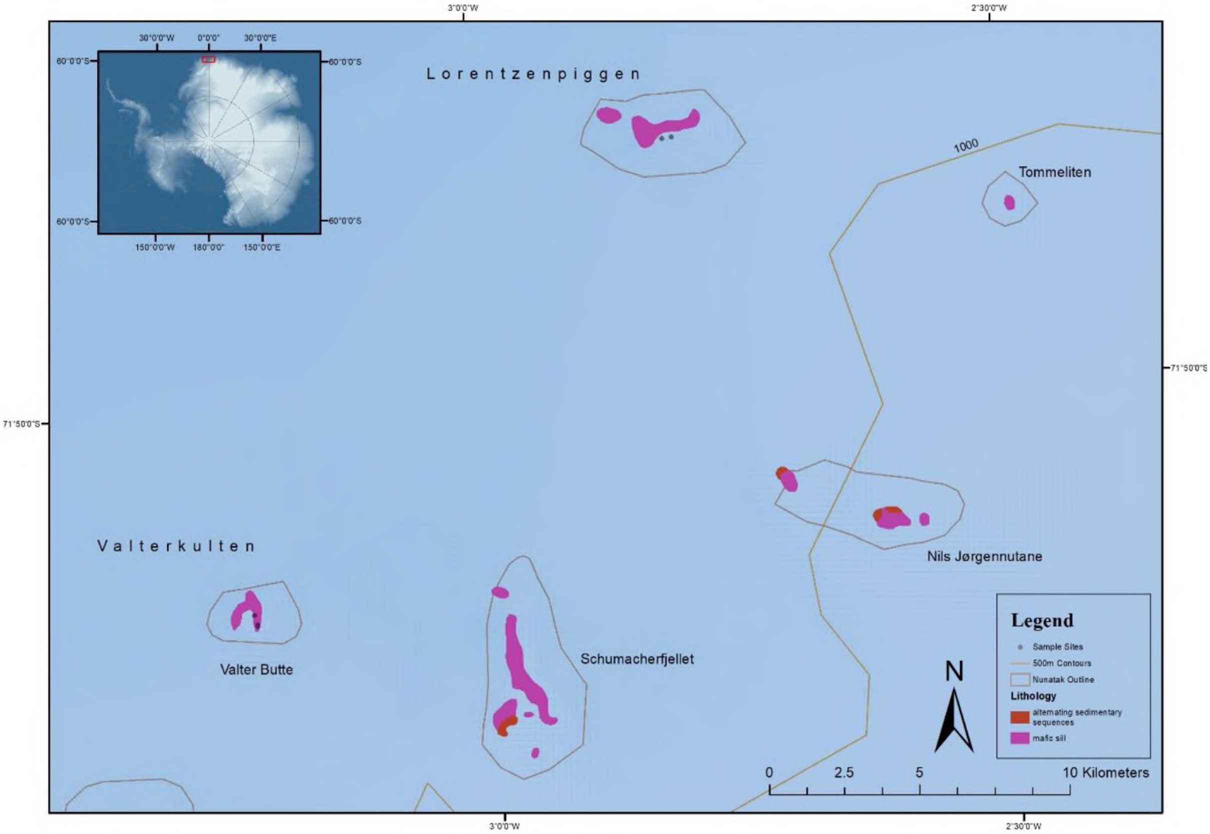

Figure 5.2.3: Lithology of Lorentzenpiggen and Valterkulten study areas. Based on data from O'Kennedy (2016)

Slettfjell (seen in Fig. 5.2.4) is comprised of Boreas dolerite and the Borg metamafics, while towards Aurho Peak a 60m wide aureole of contact metamorphosed sedimentary rocks occurs at the intersection of feeder dykes (Neethling, 1969). The remaining geology of the Grunehogna and Flårjuven areas is relatively more complex. Grunehogna is dominated by a lithology named

Grunehogna speckled arenite, which is comprised of impure feldspathic quartz arenite, is parted by minor bands of dark shale, occurring in domed and faulted outcrops at the Grunehogna and Schumacherfjellet Peaks (Neethling, 1964). According to Neethling (1969), a gradational contact with the underlying cyclic sedimentary rocks is apparently present in this rock sequence. The upper part of the sequence is more reddish in colour and is overlain at the Grunehogna Peaks by polymict jasper conglomerates (Langenegger, 1964). Flårjuven is characterised by the Jorgen Syeno-diorite geology, occurring as cross-cutting plugs and dike-like, irregular bodies in the Borg Grunehogna Peaks and Flårjuven Buff (Neethling, 1969). Irregular ferromagnesian enriched, schlieren-like bodies exhibiting linear parallelism of the hornblende and mafic intrusions are present as much as 30cm in diameter (Neethling, 1964).

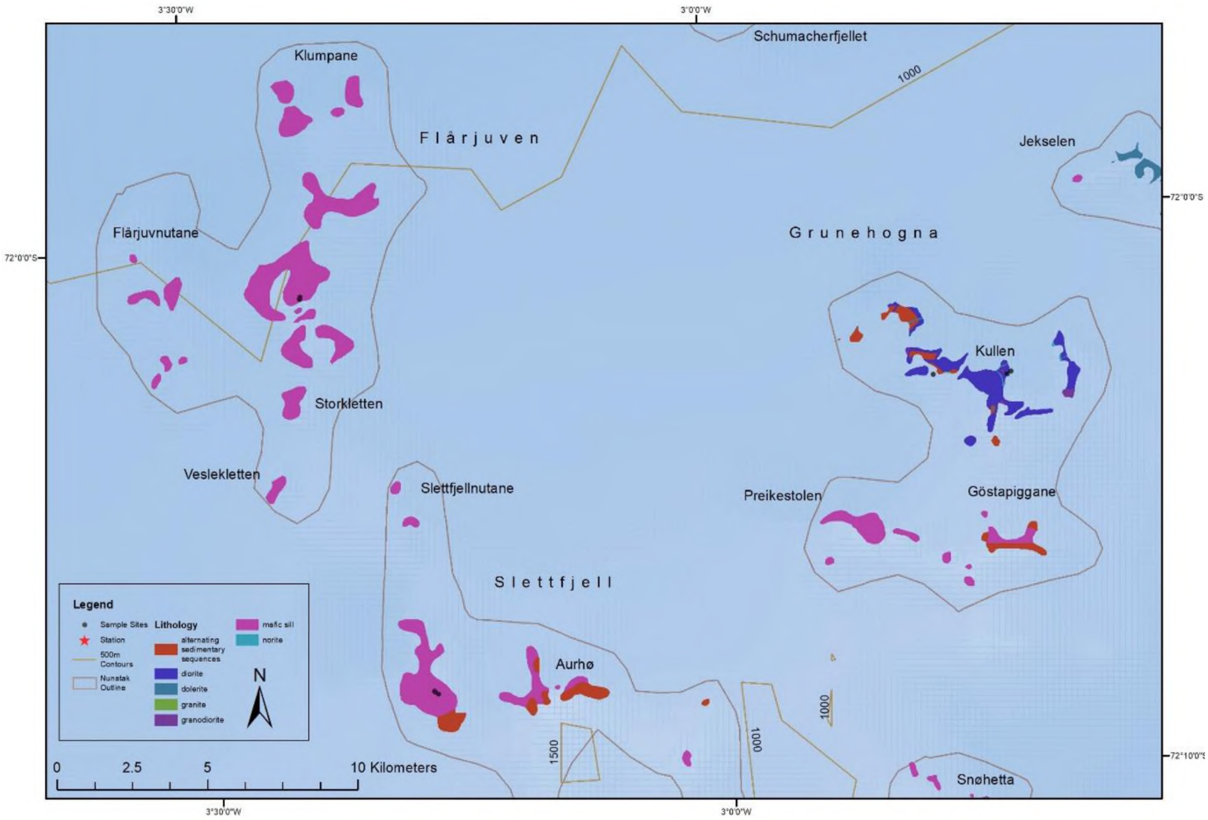

Figure 5.2.4: Lithology of Flårjuven, Grunehogna and Slettfjell study areas. Based on data from O'Kennedy (2016)

6. Methodology

In low air temperature regions, the measurement of chemical weathering can be through indirect means, such as through the analysis of river/stream solutes (Etienne, 2002). The analysis of dissolved materials in streams and soil water reflects the weathering and exchange processes that are active in an area, as well as the chemicals contained in precipitation (Anderson & Anderson, 2010). It is assumed that the solutes being tested are derived from chemical weathering of the parent material, indirectly measuring the denudation of the landscape (Pope *et al.*, 1995). Additionally, the control samples, allow for the chemicals present through precipitation to nullify, when compared to the water samples. Previous studies in Antarctica identified that bedrock weathering contributes to stream geochemistry through altering the chemical composition of the stream or standing water (Meiklejohn & Hall, 1997). The analysis of solutes is seen to provide a snapshot into the chemical processes which are present, and thus, allows one to determine if chemical weathering is occurring (Anderson & Anderson, 2010).

Analyses, such as the above, can also be direct such as through the use of rock samples, *in situ* experiments and microscopic observations of weathered samples/materials (Etienne, 2002). This type of analysis is of importance, as both the chemical and mechanical properties should both be considered in rock weathering (Oguchi, 2013). It is also important; however, to consider the environment in which the samples were taken, with this in mind opportunistic sampling occurred where possible. In rock weathering studies for example, thermal variability is influenced by both aspect and slope, especially in high latitudes (Hall *et al.*, 2002). Radiation regimes influence the extent of rock weathering, with variations resulting in changes to weathering processes (Hansen *et al.*, 2013). This is noticed in Antarctica, where North-facing rock surfaces experience higher temperatures than those facing South, as North-facing slopes in the Southern Hemisphere receive more direct rays (Hall *et al.*, 2002; Hansen *et al.*, 2013). Aspect must thus, be incorporated into the study with the FLIR camera experiment needing to take this into account (affects moisture availability) (Hall *et al.*, 2002; Hansen *et al.*, 2013).

6.1 Sampling procedure

Opportunistic sampling was undertaken for the majority of this thesis, due to the nature of the project and the terrain. Given that visible mineral precipitates are an indication of chemical weathering (the focus of this research), transects were run at each sample site when precipitates were located (Fig. 6.1.1). At each transect site, using a Garmin GPSMap 64S, a GPS point was taken as well as correlating photos, while both a rock and soil sample were taken, double bagged and labelled (Gibson *et al.*, 1983). Where visible precipitates were found, the dip angle and magnetic orientation were taken with a Brunton compass. The inputs and outputs of chemical weathering such as snow and water samples were taken next to (20-40cm) the site in question if there was snow or ice present, otherwise the closest snow/ice (within 1.5m) to the site was taken. A secondary, control sample was taken (>10m) away from each sample. Allowing for local variability to be captured and avoid sampling potentially anomalous points throughout the transect (Riebe *et al.*, 2004). Frozen snow/ice or liquid water samples were brought back to base and placed in the -20°C freezer, after which they were transported via ship in an -20°C freezer to South Africa for analysis (Gibson *et al.*, 1983). Upon arrival in South Africa, the samples were transported to Rhodes University via a dry ice cooler box and placed in the freezer in the Geography Department, where they were kept until further analysis was conducted.

Figure 6.1.1: Measurement of the extent of precipitation at Flåjuven, circles indicate precipitate samples and fine particles in the area, arrow showing the direction and extent of measurement, geopick for scale

6.2 Rock weathering

In order to help document and classify differences in weathering products at each site, sediment and particle size analysis was undertaken. This provided a means for documenting the differences in substrate weathering and the subsequent products thereof. Since the geology between sites is similar, it was expected that products of weathering would be representative as a whole. Differences between sites are, thus, likely to be caused by local conditions and relevant timing since deglaciation events.

6.2.1 Sediment analysis

6.2.1.1 Particle size analysis

A Endecott test-sieve sequence was arranged in order of decreasing mesh size, with the coarsest sieve size (4 mm) being at the top, with a base at the bottom, where material less than 0.063 mm collected (Briggs, 1977b). Individual samples were weighed to two decimal places, added to the top sieve, the lid secured and mechanically agitated for 15 minutes (Briggs, 1977b). The material within each sieve were weighed, documented and clearly labelled within zip-lock bags. The sediment in the base was, further dispensed into a separate labelled zip-lock bag, in order to differentiate the fines from the coarser particles. The recorded weight was then expressed as a percentage of initial sample weight and plotted as a cumulative percentage frequency curve (Briggs, 1977b). Recorded weights were analysed and classified according to the relevant Wentworth Grade (Table 6.2.1). Expressed as a function of cumulative percentage, producing a stacked bar chart for each sample.

6.2.1.1.1 Particle size statistical analysis

Particle size measurement is an integral sediment analysis technique, as it provides an understanding of the processes of transport and sediment deposition (Briggs, 1977b). Particle size analyses are used primarily in the classification and description of sediment deposits, typically displayed and arranged on an ordinal scale (Briggs, 1977b). An adapted size grade of sedimentary particles can be viewed in Table 6.2.1, a commonly accepted scale used by the Soil Survey of England and Wales (Briggs, 1977b). Numerous different scales of particle size can exist simultaneously, with the simple division of soils into categories such as clay, silt, and sand which, can be described as somewhat rudimentary, as this method is neither precise nor flexible (Briggs, 1977b).

Table 6.2.1 : Size grades of sedimentary particles (adapted from Briggs, 1977b)

Phi Size (ø)	Millimetres (mm)	Micrometres (µm)	Wentworth Grade
-2	4	4000	Fine Gravel
-1	2	2000	
0	1	1000	Coarse Sand
+1	0.5	500	Medium Sand
+2	0.25	250	
+3	0.125	125	Fine Sand
+4	0.063	63	
+5	<0.063	<63	Silt & Clay

The use of an ordinal scale, although effective as a descriptive means of classification, it is not suitable for detailed quantitative analysis (Briggs, 1977b). To circumvent this, a logarithmic scale called the Phi (ø) scale becomes of importance, expressing the particle size as the negative logarithm, to the base of two, of the diameter in millimetres (Briggs, 1977b):

$$\text{ø} = -\,log_2\, d$$

where d equals the diameter of the particle expressed in millimetres. Phi scale is a logarithmic transformation, which converts the data from a non-normal distribution into a normal distribution, normalising the data and making it suitable for statistical analysis (King, 1975; Briggs, 1977a).

Descriptive statistics are used to describe the particle size distribution, involving the calculation of diagnostic values known as size parameters (Briggs, 1977b). To attain these parameters the results of size analysis were plotted on a curve, giving the percentage coarser above each fixed value (phi size), resulting in an increase of phi units from left to right, plotting finer sediments at the right side of the curve (King, 1975). From this cumulative frequency plot, the values of significant percentage courser are able to be read directly off the graph and are known as percentile values, allowing the sediment to be described in terms of measures of central tendency, scatter and non-normality (sorting, kurtosis and skewness) (King, 1975; Briggs, 1977b). Measures of central tendency reflect the average particle size of the sample, while the latter describe the shape of the particle size distribution (Briggs, 1977b).

The following paragraphs describe in detail, the various equations and statistical methods used to determine measures of central tendency, scatter and non-normality of the samples. These measures include the phi mean, sorting, skewness and kurtosis of the samples.

i. Phi (ø) Mean

Typically, the mean locates the weighted central point in the distribution; however, the phi (ø) mean is the mean value of the logarithmic distribution, calculated from the phi values (Briggs, 1977b). The estimation of the mean value would involve summing all the particle phi values and dividing by the number of particles, with the use of a sieve stack however, this becomes almost impossible due to the high number of particles (Briggs, 1977b). For this method, the use of percentile values becomes appropriate, taken directly from the before mentioned cumulative frequency graph of particle size distribution (Briggs, 1977b). The size values for each percentile were read from the graph, summed and divided by the number of percentiles, as seen in the equation below (Briggs, 1977b):

$$D\bar{x} = \frac{ø25 + ø50 + ø75}{3}$$

importantly, this is the phi (ø) mean and can only be calculated from the values of the phi size.

ii. Phi (ø) Skewness

In a normal distribution the mean and median values are identical, if this is not the case and the distribution deviates from the normal, it is a non-normal distribution; with the difference in values being the measure of the degree of non-normality (Briggs, 1977b). The non-normality is apparent through a tendency towards asymmetry, the more asymmetrical the curve the greater the non-normality (Briggs, 1977b). For example, in the cumulative frequency graph of particle size distribution, this is produced through the deviation of the straight line, known as skewness (Briggs, 1977b). The evaluation of skewness from the particle size distribution were calculated as follows (King, 1975; Briggs, 1977b):

$$Sk = \frac{ø84 - ø50}{ø84 - ø16} - \frac{ø50 - ø10}{ø90 - ø10}$$

distributions are either negatively or positively skewed, negative represents a coarse tail while positive relates to a fine tail to the distribution. If skewness is positive the distribution is skewed towards higher phi values (finer particles), with negative skewness the distribution is skewed towards the lower phi values, or coarser particles (King, 1975).

iii. Phi (ø) Sorting

Sorting is the measure of scatter or dispersion and is an expression of the standard deviation of the size distribution (Briggs, 1977b). According to Briggs (1977b), very coarse or very fine sediments tend to have a high standard deviation (poorly sorted), whereas sands have a low standard deviation (are well sorted). The equation for sorting is as follows (Briggs, 1977b):

$$So = \frac{\text{ø}90 + \text{ø}80 + \text{ø}70 - \text{ø}30 - \text{ø}20 - \text{ø}10}{5.3}$$

with a high degree of sorting being represented by a low sorting value. The sorting of a sample is directly related to the ability of the sorting agent to separate its load according to size (Briggs, 1977b).

iv. Phi (ø) Kurtosis

Kurtosis measures the change in peak of the size distribution, indicating the average ratio of average spread of the tails of the distribution to the standard deviation (King, 1975; Briggs, 1977b). A poorly sorted sediment will have a relatively flat particle size distribution, it may differ from a normal distribution although showing no skewness (asymmetry) (Briggs, 1977b). Similarly, a well sorted sediment may have a peaked distribution in comparison to the normal curve (Briggs, 1977b). This calculation is below (Briggs, 1977b):

$$Kg = \frac{\text{ø}90 - \text{ø}10}{1.9\ (\text{ø}75 - \text{ø}25)}$$

the results are interpreted according to the peak of the distribution curve, a flatter than normal distribution curve is classified as platykurtic, one more peaked than normal is similarly classified as leptokurtic, while a normal distribution is classified as mesokurtic.

v. Bivariate Scattergrams

Bivariate scattergrams are graphs of any two size parameters (*e.g.* skewness and kurtosis), and are used in classifying and correlating sediments (Briggs, 1977b). The theory behind the use of these parameters states that processes of transport and deposition produce sediments with characteristic ranges of particle size distributions (Briggs, 1977b). The size parameters, are thus, indicative of the environments in which they are found and, as such, plots of skewness against kurtosis or mean phi size against sorting can distinguish sediments from different environments (Briggs, 1977b). Bivariate scattergrams were produced for the following parameters:

a. Phi mean against phi sorting,
b. skewness against kurtosis, and
c. phi mean against skewness.

vi. Spearman's Rank Correlation Coefficient

Although the use of bivariate scattergrams are of importance as a visual representation of the relationships between two parameters, it is often difficult to visually assess the degree of the relationship (Briggs, 1977b). A Spearman's rank correlation coefficient is, thus, used to investigate these relationships. The variables were ranked separately, in ascending order after which the difference between these values was determined, squared and summed using the following formula (Briggs, 1977b):

$$D^2 = (R1 - R2)^2$$

where R1 is the rank value of the first variable, R2 is the rank value of the second variable of the same sample. The values of D^2 were then summed (ΣD^2) and entered into the equation for calculating the Spearman's rank correlation coefficient (R_s) (Briggs, 1977b):

$$R_s = 1 - \frac{6\,X\,\Sigma D^2}{n^3 - n}$$

where n is the sample size. Values range from negative one (negative correlation) to positive one (positive correlation) while a zero value represents no correlation (Briggs, 1977b). The results simply reveal the strength and direction of the correlation, but, not if the relationship is statistically significant (Briggs, 1977b). Probability must, thus, be measured and a null hypothesis developed, one such method is the use of a table (Table 6.2.2) showing the critical values of R_s, but this is only applicable to small samples (Briggs, 1977b). To do this, a significance level is chosen (0.01 or 0.05) and the calculated value of R_s is entered into the table at the appropriate value of n (sample size) (Briggs, 1977b).

Table 6.2.2: Critical values of Spearman's rank correlation coefficient (R_s) (copied directly from Briggs, 1977b)

	Significance Level	
n	**0.05**	**0.01**
4	1.000	
5	0.900	1.000
6	0.829	0.943
7	0.714	0.893
8	0.643	0.833
9	0.600	0.783
10	0.564	0.746
12	0.506	0.712
14	0.456	0.645
16	0.425	0.601
18	0.399	0.564
20	0.377	0.534
22	0.359	0.508
24	0.343	0.485
26	0.329	0.465
28	0.317	0.448
30	0.306	0.432

vii. Student's t Test

Another approach is that of the Student's t test, typically used for samples of ten or more the formula for this can be found below (Briggs, 1977b):

$$t = R_s \sqrt{\frac{n-2}{1 - R_s^2}}$$

this value is compared with the critical values of a Student's t at a chosen significance level (0.01; only accepted as valid if it occurs by chance less than one case in a hundred) and for df (degrees of freedom) = n-2. The critical value was obtained from the Student's t table of critical values (Table 6.2.3), if the calculated value exceeded the critical value the null hypothesis was rejected, if it was less than the critical value the null hypothesis was accepted (Briggs, 1977b).

Table 6.2.3: Critical values of Student's t test (copied directly from Briggs, 1977b)

	Levels of significance			
df (n-2)	**0.10**	**0.05**	**0.02**	**0.01**
5	2.02	2.57	3.37	4.03
6	1.94	2.45	3.14	3.71
7	1.90	2.37	3.00	3.50
8	1.86	2.31	2.90	3.36
9	1.83	2.26	2.82	3.25
10	1.81	2.23	2.76	3.17
11	1.80	2.20	2.72	3.11
12	1.78	2.18	2.68	3.06
13	1.77	2.16	2.65	3.01
14	1.76	2.15	2.62	2.98
15	1.75	2.13	2.60	2.95
16	1.75	2.12	2.58	2.92
17	1.74	2.11	2.57	2.90
18	1.73	2.10	2.55	2.88
19	1.73	2.09	2.54	2.86
20	1.73	2.09	2.53	2.85
25	1.71	2.06	2.49	2.79
30	1.70	2.04	2.46	2.75
40	1.68	2.02	2.42	2.70
50	1.68	2.01	2.41	2.68
60	1.67	2.00	2.39	2.66
120	1.66	1.98	2.36	2.62
∞	1.65	1.96	2.33	2.58

6.2.1.2 Loss of moisture

Figure 6.2.1: **All wet samples placed in the drying oven**

The gravimetric method for measuring soil moisture was used as a means of measuring weight percentage loss (Brady, 1974). A known weight of a sample of moist soil (Fig. 6.2.1), was placed in the drying oven on melamine plates at a temperature of 105°C for 24 hours (Brady, 1974). After which, the sample was placed into a desiccator containing silica gel until cool and weighed again (Brady, 1974; Briggs, 1977a). The weights of samples before and after drying were recorded and the loss of moisture values calculated for each site.

The change in weight of the sample before and after, represents the soil moisture present in the soil sample (Brady, 1974; Briggs, 1977a). The percentage moisture content for each sample was acquired through the following equation (Briggs, 1977a):

$$\frac{(W1 \ - W2)}{W1} \times 100$$

where W1 equals the sample before drying and W2 equals the weight of the sample after drying. Then plotted as a function of percentage moisture loss, as a bar chart format for comparison between various sites.

6.2.2 Rock hardness

Rock hardness values provide an insight into the relative strength of a rock, and thus its degree of weathering (Aoki & Matsukura, 2007). When rocks undergo weathering their strength decreases, allowing for erosion to occur due to decreased resistance (Aoki & Matsukura, 2007). Both the Schmidt hammer and Equotip hardness tester provide rebound values which are indicative of the degree of weathering which has occurred (Aoki & Matsukura, 2007; Hansen *et al.*, 2013). Generally higher rebound values are indicative of less weathered material and rock which is less susceptible to weathering (Aoki & Matsukura, 2007). For weathering studies, the use of a Schmidt hammer has four positive aspects (Aoki & Matsukura, 2007):

i. portability and cost effectiveness,
ii. easy operation,
iii. convertible readings, and
iv. non-destructive.

There are issues with using the Schmidt hammer, however, these are namely, the high impact energy of the plunger and a large impact area (Aoki & Matsukura, 2007). An issue in using the Schmidt hammer is the effect of rock moisture as, moisture content is seen to decrease rebound values (Sumner & Nel, 2002). This becomes troublesome when comparing the state of weathering as the internal moisture environments may differ between sites, such as on different slopes (Sumner & Nel, 2002). In this thesis, however, the impact and availability is water is limited within the continental Antarctic environment. With the subsequent impact of moisture availability questioned.

The main problem with Schmidt hammer values is the influence of underlying properties within the sample rock (Aoki & Matsukura, 2007). Due to the high impact energy of the Schmidt hammer, the rebound values are influenced by the properties of minerals centimetres below the surface (Aoki & Matsukura, 2007). The problem arises when looking at fragile rock, or severely weathered rock as the plunger tip is likely to sink into the soft material and damage the sample, decreasing its applicability to heavily weathered material (Aoki & Matsukura, 2007).

Figure 6.2.2: An Equotip 3 D-Type (copied directly from Proceq, 2012)

In order to circumvent the issues with the Schmidt hammer, an Equotip hardness tester was used (Fig. 6.2.2). The Equotip is a small, hand held, electronic device which displays the impact and rebound velocities of a rock surface as a hardness value (L) on the display (Verwaal & Mulder, 1993; Hansen *et al.*, 2013). The rebound values provide a relative value of the compressive strength of the rock surface under investigation and are thus, an indicator of surface hardness and indirectly the susceptibility of a rocks surface to weathering (Hansen *et al.*, 2013). Essentially, the Equotip uses the same fundamental concepts as the Schmidt hammer, however, it uses a smaller impact energy and a smaller surface area to do so (Aoki & Matsukura, 2007). The Equotip, thus has applications when looking at heavily weathered materials over large distances (Aoki & Matsukura, 2007). The lower impact energy used by the Equotip has applications at the surface layer, in producing hardness values of a very thin layer and the subsequent weathering of a rock at surface level (Aoki & Matsukura, 2007). It is important to note, however, that the Equotip is not without its flaws, as surface roughness is one of these, exerting an influence on rebound values and weathering studies (Verwaal & Mulder, 1993).

For this study into chemical weathering, the Equotip 3 D-type hardness tester, produced by Proceq was used (Fig. 6.2.2) to determine rock hardness and subsequent weathering. For each rock surface, fifteen samples of single impact rebound testing occurred on each surface of the sample, the mean of the 15 readings was then expressed as the hardness number (L) (Verwaal & Mulder, 1993; Aoki & Matsukura, 2007). These measurements were recorded on selected rocks at selected sites, for example, rocks in a meltwater pool at Vesleskarvet and rocks 20m away. Single impact rebound testing was employed for this study as, with consecutive rebound testing the rebound values increase, reflecting compaction rather than weathering of the surface layer (Aoki & Matsukura, 2007). One individual was responsible for all rebound readings in order to decrease the likelihood of operator error and variation (Hansen *et al.*, 2013). The results of the rebound values were standardised, with all values below one standard deviation of each rock face being excluded from the study. This reasoning is in part due to values that are lower than one standard deviation of the sample being erroneous in nature and thus, are responsible for skewing the overall results.

6.2.3 Thermistors and FLIR camera

In order to accurately log the temperatures at the near-surface layer, ACR ET-004-GP series thermistor probes were used, in conjunction with an 8 channel ACR Smart Reader Plus 8, 1.5 MB memory data logger (Fig. 6.2.3), while older data is sourced from a 128 KB memory ACR Trend Reader data logger (Hall, 2003; Hall & André, 2003). Logger resolution was 0.2°C recording at intervals of 10 minutes, while the older loggers recorded at hourly intervals (Hall, 2003). The thermistors used in this study (Fig. 6.2.3) were cased in a stainless steel sheath, with a temperature recording range of -60°C – 55°C (ACR Systems Inc., 2016). The thermistor sensors were buried at the near-surface layer of the ground, and have been operational since 2013. It must be noted that this instrument is sensitive to incoming solar radiation but, not to short term, wind induced thermal fluctuations (Hall, 2003).

Figure 6.2.3: ACR Smart Reader Plus 8 and ACR ET-004-GP series thermistor probe (copied directly from ACR Systems Inc., 2016)

In Antarctic environments, rock thermal temperatures, in conjunction with near-surface rock zone monitoring has not been extensively studied in geomorphology, with limited knowledge into how these factors react to one another and in conjunction with each other (Hall & André, 2003). This directly leads to the use of a thermal imagery camera to determine rock temperatures, providing the basis for linking thermocouple near-surface data and actual rock temperatures.

This additional method, used in determining rock temperature, was the FLIR E8 series camera (Table 6.2.4), which takes spot measurements of infrared thermal imagery. This thermal imagery was recorded as both a high frequency data collection method and as an in situ method of temperature recording. The high frequency data were collected at two hourly intervals from 08h30 on 8 January 2017 until 06h30 on 9 January 2017 on the Vesleskarvet nunatak, Southern Buttress. *In situ* thermal imagery was collected at various other study sites, with particular attention being paid to areas where chemical precipitates were prevalent.

Table 6.2.4: Breakdown of FLIR E8 series specifications (adapted from FLIR Systems Inc., 2017)

Handheld FLIR E8	
Accuracy	±2% or 2°C
Thermal Sensitivity	<0.06°C
Emissivity Correction	Variable from 0.1 – 1.0
IR Resolution & MSX Resolution	320 × 240

The use of high frequency thermistor data (1 minute intervals), identifies the occurrence of an exotherm, indicative of water freezing, however, this is not an indicator of weathering per say (Hall, 2003). Due to the phase change of water within rock, an exotherm signal is produced, demonstrating that water, although frozen, is available for chemical weathering to occur (Hall, 2003). An exotherm is commonly described as the sudden, short term rise in rock temperature associated with the release of latent heat upon water freezing (Hall & André, 2003). In an Antarctic context, the high rock temperatures in conjunction with the presence of water allow for thermal conditions supportive of chemical weathering, for nearly six months of the year (Hall, 2003). This may extend further than this as sunlight hours change with the seasons. The relation between chemical weathering and other processes such as freeze thaw needs reconsidering at a synergistic level (Hall, 2003).

6.2.4 Thin sections

Chemical weathering either assists in the removal or addition of mass in solution, at a subsurface or surface level (Anderson & Anderson, 2010). At a subsurface level, minerals are connected through pore spacing and fractures within a rock, allowing chemical weathering to occur through the volume of said rock (Anderson & Anderson, 2010). The use of thin sections, thus, resulted in a detailed investigation of the weathering rinds and the change in rock properties throughout the rock surface (Oguchi, 2013).

Rocks, which were covered in precipitates and not able to be cut with the diamond saw, due to the use of water in the cutting process, were impregnated with resin in a vacuum. After the resin had set, the rocks were cut with the diamond saw, photographed and sent for thin sectioning (Hindshaw *et al.*, 2014). Thin sections were cut at a perpendicular orientation to the rock surface at depths of two centimetres, polished and varnished (Glasby *et al.*, 1981; Guglielmin *et al.*, 2005). This distance was chosen as it allows for the observed change of weathering between the rock surface and interior to be documented (Guglielmin *et al.*, 2005).

This analysis relied strongly on detailed petrographic analysis of thin sections under optical microscopes, from which the relationships between diagenetic products and their spatial links were assessed (Perrin *et al.*, 2014). Due to this, thin sections were analysed and photographed in both polarised and ordinary light (colour and black/white) under a petrographic microscope (Guglielmin *et al.*, 2005). The minerals were identified from optical properties in transmitted light (Perrin *et al.*, 2014).

6.2.5 Scanning Electron Microscopy (SEM)

The use of scanning electron microscopy (SEM) in geomorphology, permits the user to visually observe the effects, impacts and results of chemical weathering on a small scale, as well as the micro-topography of the mineral surface (Pope, 2013). At the mineral grain scale the processes of case hardening, rind formation, dissolution and micro-fracturing are apparent and quantifiable (Pope, 2013). The magnification used is variable and dependant on the surface texture and the size of the grain being examined (Goudie, 1990). In this thesis the Scanning Transmissive Electron Microscope (STEM), was used (TESCAN Vega TS 5136LM) with the Oxford Instruments silicon lithium detector (INCA PentaFETx3 series) Energy Dispersive Spectroscopy (EDS) system. A cobalt standard was used for peak calibration of the detector, maintaining a peak resolution better than 129 eV (MnKα) using a 30 mm^2 detector crystal. The STEM maintained a 20 kV acceleration potential, with a process time of ~5 and ~ 50-55% dead time of the detector, >300 000 counts per single point and small area analysis were recorded during 40-60 net seconds of data acquisition.

The EDS analyser is of importance as it examines the x-rays emitted by the specimen, producing a graph of the elemental composition of the sample, as such it is a semi-quantitative tool for elemental analysis (Goudie, 1990).

Coarse grains of weathering material from the thin section analysis were used for grain size analysis, followed by a coating of carbon to avoid artefacts (Glasby *et al.*, 1981; Borsato *et al.*, 2000; Guglielmin *et al.*, 2005). The carbon coated sample was viewed under a scanning electron microscope to observe mineralogy and chemical weathering changes (Guglielmin *et al.*, 2005). The resultant backscattered SEM images revealed varying, unambiguous, elemental compositions within the sample, and ubiquity of chemical weathering, where black areas symbolise micro-porosity from dissolution (Giovanoli *et al.*, 1988; Pope *et al.*, 1995). Magnification under which the samples were looked at varied between 44 – 800 times magnification, however, one has to be careful as, picture resolution decreases with increased magnification (Goudie, 1990). Mineral abundance was obtained through a combination of; point counting in thin sections and backscattered SEM images which reveal varying elemental compositions within the sample as well as element maps, which were electronically processed to remove background radiation (Giovanoli *et al.*, 1988; Hindshaw *et al.*, 2014). The elemental maps produced covered the zone from the internal to external structure of the thin section, whereby colour steps and apparent abundance indicated the relevant content of each element (Oguchi, 2013).

6.2.6 X-ray diffraction

X-ray diffraction (XRD), occurs using an X-ray diffractometer in order to analyse mineral identification, specifically the original rock forming minerals and clay minerals (Gibson *et al.*, 1983; Oguchi, 2013; Chiu & Ng, 2014). XRD, however, was omitted in this thesis, with Energy Dispersive Spectroscopy (EDS) rather providing this information. Elemental analyses were obtained using Energy Dispersive Spectrometry (EDS), providing a more quantitative measure of element composition and allowing for the user to select the region which is to be analysed. Allowing for smaller sections of rock to be analysed in detail. The use of EDS as opposed to XRD is also a much easier, cheaper and more readily available at Rhodes University, EDS in this regard, also allowed for relationships between minerals to be analysed as opposed to whole rock material in XRD.

6.3 Water/Soluble geochemistry

The use of water geochemistry or soluble geochemistry allowed for the inputs and outputs of chemical weathering to be assessed. The inputs consisted of the snow found in the surrounding area of the sample, while the outputs were comprised of the water/ice found in the region directly next to the sample. Inputs (precipitation) were assumed to be the norm for each nunatak, with differences attributed to local conditions. Outputs were directly compared with the inputs to determine changes in geochemistry, any changes that occurred were assumed to be products of chemical weathering processes.

6.3.1 Chemical analysis

Opportunistic sampling, where water or meltwater pools were present (Vesleskarvet, Robertskollen and Valterkulten) was conducted during the 2016-2017 summer season at all sites. All of the stream/meltwater pool/snow samples were collected in 250ml impermeable, polyethylene bottles, rinsed several times with distilled, deionised water in South Africa prior to sampling. In the field, the sample bottles were rinsed out with the sample twice before being filled (Green *et al.*, 1988; Borsato *et al.*, 2000). The samples were transported to base and stored in a -20°C freezer until the end of the season, thereafter, they were transported via a cooler box into a -20°C freezer on-board the SA Agulhas II. Samples were further transported via a cooler box filled with dry ice to the Geography Department, Rhodes University, South Africa. This, allowed for samples to be kept at relatively stable temperature conditions until examined, preventing any chemical reactions from taking place (Borsato *et al.*, 2000; Stumpf *et al.*, 2012).

Prior to analysis, the samples were removed from the -20°C freezer at Rhodes University and stored in refrigerated conditions allowing for thawing (Meiklejohn & Hall, 1997). Ten samples were decanted (25-30ml) into Falcon 50ml capacity, conical centrifuge tubes, labelled and stored upright, until sent to *V&M Analytical Toxicology Laboratory Services (Pty) Ltd* an ISO17025 accredited testing laboratory (*T0610*), in George for semi-quantitative ICP – MS analysis. The accuracy of this technique with regard to concentrations (solubility), of samples were within 30% or better for unknown samples.

Statistical testing of the geochemistry samples was conducted using a multivariate analysis, to assess the geochemistry at each site and discover which sites are most dissimilar or similar (McKillup & Dyar, 2010). In order to do this, the multivariate data (elemental concentrations) needed to be simplified and summarised, reducing the number of variables is one such way to do this (McKillup & Dyar, 2010).

In doing so, the elements which have the most influence among the samples needed to be identified and the relationships among the sample units summarised and hence, visualised more effortlessly (McKillup & Dyar, 2010).

Principal components analysis (PCA) is one method of doing this, as it uses cases of redundancy (two or more highly correlated variables) to reduce the number of variables, but, does not exclude them (McKillup & Dyar, 2010). Instead, PCA identifies highly correlated variables and combines them to construct a reduced set of new variables, which still describe the differences among samples; these are called principal components (McKillup & Dyar, 2010). These principal components are listed in decreasing order of importance, beginning with the one which explains the greatest variation among sampling units (McKillup & Dyar, 2010). The two or more axes which are constructed are called eigenvectors and the relative length of each is the eigenvalue, upon which the longest eigenvalue becomes the principal axis and is named principal component 1 (PC1) (McKillup & Dyar, 2010). The following components are independent and uncorrelated with PC1, named in consecutive order (PC2, PC3, PC4) (McKillup & Dyar, 2010). Eigenvalues of 1.0 or less were excluded, as this is the level of variation expected by chance, when there is no correlation among variables (McKillup & Dyar, 2010). Generally, if the first two or three principal components explain more than 70% of the variation among sampling units, then the analysis will produce a plot which is reasonably realistic (McKillup & Dyar, 2010).

In addition to stream samples, pH and electrical conductivity was measured at Rhodes University, Geography Department laboratories, due to the adverse conditions found in the field. A Eutech Con 700 electrical conductivity meter, identified the electrical conductivity (EC) of the samples, while a Eutech pH 700 meter, determined the pH of samples. The instruments were calibrated before use and rinsed with distilled ionised water, following this automatic calibration of known ion concentrations or pH values for each instrument respectively were acquired. Before each subsequent sample, distilled, deionised water rinsed the probes of both instruments, followed by a dab dry with paper towel. Approximately 30ml of sample were decanted into sterile, glass beakers, followed by testing for pH and EC with each instrument

6.3.2 Additional considerations

I have read and understood the Rhodes University Field Worker Safety Guidelines and have followed them, where applicable (Rhodes University, 2016b). I have also read and understood the Rhodes University Ethics Guidelines and have adhered to all precautions as stated (Rhodes University, 2016a).

7. Results and Discussion

7.1 Sediment analysis

The following sections of this thesis were designed as a combined results and discussion section in order for the reader to quantify the differences between results more efficiently and effectively. The first section attempts to analyse and link the differences of soil particle size and distribution between sites, as a means of quantifying soil formation at a substrate level.

7.1.1 Particle size analysis

Throughout all the samples in Fig. 7.1.1, fine gravel was the highest total proportion of the sediment types, while medium sand was the next most abundant sediment type. Interestingly in the case of Valterkulten (sites J12 H2O, J12 edge and J13), the next highest proportion of sediment after fine gravel, was that of coarse sand as opposed to medium sand as found at the other sites. Coarse sand was found to be the second highest proportion of sediment (excluding J12 and J13), followed by fine sand, with coarse silt and clay being the least abundant. Valterkulten sites J12 H2O (in the water) and J12 edge (0m) had almost no coarse silt and clay sediments, while J13 (3.52m) followed a similar trend, with a very low proportion occurring.

Overall, a pattern was identified where samples consisted primarily of fine gravel, medium sand, coarse sand and fine sand with the lowest proportions of sediment being coarse silt and clay. These results link to the limited production of fine-grained material in polar (cold based) glacial environments, which are typically ineffective at basal erosion and subsequent limited sediment production during deglaciation processes (Stumpf *et al.*, 2012; Marra *et al.*, 2015). This is due to these glaciers remaining at sub-freezing temperatures (-20°C), where no basal melt occurs and are subsequently frozen to the underlying rock substrate (Chinn, 1994; Stumpf *et al.*, 2012; Atkins, 2014; Marra *et al.*, 2015). As such, polar glaciers have little influence on the production of fresh, fine grained materials for silicate weathering (Stumpf *et al.*, 2012; Marra *et al.*, 2015).

The influence of deglaciation is thus, seen in Fig. 7.1.1, where a lack of fine-grained material, such as course silt and clay occurred throughout the sites. This lack of fine material relates to the amount of time since deglaciation, sites that have been recently deglaciated portray smaller amounts of fine materials in comparison to those that experienced deglaciation in the past. For example at Valterkulten, JV123 has a larger proportion of fine-grained sediment (fine sand, course silt and clay) than J12 H2O, J12 edge and J13. Considering the area where these sediments were sampled, JV123 was on the very top of the nunatak, while the remaining samples were found within the basin like structure at Valterkulten. As such, as the polar glacier melted and subsequent basal sliding occurred, the top of the nunatak would have deglaciated first.

Samples with a high proportion of fine gravel tend to have the lowest proportions of coarse silt and clay, such as Slettfjell (001J) and Valterkulten (J12 H2O, J12 edge). In the case of the Valterkulten sites (J12 H2O, J12 edge, J13 and JV123), the proportion of coarse silt and clay increased with distance from the meltwater pool. The increase of fine material away from the pool is linked to the dissolution of fine-grained materials (more chemically reactive by mass/volume) within the meltwater pool (increased sediment surface area), whereby fine grained materials are deposited in excess, due to the glacial movement downslope (Marra *et al.*, 2017). As water levels in the meltwater pool increased, further fine particles undergo dissolution, until the meltwater pool reached maximum water capacity, resulting in higher quantities of fine particles further away from the meltwater pool, as seen in Fig. 7.1.1.

Slettfjell (001J and 002J), Fig. 7.1.1 displayed varying soil compositions, where 001J obtained more fine gravel, while 002J, contained higher proportions of the remaining soil composition types. An influence on the difference in amount of sediment present at each site, likely occurs due to the wind patterns which this site experiences. Variable wind patterns occur throughout the year, and are said to influence the redistribution of sediment and organic particle matter (such as lichen) (Sabacka *et al.*, 2012; Fortner *et al.*, 2013; Marra *et al.*, 2014; Marra *et al.*, 2015). Sediment then becomes trapped on glaciated surfaces, and reintegrated into the environment during summer melt (Sabacka *et al.*, 2012; Fortner *et al.*, 2013; Marra *et al.*, 2014; Marra *et al.*, 2015).

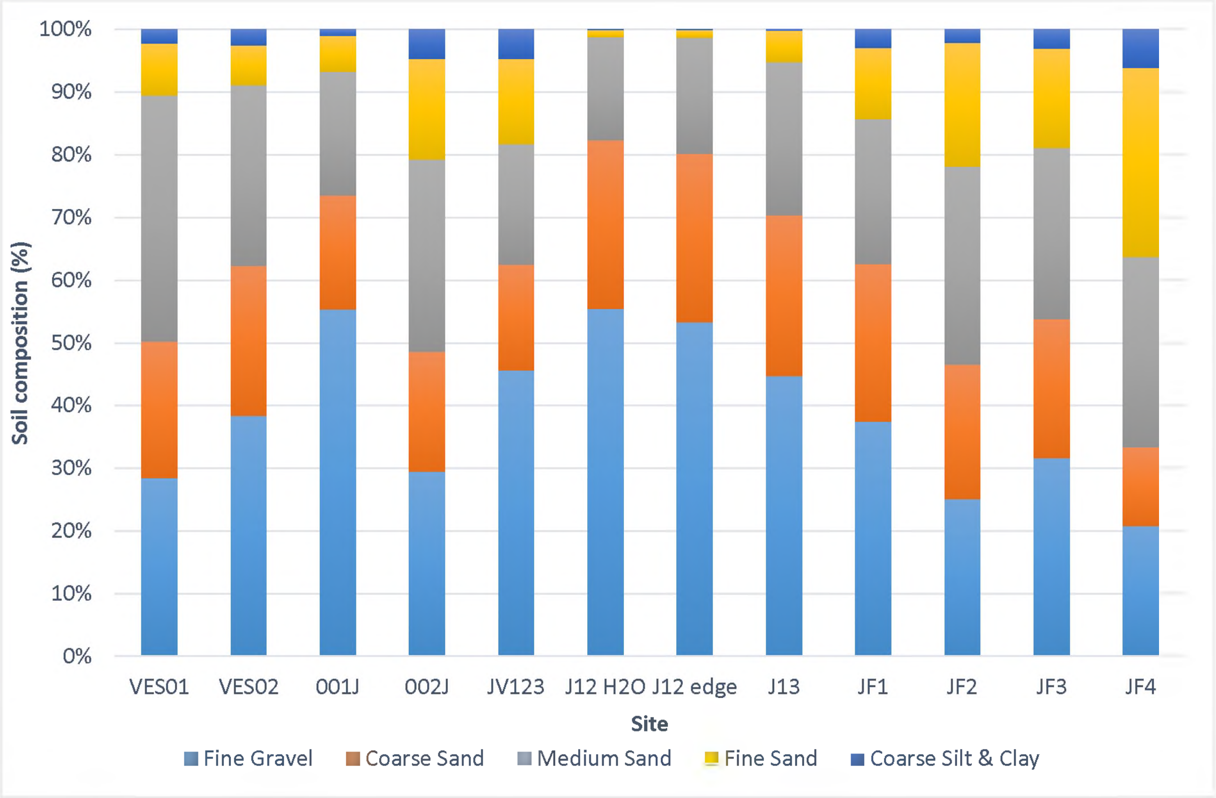

Figure 7.1.1: Stacked Wentworth grade results

Samples (Fig. 7.1.2) that displayed a rapidly increasing curve (high cumulative percentage with low phi size), consisted of a higher proportion of coarse sediments than fine. Similarly, samples which displayed a low curve (low cumulative percentage with a low phi size), had a higher proportion of fine sediment than coarse. While samples found in the middle range (uniform increase in cumulative percentage and phi size), displayed an even distribution of coarse and fine sediment (*e.g.* Vesleskarvet, VES01). VES01 showed the common s-shaped curve, expected for a normal distribution of particles. Two samples exhibit curves lower than the VES01 sample for the entirety of the graph, these being from the Flårjuven sites, JF2 and JF4 respectively. One other sample crossed the central threshold before the 50% mark, Slettfjell (002J), while Flårjuven (JF1, JF3) and Valterkulten (JV123) all fall below the s-shaped curve after the 50% mark. The remaining five samples were above the s-shaped curve for the entire duration of the cumulative frequency curve. The curves furthest away were those of Valterkulten (J12 H2O and J12 edge), displaying a curve almost identical to that of Valterkulten (J13), but at a higher displacement.

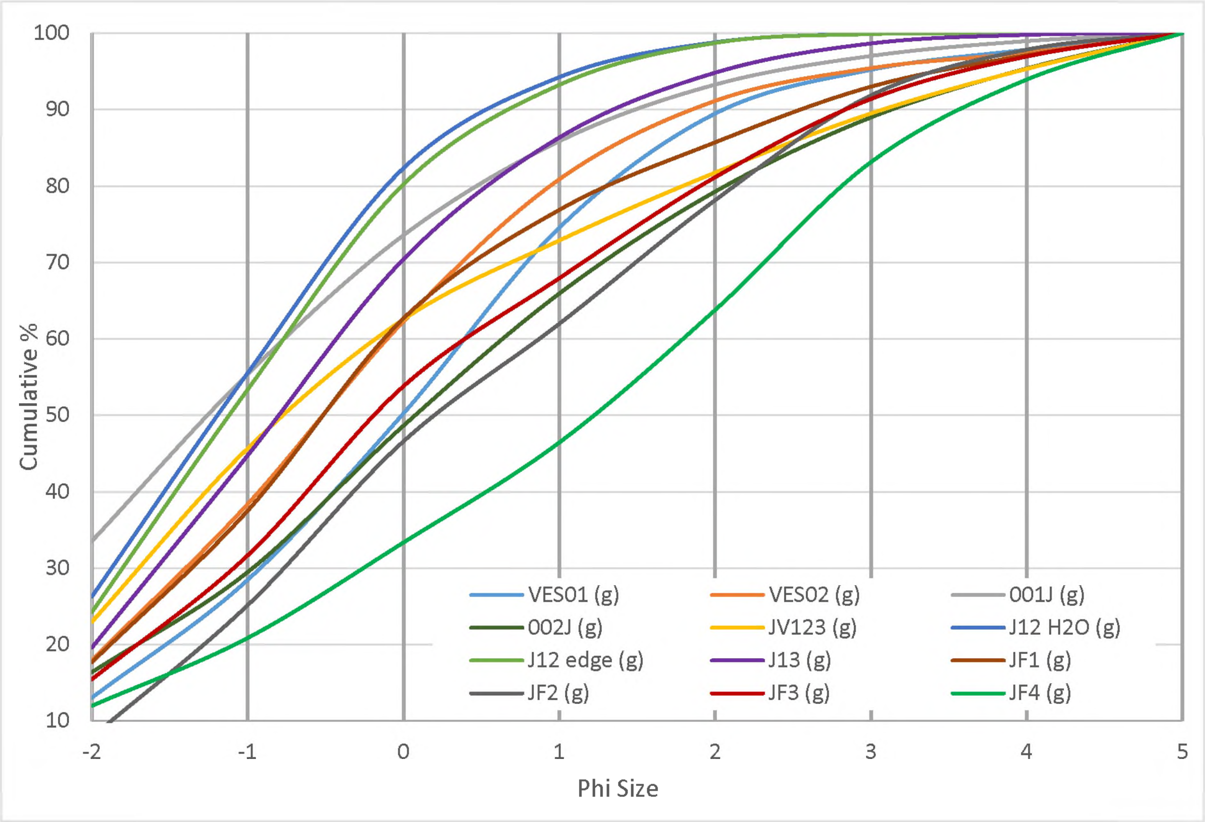

Figure 7.1.2: Cumulative percentage frequency curve

7.1.2 Particle size statistical analysis

Mean phi size (Table 7.1.1) or, estimated average grain size, was found to be the highest (largest grain size) in the samples from Valterkulten (-2.6 phi size), in particular those of J12 H2O and J12 edge. The lowest average grain size was found in samples from Flårjuven (0.72 phi size), in particular the values of 3.2 and 1 found at JF4 and JF2 respectively. In regards to Slettfjell and Vesleskarvet N. Buttress, the former has a larger average grain size (-1.35 phi size), with higher negative values, while the latter consisted of a smaller average grain size (-0.8 phi size).

Only one sample was found to be negatively skewed, that of JF4 (-0.18) from Flårjuven (Table 7.1.1). Negative skewness values display a coarse tail to the distribution, indicating a larger amount of coarse material in the sample than expected in a normal distribution (Briggs, 1977b). Two sites were found to be symmetrical in nature, those of Flårjuven, JF2 (0.09) and Vesleskarvet, VES01 (-0.06). Two sites were found to be very positively skewed, Slettfjell, 001J (0.56) and Valterkulten, JV123 (0.48), the remaining samples were found to be positively skewed. Positive skewness is a representation of a fine tailed distribution and is characterised by greater amounts of fine material occurring than would be expected in a normal distribution (Briggs, 1977b). The positive skewness of the majority of the samples, display a trend where greater amounts of fine particles occur than expected in comparison to the normal distribution of the sediment.

Four of the samples were very poorly sorted (Table 7.1.1); they contained values, which were found in the 2.00-4.00 category (Table 7.1.2) these being Flårjuven (JF3, JF4), Slettfjell (002J) and Valterkulten (JV123). The highest sorting value found was that of Flårjuven, JF4 (2.28) while the lowest sorting value was that of Valterkulten, J12 H2O (1.09). The remaining samples demonstrated lower sorting values, falling into the category of poorly sorted (Table 7.1.2). All the samples can thus be described as being representative of either a very coarse or very fine sediment deposits. This was related to the poorly sorted nature found throughout (Briggs, 1977b). The sorting value of a sample is directly related to the ability of the transporting agent to segregate load (Briggs, 1977b). In this case, the sorting processes is comparatively inefficient, due to the poorly sorted nature of the sediments, typical of glacial environments (Briggs, 1977b).

From Table 7.1.1, the majority of the samples were in the platykurtic (0.67-0.90) (Table 7.1.2) range. The classification of platykurtic was indicative of the samples following a distribution curve flatter than the normal distribution (Briggs, 1977b). The dominance of platykurtic distributions, indicated poorly sorted sediment due to the relatively flat particle size distribution (Briggs, 1977b). The samples that did not follow the same pattern are those of Vesleskarvet (VES01), and Flårjuven (JF1, JF4), which displayed mesokurtic distributions also known as normal distributions (Briggs, 1977b).

Overall, the majority of samples were found to display a positive skewness, comprising of finer sedimentary material than was expected, in comparison to the normal distribution of sediment. All the samples were very poorly sorted, or poorly sorted, indicating very fine sediment or very coarse sediment types throughout the sites. In terms of kurtosis, the samples displayed platykurtic distributions and normal distributions, that indicated poorly sorted sediments.

Table 7.1.1: Particle size descriptive statistics for various samples

	Vesleskarvet Northern Buttress		**Slettfjell**		**Valterkulten**				**Flårjuven**			
Statistical Test	**VES 01**	**VES 02**	**001J**	**002J**	**JV 123**	**J12 H2O**	**J12 Edge**	**J13**	**JF1**	**JF2**	**JF3**	**JF4**
Mean	-0.2	-1.4	-3.2	0.5	-1.4	-3.5	-3.3	-2.3	-1.2	1	-0.1	3.2
Skewness	-0.06	0.15	0.56	0.17	0.48	0.30	0.26	0.21	0.27	0.09	0.21	-0.18
Sorting	1.60	1.58	1.47	2.11	2.11	1.09	1.15	1.40	1.81	1.98	2.02	2.28
Kurtosis	0.96	0.87	0.88	0.89	0.82	0.77	0.79	0.83	0.95	0.88	0.87	0.92

Table 7.1.2: Descriptive terms for sorting, kurtosis and skewness (measured on phi scale), (copied directly from Briggs, 1977b)

Sorting		Kurtosis		Skewness	
Very well sorted	<0.35	Very platykurtic	< 0.67	Very negatively skewed	-1.0 – -0.3
Well sorted	0.35 – 0.50	Platykurtic	0.67 – 0.90	Negatively skewed	-0.3 – -0.1
Moderately well sorted	0.50 – 0.70	Mesokurtic	0.90 – 1.11	Symmetrical	-0.1 – 0.1
Moderately sorted	0.70 – 1.00	Leptokurtic	1.11 – 1.50	Positively skewed	0.1 – 0.3
Poorly sorted	1.00 – 2.00	Very leptokurtic	1.50 – 3.00	Very positively skewed	0.3 – 1.0
Very poorly sorted	2.00 – 4.00	Extremely leptokurtic	> 3.00		
Extremely poorly sorted	> 4.00				

The association between sorting and mean phi size is displayed in Fig. 7.1.3, with a correlation co-efficient of 0.72 for the samples. Sorting values increased with phi mean, displaying a decrease in sorting (a high degree of sorting is represented by a low sorting value) with increased phi size (Briggs, 1977b). As such, through the process of sorting, sediments were characterised as poorly sorted (such as sands). Samples that displayed high proportions of fine sediments were found in the lower left hand corner of the graph. The degree of sorting is dependent on the method of transport for the sediment, with sorting being said to improve with transport (King, 1975), but, this can be partly attributed to the decrease in the size of the particles with transport.

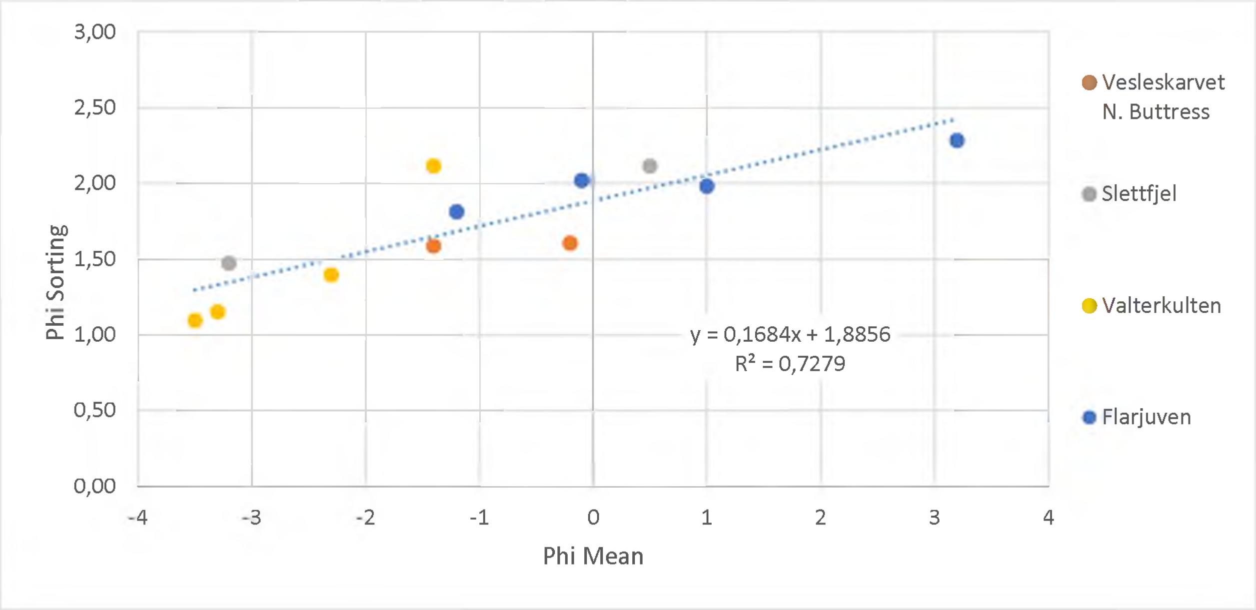

Figure 7.1.3: Bivariate scattergram of mean phi size and sorting for all sample sites

Spearman's rank correlation co-efficient values for evaluating the relationship of phi mean and sorting were displayed in Table 7.1.3. This was undertaken to determine whether there is a relationship between particle size (phi mean) and the sorting of these sediments. The Spearman's rank correlation co-efficient displayed a value of 0.89, a strong positive correlation (Briggs, 1977b). The null hypothesis, states that there is no relationship between the two variables and that the previous result, was one of chance, thus, needed to be tested. The Spearman's correlation co-efficient value (0.89) was rejected at the 0.01 significance level (Table 6.2.3), as it exceeded the critical value. A value of 6.22 was returned (Table 7.1.3), for the Student's t-test and was also rejected at the 0.01 significance level (Table 6.2.3). Since the Student's t-test value was exceeded the critical value, the null hypothesis was rejected, and the relationship shown by the Spearman's correlation co-efficient was seen as valid (Briggs, 1977b). From this result, there is a relationship between mean phi size and sorting, meaning that as phi size increases so does the sorting value.

Table 7.1.3: Summary of Spearman's rank correlation co-efficient and Student's T Test for mean phi size against sorting

	Rank Mean	Rank Sorting	D^2
VES01	8	6	4
VES02	5	5	0
001J	3	4	1
002J	10	10	0
JV123	6	10	16
J12 H2O	1	1	0
J12 Edge	2	2	0
J13	4	3	1
JF1	7	7	0
JF2	11	8	9
JF3	9	9	0
JF4	12	12	0
		ΣD^2	31

$$\boldsymbol{R_s = 1 - \frac{6\,X\,31}{12^3 - 12} =}$$

0.891608392

$$t = 0.891608392\sqrt{\frac{12-2}{1-\ 0.891608392^2}} = 6.226739556$$

The comparison of skewness and kurtosis distributions (Fig. 7.1.4) showed a relatively weak relationship, seen through the very low R^2 value (0.24). A common trend was the decrease in kurtosis with increasing skewness, depicted by the gradient of the trend line. Interestingly, a few points were relatively close to the trend line, these being predominantly samples from Flårjuven, while one sample from Valterkulten and Vesleskarvet, Northern Buttress respectively, display these features. The majority of the samples from Fig. 7.1.2, displayed positive skewness values, representing a fine tail to the distribution of particles, comprised of finer particles (King, 1975; Briggs, 1977b). Overall, the kurtosis values indicated a mesokurtic and platykurtic distribution throughout the samples, showing a relatively normal to poorly sorted sediment respectively (Briggs, 1977b).

The prominence of very high kurtosis values suggested that one type of material was sorted in a region of high energy, and transported without change of character to another environment, where it was further mixed with another sediment in equilibrium, under different conditions, possibly of lower energy than the first (King, 1975). For example, Fig. 7.1.4 consists of uniform sorting throughout the distribution, indicated by the lines drawn around relative sample points; certain samples have attributes, which makes them easy to distinguish from others. These size parameters (Fig. 7.1.4) are diagnostic of the environment, not singularly as distributions can overlap, but, in combination, allowing one to distinguish sediments from different environments (Briggs, 1977b; King, 1975). Although this is plausible, it is more likely that the very high kurtosis values are indicative of rocks of the same lithology weathering at the same rate.

In particular, Valterkulten displayed a trend whereby, the skewness values decreased and kurtosis values increased with distance from the melt pool. The highest skewness value (0.3) with lowest kurtosis value (0.77) was the sample taken in the melt pool, while the sample at the water's edge contained a value of 0.26 and 0.79 for skewness and kurtosis respectfully. The sample furthest away from the water's edge along the same transect, was the sample with the lowest skewness value and highest kurtosis value (0.12; 0.83). One of the possible reasons behind this trend could be the possible sediment type. In particular, where sediment was sorted in a high energy environment (0.12; 0.83) and transported by melting snow into the meltwater pool, whereby it became mixed with sediment of a finer grade and settled under quiet conditions (King, 1975). If both parts of sediment (fine and coarse) had been well sorted before mixing, there would be a very high kurtosis value and if the finer particles were in excess the sample would be positively skewed (King, 1975), which these particular samples are (Table 7.1.4).

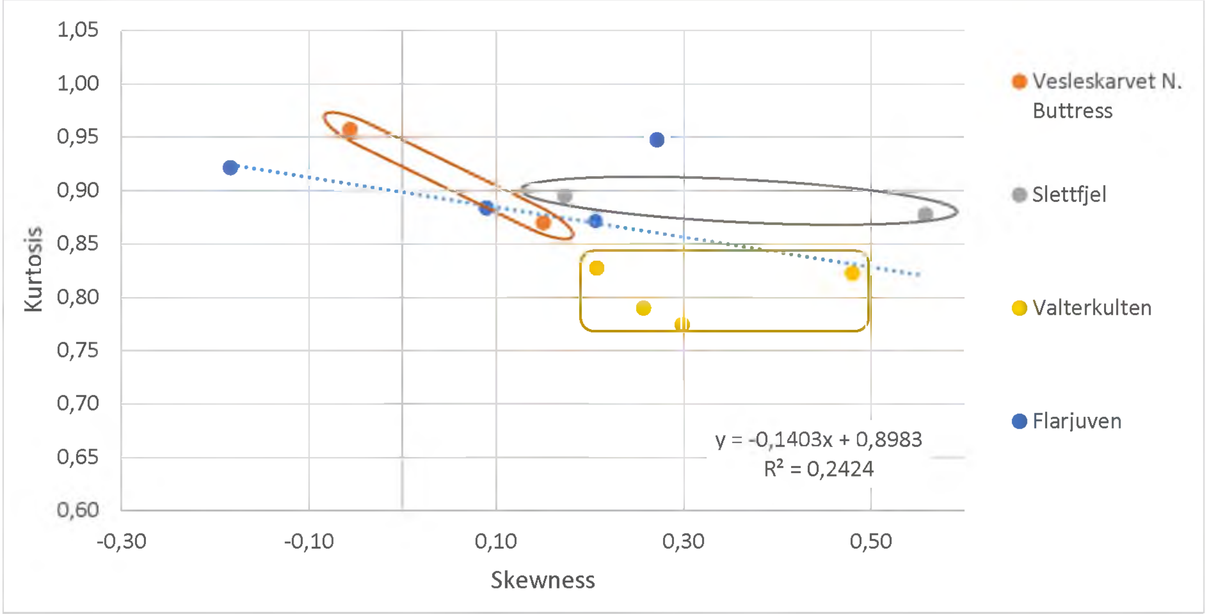

Figure 7.1.4: Bivariate scattergram of skewness and kurtosis

Spearman's correlation coefficient values for investigating the relationship between skewness and kurtosis occur in Table 7.1.4. This test aimed to determine whether there was a relationship between skewness (distribution of fine material) and kurtosis (sorting of the distribution) for the various samples (Briggs, 1977b). A result of 0.54 displayed a positive correlation, although not a particularly strong one. The null hypothesis for the Student's t-test was, thus, that there is no relationship between the two variables and that the previous result, was one of chance, and needs to be tested. The Spearman's correlation co-efficient value (0.54) was accepted at the 0.01 significance level (Table 6.2.3), as it is less than the critical value. In terms of the Student's t-test, a value of -2.05 (Table 7.1.4) was returned and when tested at the 0.01 significance level (Table 6.2.3), provided a result which was less than the critical value, and the null hypothesis was accepted. The relationship investigated in the Spearman's rank correlation coefficient was thus, seen as not valid, and that no relationship exists statistically between skewness and kurtosis for the samples.

Table 7.1.4: Summary of Spearman's rank correlation coefficient and Student's T Test for skewness against kurtosis

	Rank Skewness	Rank Kurtosis	D^2
VES01	2	12	100
VES02	4	5	1
001J	12	7	25
002J	5	9	16
JV123	11	3	64
J12 H2O	10	1	81
J12 Edge	8	2	36
J13	7	4	9
JF1	9	11	4
JF2	3	8	25
JF3	6	6	0
JF4	1	10	81
		ΣD^2	442

$$R_s = 1 - \frac{6 \, X \, 442}{12^3 - 12} = -0.54545455$$

$$t = -0.54545455 \sqrt{\frac{12 - 2}{1 - -0.54545455^2}} = -2.057983022$$

Mean phi size increased with decreasing skewness from Fig. 7.1.5, with the trend line displaying a similar decrease. A correlation coefficient of 0.56 was identified from the trend line, displaying a positive correlation, although relatively weak. In terms of fit, none of the samples were found to be very close to the trend line, with the distribution of samples being relatively similar on either side. No apparent predisposition was noted for any of the samples in terms of distribution. The relation between skewness and phi mean, was linked through the finer particles being found towards higher phi mean values, but in the positive skewness range, while coarser particles were found in negative skewness ranges and at lower phi mean sizes (below the black line). The dominance of samples in the top left corner of Fig. 7.1.5, displayed high proportions of fine particles (high positive skewness values) in low phi mean sizes. Indicating that more fine particles were found in these phi mean sizes than expected, in comparison with the normal distribution of particles, with coarser particles transported relatively less effortlessly in these environments (King, 1975). An outlier was noticed for Flårjuven, where the skewness was negative and the phi mean high, this may be an issue with non-normality and higher than usual asymmetry within the sample (Briggs, 1977b).

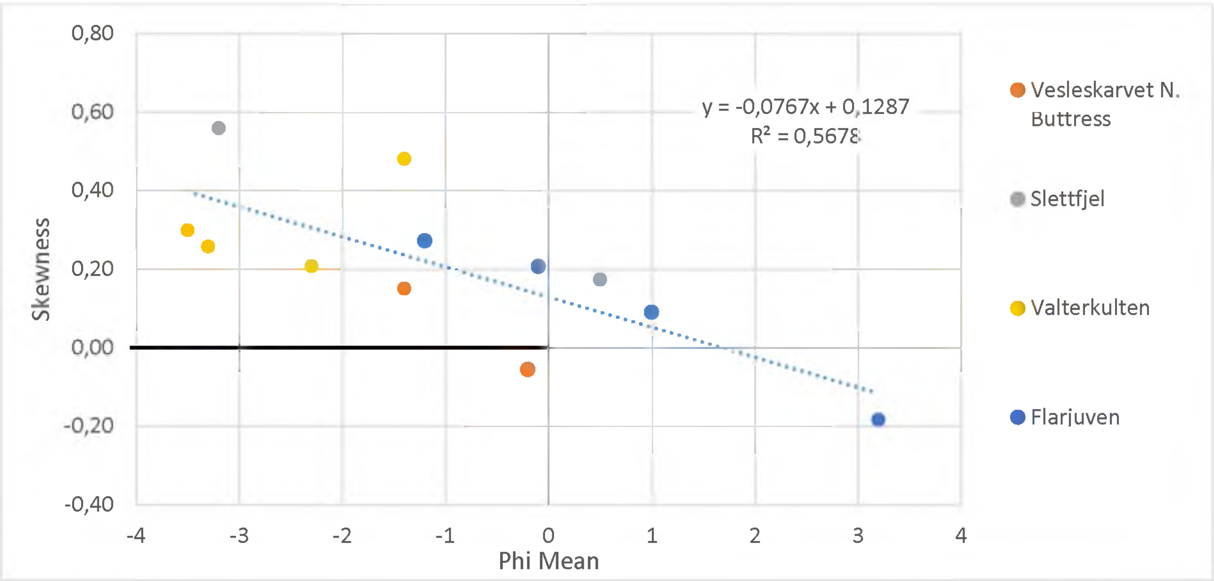

Figure 7.1.5: Bivariate scattergram of mean phi size and skewness

The relationship between mean phi size and skewness was tested by means of Spearman's rank correlation coefficient and Student's t-test. Particle size (phi mean) and distribution of fine particles (skewness), was tested in Table 7.1.6, showing a correlation coefficient of 0.72, a positive correlation, and relatively strong. The null hypothesis stated that there is no relationship between the two variables and that the result, was one of chance, needed to be tested. The 0.72 Spearman's value was larger than the critical value of 0.712 and as such, the null hypothesis was rejected. A Student's t-test value of -3.28 was returned which was also higher than the critical value of 3.17 (Table 6.2.3) although negatively correlated, the null hypothesis was rejected and the relationship between mean phi size and skewness seen as valid. The correlation was, hence, seen as negative, due to the result from the Student's t-test and the gradient of the trend line from Fig. 7.1.5. A negative correlation displays a relationship whereby, a small rise in one variable causes a proportionate fall in the other, as displayed in Fig. 7.1.2 (Briggs, 1977b).

Table 7.1.5: Summary of Spearman's rank correlation coefficient and Student's t-test for mean phi size against skewness

	Rank Mean	Rank Skewness	D^2
VES01	8	2	36
VES02	5	4	1
001J	3	12	81
002J	10	5	25
JV123	6	11	25
J12 H2O	1	10	81
J12 Edge	2	8	36
J13	4	7	9
JF1	7	9	4
JF2	11	3	64
JF3	9	6	9
JF4	12	1	121
		ΣD^2	492

$$R_s = 1 - \frac{6 X 492}{12^3 - 12} = -0.72027972$$

$$t = -0.72027972 \sqrt{\frac{12-2}{1- -0.72027972^2}} = -3.283520072$$

In summary, there was a positive correlation between mean phi size and sorting, no relationship between kurtosis and skewness, and negative correlation found between mean phi size and skewness. Positive correlations are concerned with the proportional increase in one factor as another variable increases, while negative correlations proportionally decrease as one variable is increased (Briggs, 1977b). The majority of the samples fall under the category of coarse material, with very little to no fine particles present. The majority of samples also display the characteristic s-curve, which was expected for a normal distribution of particles. Outliers in the case of Valterkulten display curves that have a higher proportion of fine sediment than coarse and this can be related to the amount of chemical weathering occurring at this site. Higher rates of weathering will result in the higher production of fine particles, and subsequently an increased surface area for dissolution to occur.

7.2 Moisture content

Moisture content was used as an indicator of the moisture availability at each site, and thus, the potential for chemical weathering to occur. High moisture content values identified sites, which have the greatest potential for this to occur.

The highest percentages of moisture content loss in Fig. 7.2.1, were above seven percent and from sites at Flårjuven (JF2, JF3 and JF4), followed by one site at Slettfjell (002J) and one site at Valterkulten (JV123). The lowest percentage of moisture content loss was at Valterkulten (J13) with a 0.38% loss, followed by a Vesleskarvet Northern Buttress sample (VES01), with a loss of 1.63%. The only samples found to be relatively constant in percentage moisture content loss were those of Vesleskarvet Northern Buttress, displaying results of less than two percent for both sample sites.

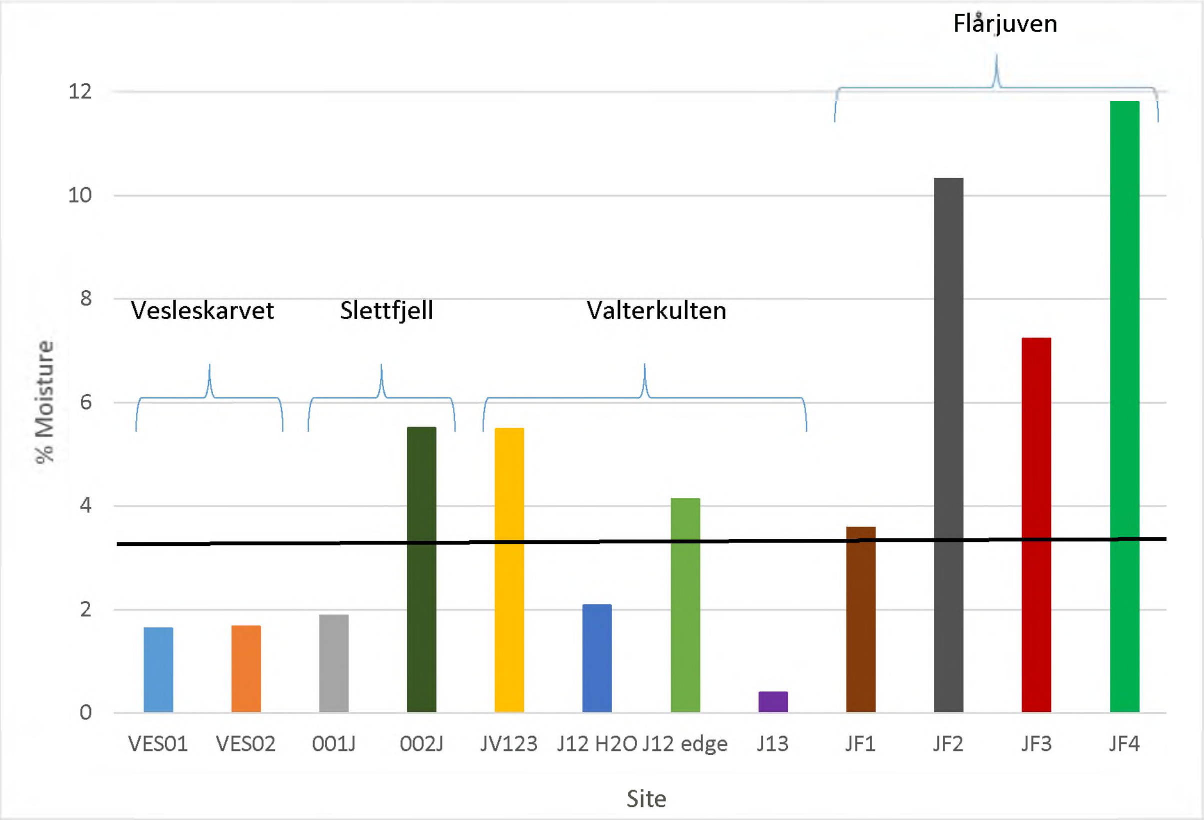

Figure 7.2.1: Moisture content per site

Figure 7.2.3: Area surrounding sample F1 at Flårjuven, geopick for scale

Figure 7.2.2: Sample F1 at Flårjuven

In Antarctica, soil moisture availability is relatively low, with this moisture only being available for chemical processes once in its liquid form (Claridge & Campbell, 1985). Thus, the amount of time that soil spends above the freezing point is relevant (Claridge & Campbell, 1985). In regions whereby the soil temperature rarely rises above freezing, soil moisture is absent and the chemical weathering processes are minimal(Claridge & Campbell, 1985). This is seen in J13 (Valterkulten) sample in Fig. 7.2.1 whereby the soil moisture loss was the least (0.38%). Consequently the results from Vesleskarvet Northern Buttress (Fig. 7.2.1), suggest that this site is also relatively inactive in terms of soil moisture due to the low moisture values. It is important to note, however, that the Vesleskarvet Northern Buttress sites moisture values are more than four times greater than the results of Valterkulten (J13), and are substantially more important to chemical weathering processes than the former. In regions where thawing is more pronounced, soils may be wet, with leaching and chemical weathering more evident (Claridge & Campbell, 1985). For example, the incredibly high values of moisture loss from Flårjuven (F2, F3 and F4), with greater than six percent moisture content. Flårjuven can, thus, be seen as a site where large amounts of chemical alteration of soils could occur.

The lower Flårjuven value (F1) in Fig. 7.2.1, could possibly be because this sample was located further away from heavily weathered material (precipitates) than the other samples at this location (Fig. 7.2.2). Although the value at this site were lower than the other three, this sample displayed more than 3.2% moisture content loss; higher than the average 2.9% moisture content loss (black line Fig. 7.2.1) seen when excluding the Flårjuven (F2, F3 and F4) values. The lower moisture content values noted for Flårjuven (F1) indicated that moisture availability at this particular site was less than the amount of moisture at sites F2, F3 and F4. A possible influence on the differences may be due to the orientation of the samples. F1 had an orientation of 180° while F2, F3 and F4 had orientations ranging between 215° and 274°. In Antarctic environments, northern-facing slopes receive more direct solar radiation than the south-facing slopes. This leads to higher snow melt, and, hence, moisture availability (Claridge & Campbell, 1985).

Figure 7.2.4: Depth of precipitates found at Flårjuven, study site F4

Figure 7.2.3 displays a change in colour of precipitates, with whiter precipitates accumulating on the underlying rock face and browner precipitates at the soil interface. This is similar to the observations made by Gibson *et al.* (1983), where the degree of weathering of mafic or ferromagnesian minerals were found to increase progressively towards the surface, with progressive oxidation toward the top. The major movement of water soluble anions and cations within the active zone depends on the climatic conditions and seasonal influences which affect ionic transport (Gibson *et al.*, 1983).

The moisture value on an inter- and intra-nunatak level was that of Flårjuven, study site F4 (Fig. 7.2.1), with a value of 11.8%. This site displayed high moisture values when considering the amount of moisture lost after drying the sample in the drying oven. Moisture, which is integral for soil development, is either derived from existing ice within the soil or melting snow (Claridge & Campbell, 1985), as pictured in Fig. 7.2.4.

Figure 7.2.5: Flårjuven, study site F4, geopick for scale

In young soils, permafrost tends to be found near the soil surface and, as such, undergoes melting in summer months (prevalence of an active layer) when the soil temperatures rise, adding to the amount of water available in these areas (Claridge & Campbell, 1985). In these situations of increased moisture availability, soils are able to become quite wet during the warmest part of the year (Claridge & Campbell, 1985). Soils formed under these conditions often show little profile development (Fig. 7.2.5) due to their young nature, and the disturbing processes of freeze-thaw resulting in the mixing and overturning of soils within the active zone (Gibson *et al.*, 1983; Claridge & Campbell, 1985). According to Gibson *et al.* (1983) within this zone, the percolation of fluids occurs, as well as chemical weathering and secondary mineral formation. The characteristic features of these soils are the accumulation of salts or precipitates, as seen in Fig. 7.2.5, occurring as encrustations (e.g.: Fig. 7.2.3, Fig. 7.2.4), surface coatings under stones (e.g.: Fig. 7.2.2), or concentrated as soil horizons within the profile (Claridge & Campbell, 1985). The nature of these salt deposits depends on the moisture availability of the soil and the source of the salts, *i.e.* the rock itself or neighbouring rocks (Claridge & Campbell, 1985). Since these areas are not coastal/maritime, one can assume that the salt accumulations do not originate from local marine sources or upper atmosphere circulation patterns, with no deposition of tropical marine salts through precipitation occurring (Claridge & Campbell, 1985).

Figure 7.2.6: Transect of J12, arrow indicating J12 H2O and circle J12 Edge

Figure 7.2.7: J12 H2O sample site, trowel for scale

Figure 7.2.8: J13 sample site, Garmin GPS for scale

The data from Valterkulten displayed a wide range of values, being both in the low and high range, 0.38% (J13) and 5.47% (JV123) respectively. The moisture contents for this site were of particular interest, as these samples were taken from various points around a meltwater pool (Fig. 7.2.6) and at a high altitude area. The sample that was closest to the meltwater pool (arrow in Fig. 7.2.6) was that of J12 H2O (Fig. 7.2.7), found at the edge of the meltwater pool. Seconded by J12 Edge (Fig. 7.2.8) which was the end of the transect (3.52m away), displaying visible precipitates throughout the extent of the transect. J13 (Fig. 7.2.8) was approximately 22m away from J12 H2O, where there were no visible precipitates on the surface but were found underneath rocks. The ground surface was visibly less moist at this site, in comparison to the others, comprised of fine particles beneath the rock.

An interesting component of this transect and subsequent samples from this nunatak was the influence of elevation. Moisture contents for this nunatak increased with an increase in elevation, noted in Table 7.2.1. To test whether or not the percentage moisture loss values were significantly related to the elevation values, a statistical analysis in the form of a one-tailed Pearson's correlation co-efficient was used, with the relationship plotted as a scatterplot diagram (Fig. 7.2.9). Fig. 7.2.9 displayed a positive correlation between the two variables, as well as the normal distributions of the various datasets outside the scatterplot. This positive correlation was strong (0.86), indicating that even though the points were scattered, both variables tended to increase together (McKillup & Dyar, 2010). Upon further statistical investigation, however, the correlation coefficient was 0.86 (Fig. 7.2.9) when compared to the critical values at two degrees of freedom (DF= n-2), this value was lower than the 0.900 value at a .05 significance level. Since the calculated value was below the table value, the relationship was insignificant, however with a strong positive correlation found between the variables. Perhaps this result was the influence of a small sample number at the Valterkulten site; with more samples, this result may be further disproved.

Table 7.2.1: Percentage loss of moisture values and relative elevation

Sample Naming Convention	*LOM (%)*	*Elevation (m.a.s.l)*
J13	0.38	927
J12 H2O	2.07	1022
J12 Edge	4.13	1022.5
JV123	5.47	1292

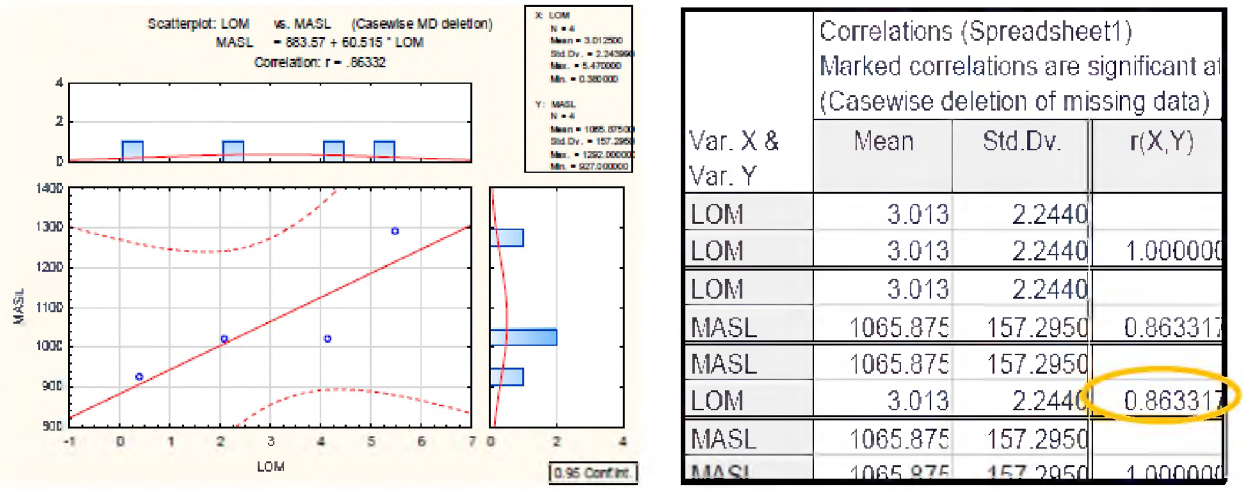

Correlations (Spreadsheet1)
Marked correlations are significant a
(Casewise deletion of missing data)

Var. X & Var. Y	Mean	Std.Dv.	r(X,Y)
LOM	3.013	2.2440	
LOM	3.013	2.2440	1.00000
LOM	3.013	2.2440	
MASL	1065.875	157.2950	0.863317
MASL	1065.875	157.2950	
LOM	3.013	2.2440	0.863317
MASL	1065.875	157.2950	
MASL	1065.875	157.2950	1.00000

Figure 7.2.9: Scatterplot of the relationship between elevation and percentage loss of moisture, for the four sites at Valterkulten and the Pearson's correlation co-efficient (r) of the two variables and other statistical values

The Slettfjell nunatak displayed two varied soil moisture contents from samples collected, with 001J (1.87%) being substantially lower than 002J (5.50%). The smaller soil moisture values noted for site 001J could be related to the amount of snow in the region, as from visual observation, there was a larger area of snow in Fig. 7.2.10 in comparison to the area covered in Fig. 7.2.11 for site 002J. The surface area of snow is an important observation as, snow has an insulating effect, thus, larger quantities of snow provide more insulation to the underlying soil and to a certain extent prevent melting (through reduced frost action) due to the inactive thermal regime of snow (Washburn, 1979; Hedding, 2008). The insulation effect is important as it decreases the moisture availability in an area, limiting the development of permafrost (Hedding, 2008). According to Washburn (1979), ice is a less effective insulator than an equal thickness of snow in preventing freezing and thus inhibiting the development of underlying permafrost (Gold & Lachenbruch, 1973). This characteristic of snow is a possible contributor to the smaller amount of soil moisture found at site 001J in comparison to site 002J. It is important to note however, that the distribution of snow at this site is a snapshot of the possible extent of snow cover during the year. Although snow was present at these sites when sampling, the impact of radiation was not investigated, with this possibly playing a greater role in precipitate development than currently acknowledged.

Figure 7.2.10: Sample 001J at Slettfjell, geopick for scale

Figure 7.2.11: An overview of sample site 002J at Slettfjell

When considering Fig. 7.2.10 and Fig 7.2.11, it was apparent that the relative distribution of precipitates was visually different. Both displayed precipitates in close proximity to snow, however, in Fig. 7.2.10 snow cover was larger and surrounded the precipitates (as seen in the precipitates below the sample site). The effect of insulation of snow can, thus, also be applied to this example, as surrounding snow will insulate the precipitates, effectively isolating them and resulting in lower soil moisture values.

The size of the area covered by the precipitates in Fig. 7.2.10 and Fig. 7.2.11 also differed. When comparing the two using the geopick as reference, it is clear that in Fig. 7.2.11 the extent of salt accumulation on the surface is greater. Fig’s 7.2.12 and Fig. 7.2.13 reiterate this view, which, display

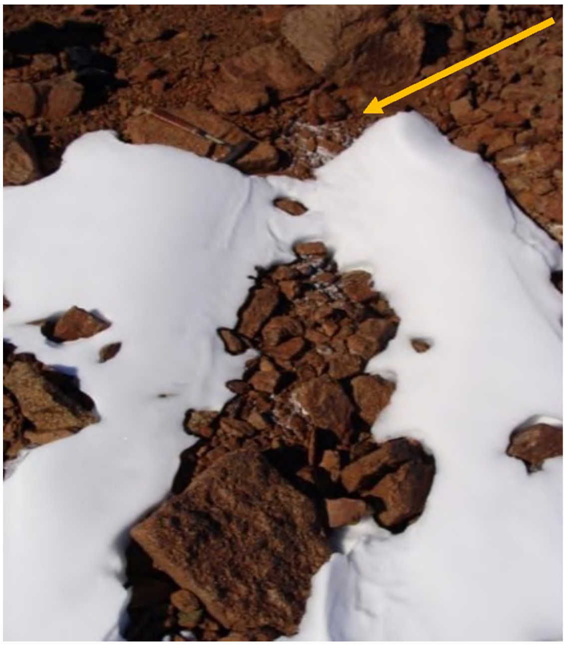

Figure 7.2.12: An overview of the setting of sample 001J (Slettfjell), geopick for scale

Figure 7.2.13: 002J site on the Slettfjell nunatak, geopick for scale

in detail, the size of the precipitate accumulations. Precipitate accumulations were used as a proxy measure of soil moisture. The greater the extent of precipitate or the depth of precipitate, the higher the soil moisture. As chemical weathering processes required liquid water in order to occur so the evidence of precipitates indicated the availability of water. Greater amounts of water resulted in larger deposits of precipitates; hence, a site, which had a large extent or deep extent of precipitates, had greater soil moisture. This argument is supported in Fig. 7.2.10 – Fig. 7.2.13, while also being directly linked to the calculated loss soil moisture values in Fig. 7.2.1. In particular, where Slettfjell site, 001J (Fig. 7.2.10) contained a lower soil moisture content than Slettfjell site 002J (Fig. 7.2.11 and Fig. 7.2.13).

The percentage loss of moisture values for Vesleskarvet, Northern Buttress, both fell below the average loss of moisture value in Fig. 7.2.1. The two sites at Vesleskarvet, VES01 (1.63%) and VES02 (1.66%) were similar in their loss of moisture values, and when looking at Fig. 7.2.14 and Fig. 7.2.15, both sites displayed visible precipitates and no snow. Snowfall, however, is known to occur at Vesleskarvet and may sublimate (evaporate directly from ice crystals), rather than melt, due to the aridity of the region, therefore, not supplying moisture directly to the soil (Gibson *et al.*, 1983; Meiklejohn & Sumner, 2008). This relationship may account for the extremely low soil moisture values at this nunatak. Visual inspection of Fig. 7.2.14 and Fig. 7.2.15 provided information on the extent of precipitates at each site; VES01 displayed less visual precipitates than VES02, while both sample sites were relatively similar in extent when using the geopick as a scale bar.

Figure 7.2.14: Sample VES01, geopick for scale

Figure 7.2.15: Sample VES02, geopick for scale

The colour and texture of precipitates varied between both sites, with VES01 displaying off brown, "dry" precipitates (Fig. 7.2.14), while VES02 displayed whiter, "dry" precipitates (Fig. 7.2.15). The colouration and apparent state of saturation of these precipitates were possibly related to the moisture availability, and input, for each site. In particular, these results are most likely connected with the microclimate and micro-topography of the area and as such, the influence of ground-surface characteristics. For example, moisture, air-earth and air-water interface effects (Geiger, 1965; Washburn, 1979). Micro-climate has the ability to vary with distance, in both a vertical and lateral orientation, strongly influenced by wind velocity, the distribution of snow and vegetation (absent in this case) (Washburn, 1979).

Sites with lower moisture availability (VES01 with 1.63% and VES02 with 1.66%) display precipitates visibly less saturated, than at higher moisture availability sites (Valterkulten, J12 Edge with 4.13%). When comparing Fig. 7.2.14 and Fig. 7.2.15 to Fig. 7.2.2 – Fig. 7.2.5 and Fig. 7.2.10 – Fig. 7.2.13, a notable difference in moisture saturation of precipitates became apparent. Higher soil moisture samples, such as those seen in Fig. 7.2.2 – Fig. 7.2.5 were characterised by larger accumulations of precipitates, and precipitates which were visually more saturated than sites with lower soil moisture values, such as Fig. 7.2.14 and Fig. 7.2.15 at Vesleskarvet. In relation to this, the presence of precipitates in Antarctic environments indicated ionic migration and chemical activity, even in areas with a permanently frozen zone, such as Vesleskarvet (Gibson *et al.*, 1983).

Overall the high percentage soil moisture loss at the Flårjuven and Valterkulten sites may be attributed to the permafrost levels at these sites and the local temperatures which are experienced (Claridge & Campbell, 1985). Temperatures have a great influence on the amount of moisture found within a soil profile, typically younger soils are underlain by a layer of permafrost close to the surface, while older soils maintain permafrost levels at depth (>1 m) (Claridge & Campbell, 1985). Where ice crystals are present, either between the soil grains or above the soil surface layer, the soil has a high probability of becoming more saturated due to higher surface temperatures in summer months (Claridge & Campbell, 1985). As a consequence of increased moisture availability, these sites have more available moisture, with deeper penetration of weathering, and to an extent, greater degrees of weathering, with the resultant chemical precipitates found in these areas being an indicator of this (Claridge & Campbell, 1985).

The results of the relationship between elevation (MASL) and loss of moisture (LOM) at Valterkulten in Fig. 7.2.16, returned a positive correlation, however, it displayed no statistical significance. To further test this result against all sample sites, the relationship between MASL and LOM was investigated (Fig. 7.2.16). From Fig. 7.2.16, a positive correlation between MASL and LOM was found to exist, where as one variable increased as did the other, however, when looking at the Pearson's correlation co-efficient there was no statistical significance for the relationship ($p < .05$). The reiteration of results from Fig. 7.2.9 contribute to the rejection of the relationship between elevation and moisture loss at these sites. The positive correlation of these variables, however, warrants further investigation, with more samples across various nunataks and at various elevations having the possibility of improving this correlation and relationship.

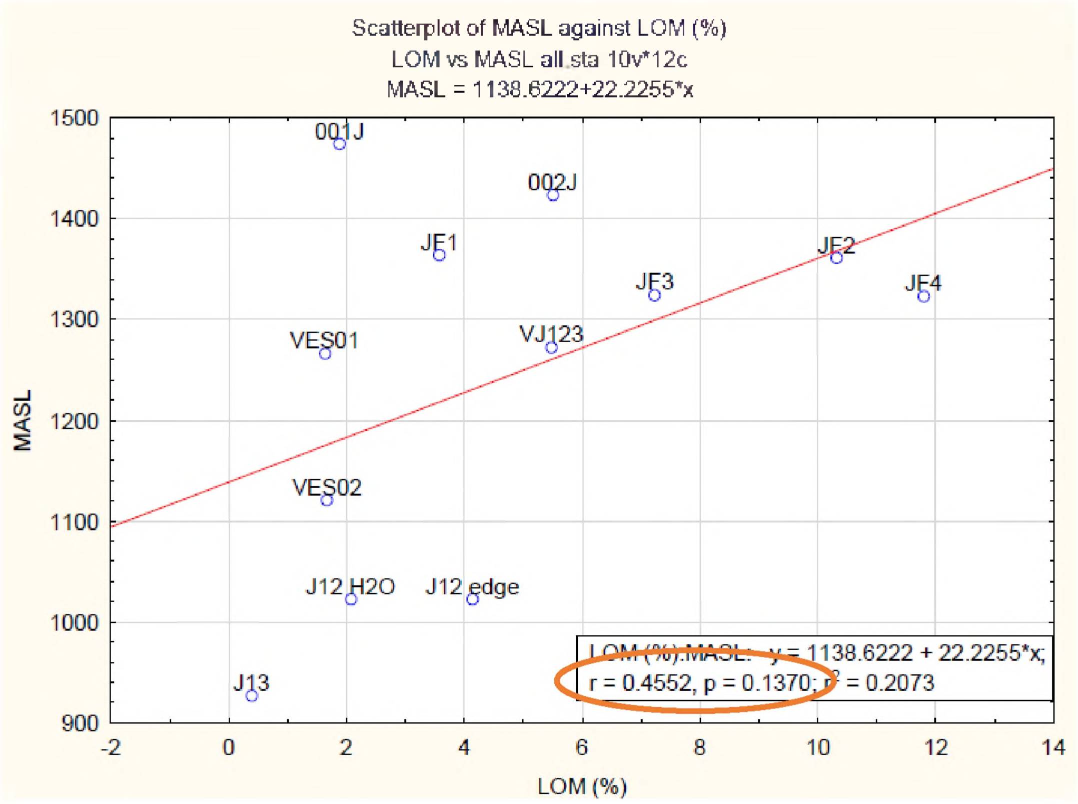

Figure 7.2.16: Relationship between percentage moisture loss and elevation

Loss of soil moisture was controlled by the availability of snow at each study site and the subsequent melting thereof, such as at Slettfjell, where areas with smaller snow cover experienced greater soil moisture loss values. This was in part due to the insulation effect of snow, which provided shelter to the soils underneath and decreased the amount of moisture added to the environment. Snow accomplished this through increasing the amount of energy needed to melt larger portions, maintaining a relatively constant temperature; hence taking longer to melt than areas containing small amounts of snow whose temperatures are likely to change relatively quickly in comparison. Although the influence of the insulating effect of snow contributed to soil moistures, it is also important to note that local microclimates also had an influence on soil moisture loss. Local climate influenced temperatures, which in turn influenced the melting of surrounding snow and underlying permafrost, adding moisture to these environments. Although local climate influenced temperature, it also had an influence on the desiccation of soils, through evaporation via wind (Meiklejohn & Sumner, 2008). The local climate in relation to wind action in polar desert environments was hence of importance, as, it influences the positioning of snow (French, 2011). The deposition of snow influenced the moisture availability through snow melt. Typically, in these environments snow is blown clear of upland surfaces while the lee-slopes and lower valley sides are sites of snow bank accumulation (French, 2011). In this regard, soils, which contain high moisture values and small areas of snow, are more likely to desiccate faster than those that do not. Consequently, areas experiencing decreases in the insulating effects of snow, are more likely to exhibit previously covered rocks with a more dynamic thermal regime, aiding thermally-induced weathering processes, through limiting the prolonged wetting of melting snow (Hedding, 2008). While frost processes may accelerate due to increased radiational heat exchange, a result of decreased snow cover (Matsuoka, 1996; Hedding, 2008). This result however, will only occur if the environmental conditions enabling frost action do not reach the warming limit over which the ground freezes too little to contribute to effective and prolonged frost action (Matsuoka & Moriwaki, 1992; Hedding, 2008).

Precipitate deposition and apparent saturation between sites varied with soil moisture content, sites with higher soil moisture values presented more developed, inundated precipitates, with a whiter colouration. The development of precipitates was linked to the moisture availability in the area. Hence, higher moisture loss areas should display more precipitate development than sites with low loss of moisture values. This suggestion was based on a contention that an increase in rock moisture content through decreased rock temperatures; condensation, precipitation or increased atmospheric moisture, caused hydration of rock minerals, precipitated salts, clay minerals, and chemical alteration through hydrolysis and solution of rock minerals and precipitates (Meiklejohn & Sumner, 2008). Seen in the case of Vesleskarvet, Northern Buttress and Flårjuven, Valterkulten and Slettfjell. Decreases in rock moisture or soil moisture content resulting from increased rock temperature, decreased the moisture movement along discontinuities, and hence decreased atmospheric moisture, causing the dehydration of rock minerals, clay minerals and precipitated salts, resulting in the precipitation (crystallisation) of solutes (Meiklejohn & Sumner, 2008). Areas that have extensive quantities of precipitates or saturated precipitates were argued to be places with increased water mobility. Sites whereby deep precipitate accumulation or large-scale accumulation occurred were attributed to multiyear time scales, or products of excessive precipitation and evaporation processes.

7.3 Rock hardness

The following sections interprets rock hardness values, which were used as a relative measure of comparison between sites in terms of pitting, flaking and surface disintegration. Higher rock hardness values indicated more intact rock surfaces with little weathering having occurred while low rock hardness values were indicative of more weathered and hence “softer” rock.

The naming conventions found in Fig. 7.3.2 were related to the distance from the meltwater pool; the sample site closet to the pool was named Near (0m) and that sample furthest away from the pool was named Far (3.52m). The use of impact values in determining rock hardness and subsequent weathering was of importance as it allowed one to test the differences in weathered products between rocks at the same site. Essentially rock hardness (impact values) provided a proxy for measuring the extent of weathering between sites with similar lithology.

Rock hardness values (impact values) at the Valterkulten Far site (3.52m) (Fig. 7.3.2) were much higher than those found at Valterkulten Near (0m). Valterkulten Far indicated rock hardness values, which were of a higher median than at Valterkulten Near (0m), characterised by a larger percentile distribution and range of values (Fig. 7.3.2). This change between the two sites indicated that the Far (3.52m) site was slightly more resistant to weathering (high rock hardness values) than the Near site (0m).

The above results were further supported by the observed change in colour of the rocks around the meltwater pool as one moves away from the water’s edge (Fig. 7.3.1). Rocks closest to the meltwater pool were a grey colour, which became a light grey/orange colour in the middle, to reddish-brown at the edge. This colour gradient may be a result of previous water levels. If this is the case, the Near site (0m) would have been more likely to become weathered through water based weathering processes such as hydration and hydrolysis than the Far site (3.52m), which comprised of reddish-brown rocks. Since this site was summarised overall in Fig. 7.3.3, the same interpretations above are

Figure 7.3.1: Change in colour gradient extending from the meltwater pool at Valterkulten.

valid for this site in contrast to the other sample sites.

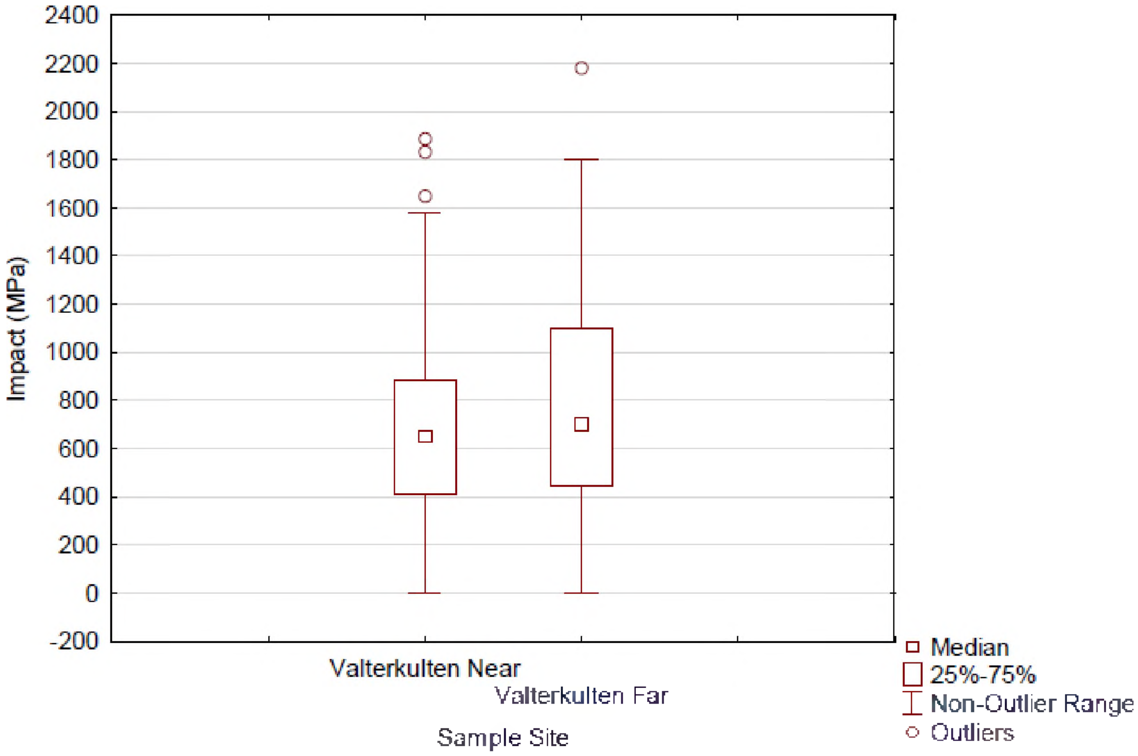

Figure 7.3.2: Rock hardness values at two sites by the meltwater pool at Valterkulten for summer 2016

Rock hardness values at various sites were previously measured in research that commenced in 2007 and complimented by 2016-2017 values all of which allow for inter-nunatak comparison (Fig. 7.3.3). The 2016-2017 values for all sites displayed a larger range of values and higher descriptive statistics than sites from previous data collection, possibly due to the smaller number of impact values taken. When analysing at intra-nunatak level, impact values for Vesleskarvet (2014-2015) decreased followed by an increase in 2016. Although changes in impact values for rock hardness occurred, the years cannot be significantly compared. Due to the small sample size of the 2016/2017 field season and the use of different rock faces. Changes in impact values relate to the microclimate at each sample site and the underlying geology. For example, the greater the amount of snow cover the higher the rebound impact values (Hansen *et al.*, 2013). In this regard, low rebound values for areas of low snow cover possibly indicate the loss of the insulating effect of snow, resulting in a more dynamic weathering environment (Hansen *et al.*, 2013; Hedding, 2008). The magnitude of impacts seen in Fig. 7.3.3 further investigated the structure of the rock and subsequent strength and resistance to weathering processes, where higher impact values identified more resistant rock surfaces (Meiklejohn & Sumner, 2008).

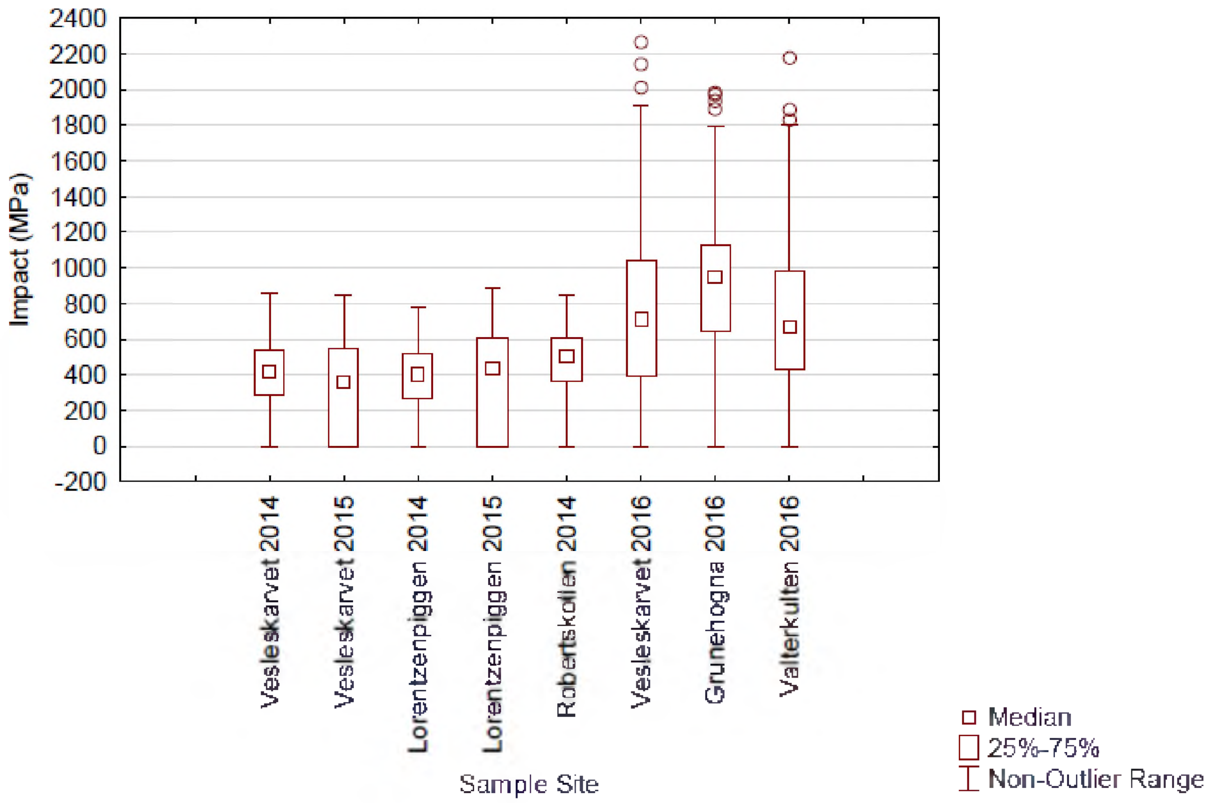

Figure 7.3.3: Relative rock hardness values for a variety of sites over numerous years

Over larger timescales, sites that display decreased rock hardness values, resulted from moisture controlled weathering processes and other processes (thermal expansion for example) related to changes in temperature, which enlarged existing pores and caused granular disintegration (Meiklejohn & Sumner, 2008). This increased rock porosity (enlargement of pores created lower micro-porosity) and widened bedding planes, allowing further weathering to occur (Meiklejohn & Sumner, 2008). Lower micro-porosity, higher porosity and the widening of bedding planes, thus, results in easier moisture infiltration and allows for further weathering processes to occur (Meiklejohn & Sumner, 2008). Low rebound impact values have relations to the influence of temperature through the amount of solar radiation which is received, high amounts of received solar radiation have been found to produce low impact values (Hansen *et al.*, 2013). Hence, sites, which display low impact values, are likely to further weather through thermal or hydrological processes over a period of years, and contribute to pedogenesis. Aspect related differences in rock hardness values reflect differences in weathering environments, with indicators of weathering such as pitting and flaking being the products of differentiated weathering of bedrock (Sumner *et al.*, 2002; Hansen *et al.*, 2013).

Increases in rock hardness values at the Lorentzenpiggen site (Fig. 7.3.4), were related to the lower likelihood of snow and ice melt availability for chemical weathering activity, especially noted on south facing slopes, which reduced rock breakdown and produced harder rock surfaces (Hansen *et al.*, 2013).

Figure 7.3.4: Sample rock at Lorentzenpiggen, displaying rock coatings and surface alteration, such as pitting (Meiklejohn, 2016)

Subsequently the higher the rebound impact values, the higher the amount of snow cover and the more stable the thermal regime on these rocks, resulting in less weathering (Hall & André, 2001; Hansen *et al.*, 2013). As previously mentioned, higher impact values tend to display more intact rock, and thus less weathered material.

When comparing the impact values for Lorentzenpiggen 2014 and 2015, and Vesleskarvet 2014-2016 the increases display either sample sites that have variation in weathering or an increase in rock hardness (lower impacts in 2014) although the time scale is too small to accurately conclude this. Increases in rock hardness were possibly due to the formation of coatings (Fig. 7.3.4) on the rock surface, which have been shown to protect the underlying rock from further weathering and erosion, partially through waterproofing the exterior (Robinson & Williams, 1989; Robinson & Williams, 1992; Robinson & Moses, 2011). This alteration of rock resulted in a colour change involving the loss or accretion of chemical minerals, either developing on the outer surface of the rock (Fig. 7.3.5) or within the original rock (Robinson & Moses, 2011). Chemicals included within the coating are either derived from external sources, or the parent material (Robinson & Moses, 2011). Over time, these crusts deteriorate (Fig. 7.3.5) and when breached, the subsurface layer which is weakened and poorly cemented is lost, undermining the crust and spalling as it falls away (Robinson & Moses, 2011).

Figure 7.3.5: Spalling crusts on Northern Buttress, Vesleskarvet

Weathering rinds, as seen in the above Fig. 7.3.4 and Fig. 7.3.5 are typical of bidirectional water movement, causing oxidation and dissolution to occur (Oguchi, 2013). These weathering rinds displayed similar characteristics to those described by Oguchi (2013), whereby rinds were parallel to the rock surface with nearly constant thickness. When precipitation was abundant, small amounts of water was supplied to the rocks through snow melt, either on or around the rock in question (Oguchi, 2013). Water was then directed from the outside of the rock to the inside, while, during periods of no/low precipitation, water movement occurred in the other direction (Oguchi, 2013), which created the white and red coloured weathering bands pictured in Fig. 7.3.6.

Figure 7.3.6: Fresh weathering rind, Robertskollen, Ice Axe Peak

Robertskollen's values (Fig. 7.3.3) are likely related to the temperatures which this site experiences and the subsequent microclimate. Temperatures at Robertskollen were the highest of all the sites, with liquid water flowing between rocks and pooling in areas. This increase in water availability provided the water needed for chemical rock weathering to occur (Fig. 7.3.6) and subsequently decreased the rock strength and rock hardness values. Since the Robertskollen site had flowing water and pooling of water, the values of rock hardness were likely to be influenced. Flowing water has the ability to transport sediment, which provides the abrasive power to wear down rock material. In this regard, the impact of water is variable, with local climatic influences determining favoured processes.

Grunehogna 2016 (Fig. 7.3.3) displayed the highest median average of rock hardness for all sites, while the range of values was relatively small in comparison. Grunehogna has a geology that comprises of an intrusive dike of Grano-diorite throughout the alternating sedimentary sequence, and thus, contributes to higher rock hardness values (more hardy material). As previously mentioned, higher rebound impact values are related to greater amounts of snow cover and stable thermal regimes, resulting in less weathering having occurred (Hall & André, 2001; Hansen *et al.*, 2013). The Grunehogna site displayed large amounts of snow cover, with the top of the nunatak covered in thick snow, a large snow scoop and a semi-permanent lake ice blister being indicator of the prevalence of snow and ice at this site.

Overall, rock hardness values and subsequent rebound values were dependent on multiple factors, such as geology, aspect, inputs of precipitation and atmospheric processes among others. The use of an Equotip indicated the degree of weathering a surface has undergone, with observed average median r values being approximately 560 MPa per site. The highest rebound values (Grunehogna) were attributed to the influence of geology and subsequent length of exposure since deglaciation, while the low values (Lorentzenpiggen and Vesleskarvet) were influenced to a high degree by the development of rock crusts, aspect, thermal regimes and snow input. Sites that returned values within these two extremes (Valterkulten and Robertskollen), displayed the influences of previous water availability and the impact of microclimatic temperatures. Weathering rinds related to rock hardness exhibited two typical bands of formation, a red (oxidised) band and a white, “bleached” zone, consisting of depleted elements. Water was the primary agent of weathering rind formation at sites, such as Robertskollen, displaying parallel, uniform thickness weathering rinds, exhibiting textbook characteristics. Weathering rind values and rock hardness were related; with decreased rock hardness values being noted, possibly due to the influence of spalling (Fig. 7.3.5), whereby the weathering rind starts disintegrating and losing its initial hard, protective layering.

7.4 Thermistors and FLIR camera

Thermistors and a FLIR camera allowed for quantitatively comparing near-surface temperatures (1cm below ground) and rock temperatures respectively. Additionally, FLIR cameras and software were used as a means of disproving the argument of negative temperatures hindering chemical weathering. This successfully allowed definite rock temperatures to be quantified and interpreted, not relying on air temperatures as a proxy.

7.4.1 ACR Thermistors

Common trends occurred in mean near-surface air temperatures (Fig. 7.4.1) in the form of peaks and depressions. Every year all sites displayed the same trend, high peaks in the summer months (November-March) and an inversion of peaks in the winter months (May-August), seen in Fig. 7.4.1. These peaks were typical of summer and winter variations in Antarctic environments, where winters (-33°C – -20°C) were substantially colder than summers (-8°C – 5°C). These variations evident in Fig. 7.4.1, occur over large time scales due to meso-scale pressure systems, controlled by the Southern Annual Osculation (SAO), which influences pressure changes and circulation around the Antarctic continent twice yearly, altering the transport and subsequent strength of air from the lower latitudes, influencing air and surface temperatures (Reijmer, 2001; Knox, 2015).

The summer months in Antarctica (November-March) are moderated by the ocean at coastal stations, while inland stations experience increased amplifications of extremes due to heat conductivity and decreased snow density (Reijmer, 2001; Knox, 2015). During winter months (May-August), however, the absence of diurnal inputs and variations such as albedo and insolation results in the forcing of metrological conditions (Reijmer, 2001; Knox, 2015). In June throughout the recorded years (excluding 2016), a trend was noticed where temperatures for all sites increased in June and decrease in July, and then increased once again. These inversions are possibly due to the influence of katabatic winds in the winter months, where stronger winds enhanced vertical mixing and reduced the strength of temperature inversions, resulting in higher than usual surface temperatures (Reijmer & Oerlemans, 2002; Knox, 2015).

Interestingly the years of 2014 and 2016 display synchronous trends in temperature, during the winter months, where the trend line decreased in July and again in September before increasing rapidly for the summer months. When comparing the 2013 and 2016 values for winter, an inverse effect was noticed, where their values were mirror images of one another.

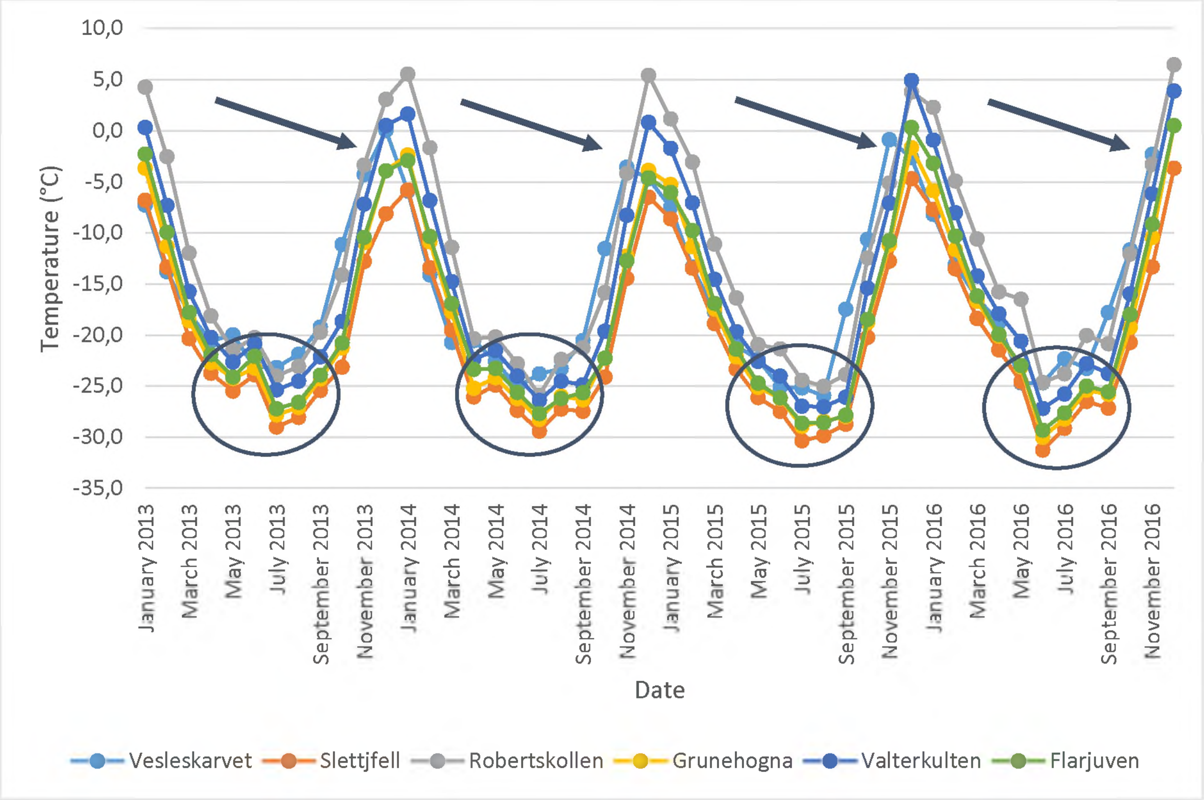

Figure 7.4.1: Average monthly near-surface (1cm below ground) temperatures at numerous sites (2013-2016)

Near-surface thermistor data (Table 7.4.1) were shown graphically as detailed graphs of the average below ground temperatures (1cm), maximum temperatures, minimum temperatures, winter and summer temperatures. Average yearly near-surface ground temperatures per site (Table 7.4.2) differed substantially, ranging from -12°C- -20.5°C, while yearly temperatures at each site also ranged from roughly 0.7°C to 1.2°C. The warmest site from Table 7.4.2 was that of Robertskollen followed by Valterkulten, Vesleskarvet, Flårjuven and Grunehogna with the coldest site being Slettfjell.

High relative near-surface ground temperatures such as Robertskollen and Valterkulten, and low relative near-surface temperatures such as Grunehogna and Slettfjell were suggested to be the result of the microclimate at each location. With the influence of characteristics such as the air-earth interface having an effect on the moisture availability at each site (Geiger, 1965; Washburn, 1979). Local and microclimatic influences are highly significant for periglacial processes such as wind, temperature, precipitation and the seasonal distribution of these factors (Washburn, 1979). Local climatic influences are typically related to the local topography of the area, noticed most in the differing temperature regimes of slopes of mountains (Washburn, 1979), especially in high latitude areas such as Antarctica. Aspect is of importance due to the North-facing slopes in the Southern Hemisphere experiencing a greater depth of thawing than southerly slopes (Washburn, 1979). This is presumed to be a reaction between the lower near-surface soil temperatures and the slower evaporation of moisture after precipitation (Hannell, 1973; Washburn, 1979).

If one only considers the topography of the relevant areas, Table 7.4.2 becomes more relevant in terms of location, for example the coldest site (Slettfjell) was the most southerly and subjected to winds from the Borgmassivet mountain range and the Plateau, even further south. The topography of the warmest site was also relevant, as Robertskollen was protected largely by Ice Axe Peak, found directly in front of the nunatak, effectively acting as a windbreak. Similarly, the second warmest nunatak (Valterkulten) contained a meltwater pool in the base of the basin-like formation, with the exterior of the nunatak protecting the hollow from high wind speeds and subsequently allowing for warming through sheltering the area. The influence of shelter provided favourable conditions for the prevalence of liquid water and decreased evaporative loss through Aeolian processes. Moisture is a limiting factor in Antarctic environments and as such, the presence of liquid water at these sites is relevant as these environments become less thermally driven (weathering regimes) allowing chemical weathering to become the major controlling process in regards to pedogenisis (Hansen *et al.*, 2013).

Daily fluctuations of below ground temperatures were influenced by diurnal temperatures, as well as external factors such as cloud cover, with temperature gradients greatest during clear free days, as opposed to the latter (Bockheim & Hall, 2002). Maximum soil surface temperatures were dominantly radiation controlled, while minimum temperatures however were strongly linked to air temperatures (Bockheim & Hall, 2002). This linkage to air temperatures, allowed for large temperature gradients to be generated (in relation to soil-surface temperatures) in one of the coldest and highest environments in the world (Bockheim & Hall, 2002).

Table 7.4.1: ACR thermistor legend for Table 7.4.2

🟦	Average Temperature
⬜	Average Minimum Temperature
🟧	Average Maximum Temperature
🟨	Average Summer Temperature (Nov-Feb)
🟦	Average Winter Temperature (May-Aug)

Table 7.4.2: One centimetre below ground ACR thermistor data for various sites over a four-year period

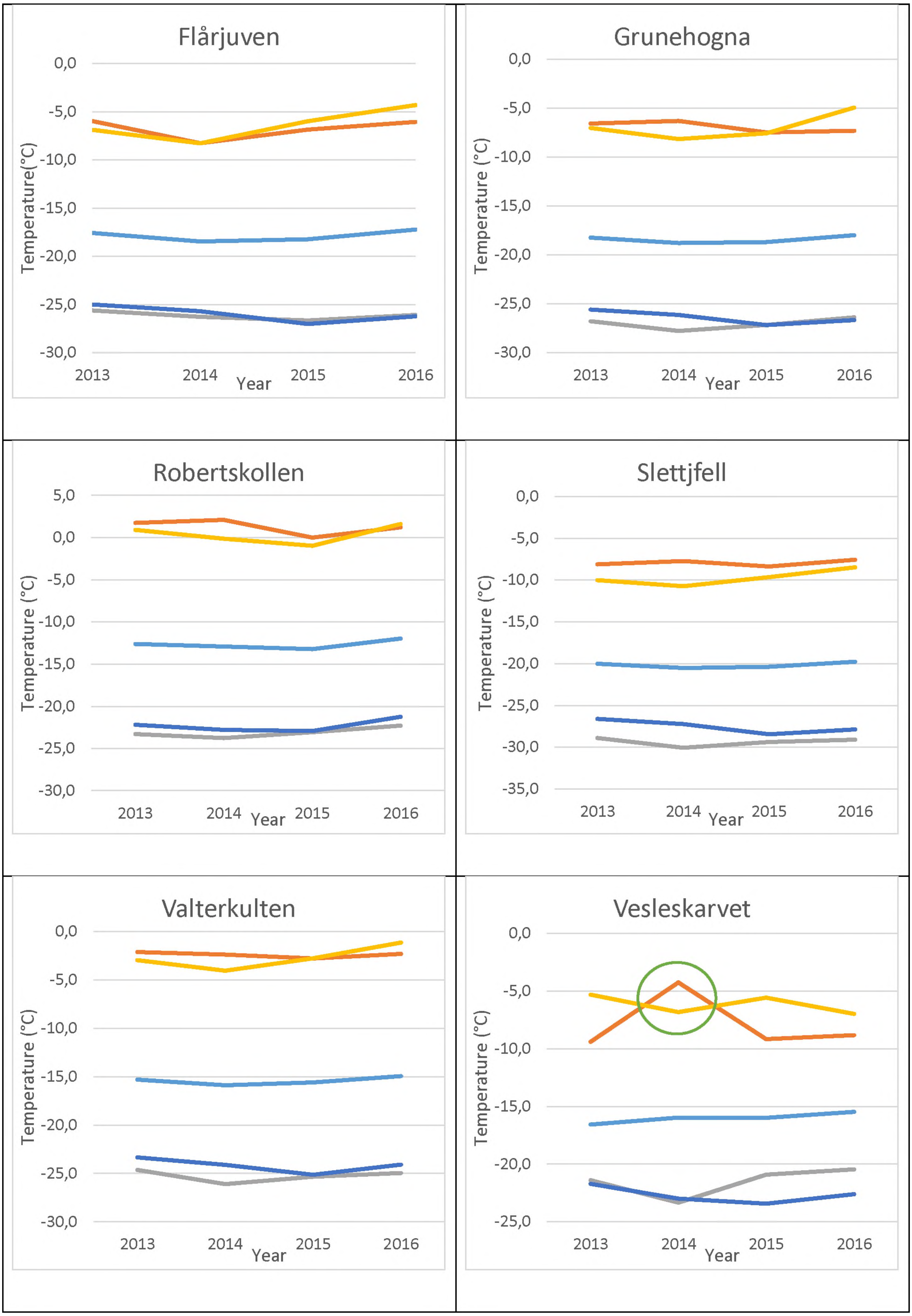

In periglacial environments, ground temperatures are more important than air temperatures for landscape dynamics, as they are direct readings and not inferred (French, 2011). However, mean annual air temperatures, such as those in Fig. 7.4.1 are important to differentiate from mean annual ground surface temperatures (Table 7.4.2), as they are responsible for surface offset, also known as the change in temperature below ground in comparison to above ground (French, 2011). Thermal offset, however, is the difference between the mean annual ground surface temperature and the temperature at the top of a permafrost layer (French, 2011). Snow cover primarily influences surface offset, while physical properties of the active layer (moisture content and thermal conductivity) largely control the thermal offset (French, 2011). The annual near-surface air temperatures and near-surface ground temperatures, found above display the relationship between these factors. Typically ground temperatures change with air temperatures, but, often a lag effect is noticed, with the below ground temperatures remaining more static than air. Chemical weathering models widely recognise that increased temperatures favour chemical activity (in both the case of air and ground), while temperatures below freezing inhibit chemical activity (Hall *et al.*, 2012). Thus, favourable conditions are typically those produced by the thermal offset, a product of both air and ground temperatures.

7.4.2 FLIR camera data

High frequency FLIR data, which was collected over a 24-hour period on the Southern Buttress of Vesleskarvet, displays an obvious trend on the major rock face that was studied. Temperature ranges were standardised across the samples (-32°C – 20°C), with a colour key indicating high temperatures (white and red) and low temperatures (dark purple and blue). Demonstrating the variability of temperatures in high mountainous regions and periglacial ecosystems (Barsch, 1993).

Over the 24 hour period monitored, this rock face experienced a temperature change of approximately 50°c, from -32°C to 20°C (where the standardised values come from). This range of values was similar to field studies in Antarctica, quoted by French (2011), where daily temperature ranges “were in excess of 40°C”. Rapid daily fluctuations of temperature were also observed by Bardin *et. al.* (1964), in Queen Maud Land where rock temperatures fluctuated between 30°C and -12°C (Bardin *et al.*, 1964; Hall & André, 2003). A study by Jonsson (1985), recorded temperature in the 20°C – 30°C range, even when air temperatures were -7°C. From the comparison of these rock temperatures, and temperatures from other undertakings, it was clear that rock surfaces were experiencing high temperatures even while atmospheric temperatures were below 0°C. Assuming these rock temperatures were recorded at high frequency intervals (< two-hourly periods), one can conclude that radiation has a great influence on rock surface temperatures. The influence of wind and cloud are likely to modify these temperatures, either through heat gain or heat loss, such as the process of convective heat transfer (Kappen *et al.*, 1981; Friedmann, 1982; McKay & Friedmann, 1985; Friedmann *et al.*, 1987; Hall & André, 2003).

The change in colour gradient of the rock face in Table 7.4.3 from 08.30 until 06.30 displayed the movement of the sun during these hours, with it moving towards the east in the images (08.30 – 16.30), until it completes one full rotation and the westerly surfaces start warming (04.30 – 06.30). The influence of aspect can hence, be brought into this discussion of temperature change on a rock face. In a study conducted by Mathys (1974), rock surface temperatures at 3500m on a north wall of the east ridge of the Jungfrau (Berner Oberland, Switzerland) never exceeded 0°C for 7 months, while at the same altitude on a south exposed wall data displayed slightly positive temperatures, even during winter on clear days (Barsch, 1993). Because the above study region is in the Northern Hemisphere and not the southern, the opposite effect of aspect was expected to occur, in that the south-facing rock surfaces are expected to be colder than north-facing rock surfaces. According to experiments by Hansen *et. al*. (2013), it was suggested that northern aspects may be influenced to a greater degree by thermal driven regimes such as thermal stress, than southern aspects. In addition, there is also a lower likelihood of moisture from melting snow being available for chemical weathering on south-facing slopes, reducing rock breakdown and producing harder surfaces (Hansen *et al.*, 2013). When considering a single rock face such as in Table 7.4.3, the rotation of the sun exposes all directions to incoming solar radiation and as such, the influence of aspect in a small-scale system. If incoming solar radiation varies according to the orientation of a rock surface and snow or ice are present in the system, aspect may be an even more influential influence on rock weathering than previously thought (Hansen *et al.*, 2013).

It is important to note that the snow around the rock face, and surrounding rocks changed temperatures together, however, never reaching above the -7°C range throughout the samples. As such, solar radiation has the potential to influence and impact rock weathering through the supply of moisture through melting snow and ice, which is a key component of chemical rock weathering (Hansen *et al.*, 2013). If no snow or ice are present, thermally driven weathering regimes are more likely to dominate, however, if moisture is present, it is able to become available as rock surfaces heat, melting the snow/ice which is in contact with it (Hall, 1992; Gardner, 1992; Hansen *et al.*, 2013).

The ice in the surrounding areas of rock in Table 7.4.3, displayed a change in ice temperatures, especially in those which were isolated (displaying warmer temperatures) than ice which was free standing and not enclosed, for example at 08.30hrs. Another interesting trend in relation to ice was that those which were touching/close to a rock face, were warmer than ice which was not (e.g.: 14.30hrs), while the inverse relationship was also noticed, (e.g.: 22.30). Surfaces covered by snow/ice exhibited a more stable thermal regime than those which did not(more dynamic thermal regime) (Gardner, 1992; Hall & André, 2001; Hansen *et al.*, 2013). Although this theory typically relates to entire clast faces/surfaces, the results of ice/snow, which were touching a rock surface, should inherently portray the same concept, over a smaller surface area.

Table 7.4.3: High frequency FLIR data taken of one rock face on Southern Buttress, Vesleskarvet over a 24 hour period

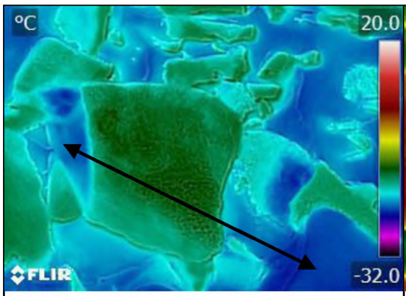 08.30	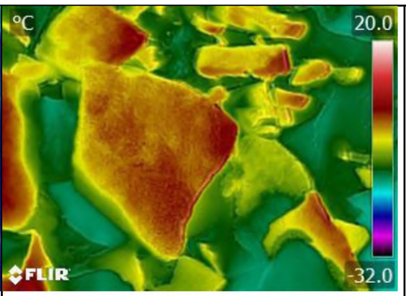 10.30	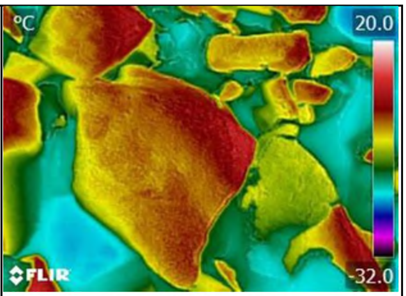 12.30
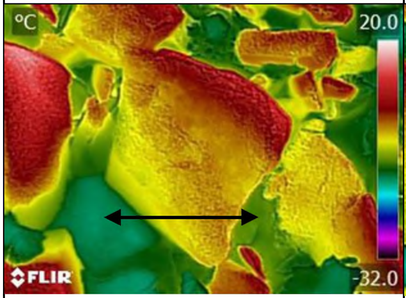 14.30	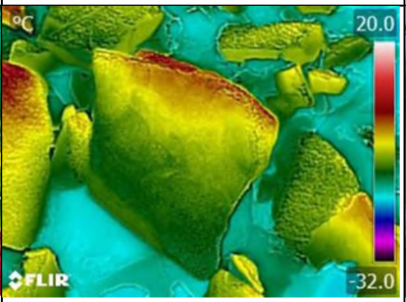 16.30	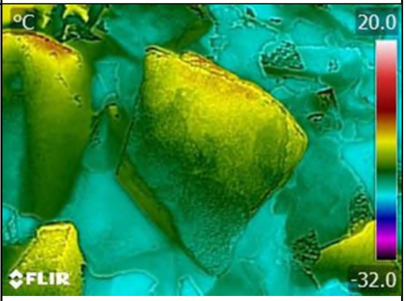 18.30
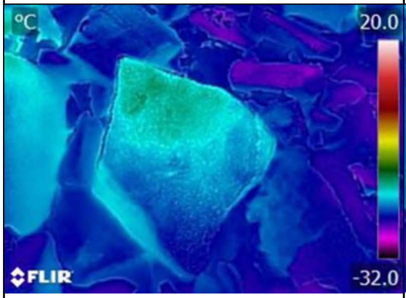 20.30	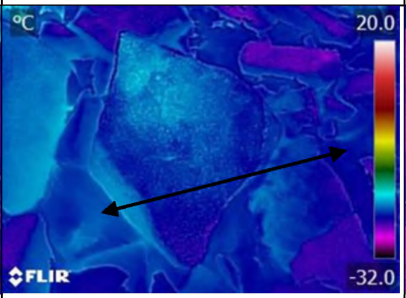 22.30	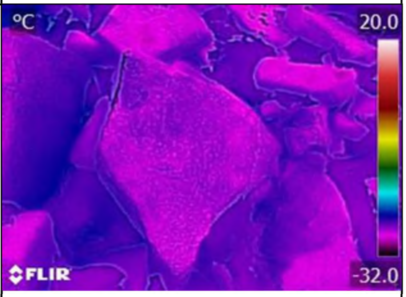 24.30
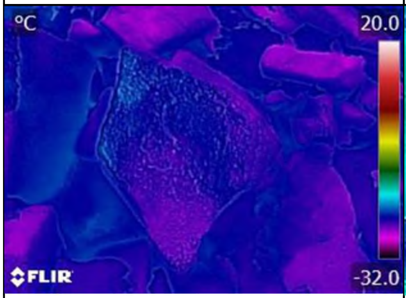 02.30	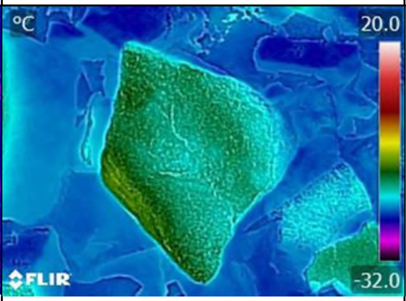 04.30	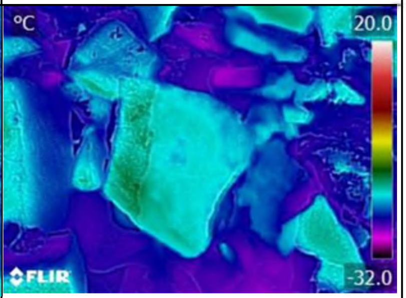 06.30

FLIR imagery of one rock face over a 24-hour period, displayed the changes in temperature (50°C range) in two-hour increments at one study site. Major changes in temperature were seen throughout the period, with the rotation of the sun influencing both rock and snow temperature regimes. Aspect played a large influence on the temperatures of the rock face, with temperatures moving as the sun moves throughout the day (east to west). Aspect also influenced the temperatures of snow/ice, with southern facing slopes contributing little to moisture availability, as less snowmelt occurred in these areas. Local climate played a major role in rock surface temperatures, with atmospheric processes such as cloud cover, wind and synoptic systems influencing heat exchange and loss. If no snow/ice were present at a site thermal weathering processes were more likely to dominate. Snow/ice displayed attributes of both being thermally stable and dynamic, dependant on the position of neighbouring rock and snow/ice. Snow/ice isolated from other snow/ice by surrounding rocks, displayed a more dynamic thermal regime, changing temperatures with the surrounding rock. While snow/ice, which was further away from rock, displayed a more typical stable thermal regime, with temperatures changing very little and the insulating effect of ice being apparent.

7.5 Geochemistry

Geochemistry provided information on the soluble ions, which occurred as products of chemical weathering, while also providing for the quantification of solutes within specific regions. In this regard, the use of inputs (such as control snow) and outputs (meltwater, snow in the region of precipitates and ice) allowed for differences between the two to be inferred as products of chemical weathering. pH and electrical conductivity results further added to this, where high values were linked to high geochemistry results in regards to solute specific ions. Additionally pH and electrical conductivity allowed for the specific chemical processes responsible to be inferred.

7.5.1 ICP

Major cation concentrations from Table 7.5.1 were magnesium, potassium, sodium, strontium, copper, manganese and calcium, while the most common anions were, iodide and sulphur. These major ion concentrations were different to a study conducted by Astrom and Bjorklund (1995), where the principal abundant ions (in descending order) were sulphur, calcium, silicon, magnesium, sodium, aluminium, potassium and iron. In Table 7.5.1, the principal abundant ions (in decreasing order), were magnesium, sodium, calcium, potassium, aluminium, iron and silica. The differences between these samples was based on the relevant abundance of ions, where the dominant elements were those of the alkali and alkaline earth metals, which was related to the geology of the area (*i.e.* alkali feldspars). As a result, acid sulphate soils were not the primary soil type in these nunataks, but, were rather more carbonaceous in composition, with extensive leaching of calcium, potassium, sodium and magnesium, expected products of cation exchange reactions under low pH conditions (Astrom & Bjorklund, 1995).

Given the low concentrations of ions in the Grunehogna control snow sample (Grun1), when compared to an ice sample (JG01), it is suggested that the underlying bedrock/dyke accounts for the observed differences in chemical composition between the two samples (Meiklejohn & Hall, 1997). The Valterkulten sites (J12 and VC1) showed similarities in the composition of ions that were present, although at various concentrations. Increased concentrations at Valterkulten (J12 as opposed to VC1) displayed the influence of increased water availability. Through the addition of meltwater into the meltwater pool, thus, increasing the concentrations of various ions. When comparing these two sites, however, it was clear that the control snow displayed ions that were not present in the lake sample, and vice versa. For example, the lake sample (J12) displayed high concentrations of lithium (37.32 µg/L), sulphur (3440.38 µg/L), chlorine (4167.74 µg/L), bromine (72.79 µg/L). Highly elevated concentrations of boron (110.31 µg/L), sodium (61162.56 µg/L), magnesium (19275.55 µg/L), potassium (124.18 µg/L) and calcium (252.13 µg/L) were also present in J12 while they were present at low levels in VC1. The high concentrations of calcium in J12 occurred due to chemical weathering of rocks and soils that were not covered by snow during summer months, which subsequently drained into the meltwater pool and accumulated there (low values in VC1 control snow sample) (Smith, 1985; Forstner, 1986; Torri *et al.*, 1989; Prendez & Carrasco, 2003).

Interestingly, all of the samples displayed not detected (ND) values of iron. Since biological consumption of iron is not a factor at the majority of these sites (excluding Robertskollen and Valterkulten), one cannot infer that this is a result of reduced iron concentrations being input into the system (Stumpf *et al.*, 2012). The absence of iron in these samples, could be a result of iron not remaining in solution in the system, either as a result of high oxidation rates, or the low nucleation kinetics for iron oxides at low temperatures (strong undercooling) in this particular system (Stumpf *et al.*, 2012).

Since the input of ions (VC1 and JGrun1) into these nunataks (Valterkulten and Grunehogna respectively) was highly differential to the output of ions (J12 and JG01), one can assume that the differences were due to the influence of chemical rock weathering within the system. Since the system was isolated from others and displayed these characteristics, it was safe to assume that this was highly probable. The differences between control samples and snow/ice samples related to the outputs of chemical rock weathering, assuming that the control samples displayed the natural geochemistry of the snow and precipitation in the local areas. Primarily based off a theory in previous studies, where (Bluth & Kump, 1994):

1. the total dissolved solids are primarily the result of runoff,
2. rates of dissolution are controlled by lithology and permeability of the soil and bedrock, and
3. bicarbonate and dissolved silica are the best elements to use to examine chemical weathering.

The idealised reactions for the dissolution of Ca, SO_4 and Na are as follows (Torres *et al.*, 2017):

a) Carbonate dissolution: $2H^+ + CaCO_3 \leftrightarrow Ca^{2+} + H_2CO_3$,
b) Silicate dissolution: $4H^+ + Ca_2SiO_3 \leftrightarrow 2Ca^{2+} + H_4SiO_4$,
c) Carbonic acid: $CO_{2\,(diss)} + H_2O \leftrightarrow H_2CO_3 \leftrightarrow 2H^+ + CO_3^{2-}$,
d) Sulphuric acid from sulphide oxidation: $FeS_2 + 15O_2 + 14H_2O \leftrightarrow 16H^+ + 8SO_4^{2-} + 4Fe(OH)_3$, with evaporites having the possibility to contribute to Ca and SO_4.

The increased magnesium ions noted in all ice, lake, and snow samples in comparison to control snow samples were a by-product of the solution of alkali feldspars in these areas, through the contribution of snow melt (Meiklejohn & Hall, 1997). The sulphate ions present in only the Grunehogna ice sample (JG01) and the Valterkulten lake sample (J12) are, however, not from the dissolution of alkali feldspars, rather, these sulphate ions originate from the re-solution of gypsum (Grunehogna) and calcite (Valterkulten) (Meiklejohn & Hall, 1997). A study by Meiklejohn and Hall (1997) in Viking Valley, Alexander Island, sampled of solutes in water flow upon analysis of standing water samples (such as Valterkulten), the ion concentrations were 10 times greater than the stream water (snow in this case). Due to the water remaining in contact with bedrock longer than the stream water (snow) resulting in a greater amount of solution (Meiklejohn & Hall, 1997). High concentrations of calcium, such those found at Valterkulten, J12 (252.13 µg/L) suggested more carbonate weathering than silicate weathering at this site (Torres *et al.*, 2017). The concentrations of carbonate weathering were likely derived from calcite cement and alkali feldspars, with low temperatures enhancing the solubility of calcite (Meiklejohn & Hall, 1997). The key observation from Meiklejohn and Hall (1997) was the influence of total residence time where water was in contact with bedrock, enhancing chemical processes in these situations. As such, moisture from snowmelt was likely to both facilitate and accelerate mechanical and chemical weathering, with the re-deposition of gypsum precipitates along drainage lines/cleavage planes indicating both evidence of chemical weathering, and of the transport of these precipitates in solution (Meiklejohn & Hall, 1997).

Table 7.5.1: Concentrations (μg/L) of detected metals for 10 sites

	Control snow	Ice	Lake	Control snow	Snow					Control snow
Detected Metals (μg/L)	**JGrun1**	**JG01**	**J12**	**VC1**	**001J**	**002J**	**JF1/2**	**JF4**	**J02**	**J04**
Li	-	-	37.32	-	-	-	-	-	-	-
B	-	-	110.31	2.48	-	-	-	-	-	-
Na	-	817.89	61162.56	666.97	670.04	968.51	278.69	327.04	322.06	175.58
Mg	21.54	1402.56	19275.55	342.04	67.94	136.88	198.16	231.86	96.22	21.64
Al	-	17.81	-	-	-	-	-	-	-	-
P	-	-	-	0.88	-	-	-	-	-	-
S	-	251.13	3440.38	-	-	-	-	-	-	-
Cl	-	-	4167.74	-	-	-	-	-	-	-
K	-	21.87	124.18	7.66	-	-	7.06	2.20	2.41	7.79
Ca	19.09	25.54	252.13	1.14	8.74	-	-	1.99	0.66	-
V	-	-	0.77	-	-	0.09	0.09	-	-	-
Cr	0.16	-	2.78	1.58	-	-	-	-	-	-
Mn	3.68	27.81	3.73	3.69	4.76	5.83	4.45	3.36	2.91	1.65
Co	-	-	-	0.07	-	0.06	0.18	-	-	-
Ni	-	-	-	-	-	0.18	-	-	-	-
Cu	-	1.36	3.00	0.18	-	0.67	1.68	0.64	1.74	0.46
Zn	7.08	-	-	3.54	1.07	0.16	8.81	64.51	11.12	11.61
Ga	-	-	-	-	0.11	-	-	-	0.11	-
As	-	-	-	-	-	0.71	0.71	-	0.71	-
Br	4.10	-	72.79	-	-	-	-	-	-	-
Sr	0.70	13.92	30.49	2.40	0.65	1.28	1.47	2.26	1.16	0.22
Y	-	-	-	-	-	-	-	-	-	0.07
Zr	-	0.14	0.14	0.14	0.14	0.14	0.14	-	0.14	0.14
Mo	-	-	-	-	0.30	0.30	0.30	0.30	0.30	0.30
Ru	-	-	0.12	0.13	-	-	-	-	-	-
Ag	0.02	0.02	-	0.02	-	0.02	0.11	-	-	-
In	-	0.06	-	-	-	-	0.06	-	-	-
Sn	-	-	-	0.19	0.19	0.19	0.19	0.19	0.19	0.19
Sb	-	-	-	0.15	-	0.15	0.15	0.15	0.15	0.15
I	1.49	5.74	30.05	-	-	0.10	2.56	-	1.72	2.98
Ba	-	-	-	-	0.51	-	-	-	0.51	-
Ir	-	-	-	-	-	-	-	0.04	0.04	-
Au	0.17	-	0.55	0.59	-	0.19	0.30	-	0.06	0.36
Hg	0.06	-	-	-	-	-	0.06	-	-	-
Bi	-	-	-	0.09	-	0.09	0.09	0.09	0.23	-
U	-	-	-	-	-	0.03	0.03	0.03	0.03	0.03

Table 7.5.2 displayed the PCA output values for the first four principal components, including the eigenvalues (which give the relative length of each eigenvector) (McKillup & Dyar, 2010). When considering that the eigenvalues gave the relative length of the eigenvectors, a hyper ellipsoid is produced (McKillup & Dyar, 2010). The hyper ellipsoid was non-spherical (Fig. 7.5.1), and as such, the variables showed redundancy, and that PCA has successfully reduced the number of variables (McKillup & Dyar, 2010). Additionally the percentage of variation for each principal component was displayed, as well as the relative contribution of the original variables to each eigenvalue (McKillup & Dyar, 2010). Since several of the initial variables were highly correlated, PC1 explained 42.8% of the variation among elements at various study sites (McKillup & Dyar, 2010). As such, PC2 explained 13.4% of the variation, PC3 explained 11.2% of the variation and the fourth, PC4, explained 9.5% of the variation. Thus, 67.4% of the variation among sites could be described by a three dimensional ellipse, with axes of PC1-PC3. This ellipse would approximate an elongated, not very wide, even less thick

object suspended in a three dimensional space, with the remaining dimension contributing little to the shape (McKillup & Dyar, 2010). Since PC1 and PC2 explained 56.2% of the variation, a two dimensional plot was created (Fig. 7.5.1), whereby the closeness of the elements in two dimensions gave an average indication of their similarities (McKillup & Dyar, 2010).

Table 7.5.2: Principal components elemental analysis summary

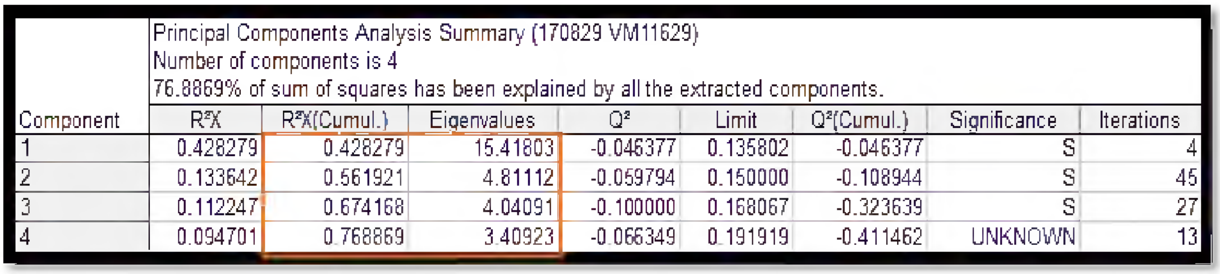

Principal Components Analysis Summary (170829 VM11629)
Number of components is 4
76.8869% of sum of squares has been explained by all the extracted components.

Component	R^2X	R^2X(Cumul.)	Eigenvalues	Q^2	Limit	Q^2(Cumul.)	Significance	Iterations
1	0.428279	0.428279	15.41803	-0.046377	0.135802	-0.046377	S	4
2	0.133642	0.561921	4.81112	-0.059794	0.150000	-0.108944	S	45
3	0.112247	0.674168	4.04091	-0.100000	0.168067	-0.323639	S	27
4	0.094701	0.768869	3.40923	-0.066349	0.191919	-0.411462	UNKNOWN	13

The relative lengths of the two axes in Fig. 7.5.1, depended upon the strength of the correlation between the two variables, with highly correlated data enclosed by a long, narrow ellipse and weakly correlated data enclosed by a more circular ellipse (McKillup & Dyar, 2010). If a more circular ellipse was present, both variables were not correlated and the first and second eigenvectors would have similar values, with neither of these values being able to be used by themselves as a good indication of the differences among sites (McKillup & Dyar, 2010). If a narrow ellipsoid was present (Fig. 7.5.1), the two variables were found to be highly correlated, with the first eigenvector being long with a high eigenvalue (PC1, Table 7.5.2), while the second will be relatively short and with a small eigenvalue (PC2, Table 7.5.2). Since this was the case as shown in both Table 7.5.2 and Fig. 7.5.1, the new combined variable of the first eigenvector was used as a good indicator of the differences among sites (McKillup & Dyar, 2010). As such, Fig. 7.5.1 displayed two differences in correlations of various elements throughout the sites, where those such as silver (Ag) and yttrium (Y) were correlated while chlorine (Cl) and bromine (Br) were not correlated. From Fig. 7.5.1 it is clear that PC2 did not explain much of the variation among the samples, as the elements were widely dispersed around the axis (short eigenvector), as opposed to PC1 which had more elements closer to its axis (largest eigenvector) (McKillup & Dyar, 2010).

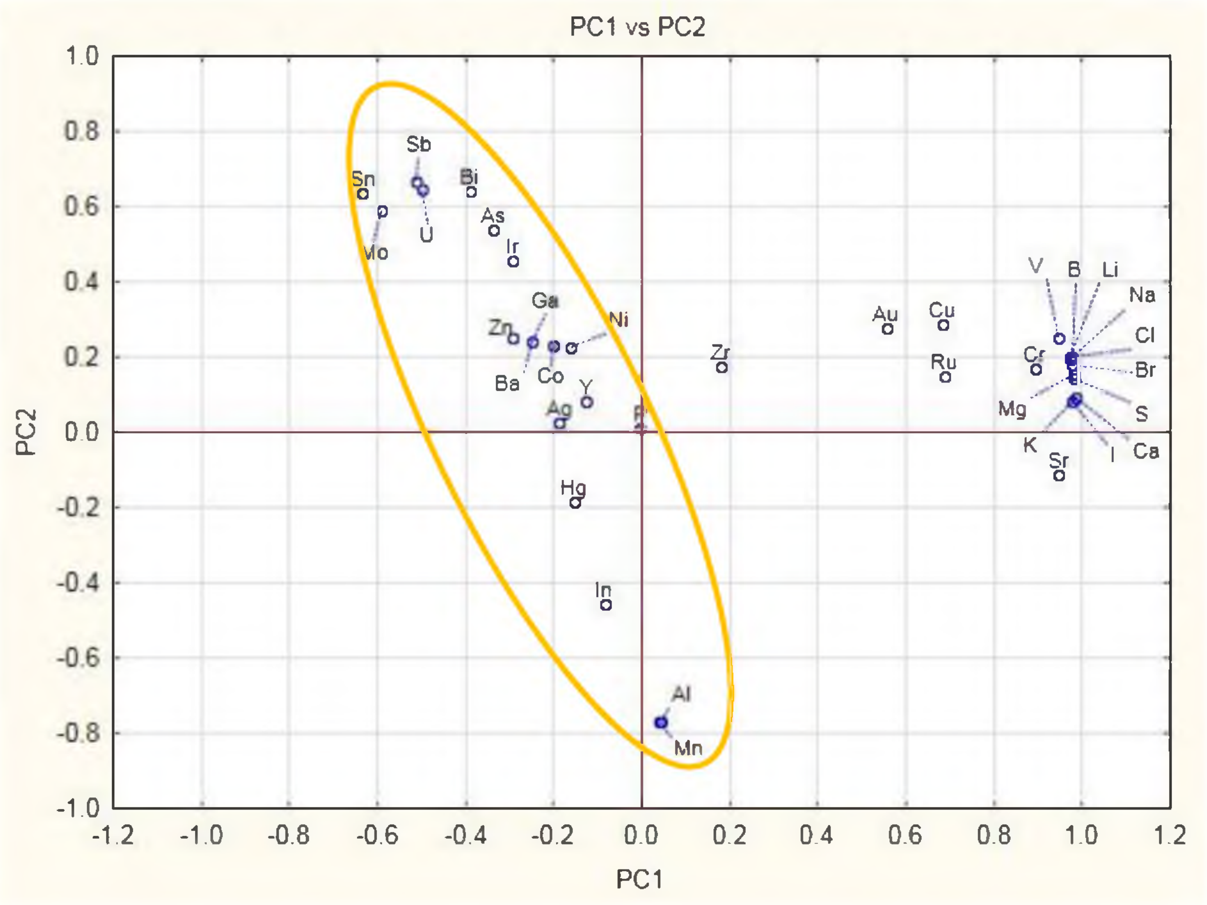

Figure 7.5.1: Principal component 1 and 2 for various elements across all study sites

From Table 5.7.3, a correlation value of 0.25 was deemed important (explained 75% of the variation) and it was clear that PC1 was primarily composed of variables 4 (Mg), 7 (S), 9 (K) and 10 (Ca), the four highest positive correlations (McKillup & Dyar, 2010). The signs of the correlations were of importance, as they demonstrated the relationships between elements. PC1 was seen to correlate most highly with calcium (0.251), and that as one value increased proportionally so do the remaining elements at each site. Therefore, study sites which have high values of calcium were likely to have high values of magnesium, sulphur and potassium. An example of where this occurred was Valterkulten (J12) (Table 7.5.3), where these values were particularly high. Component 2 was largely composed of variables 5 (Al), 13 (Mn) and 29 (Sb), of which only variable 29 was positive of the three. Aluminium was the most highly correlated variable in PC2 (-0.350), displaying a different trend whereas aluminium decreased so did manganese, while antimony increased. Therefore, sites that had these variables were likely to display the same trends. This was seen for example at Grunehogna (JGrun1) (Table 7.5.3), where the value of aluminium was the highest among all samples (17.81 µg/L), while the value of manganese was highest among the sites (27.81 µg/L) and antimony are low (not detected), validating the PCA analysis. Component 3 was only composed of variable 14 (Co), which was positive. As cobalt increases, various other elements either increased or decreased, however, at a less significant level. Finally, component 4 was composed of variables 16 (Cu) and 33 (Au), of which the former was positive and the latter negative. PC4 portrayed the trend in which copper increased while gold decreased. Since PC3 and PC4 were almost entirely excluded from the principal component analysis due to their redundancy in terms of influence between study sites, they can similarly be excluded from this study.

Table 7.5.3: Principal components correlation coefficients, their original variables, and the elements they represent.

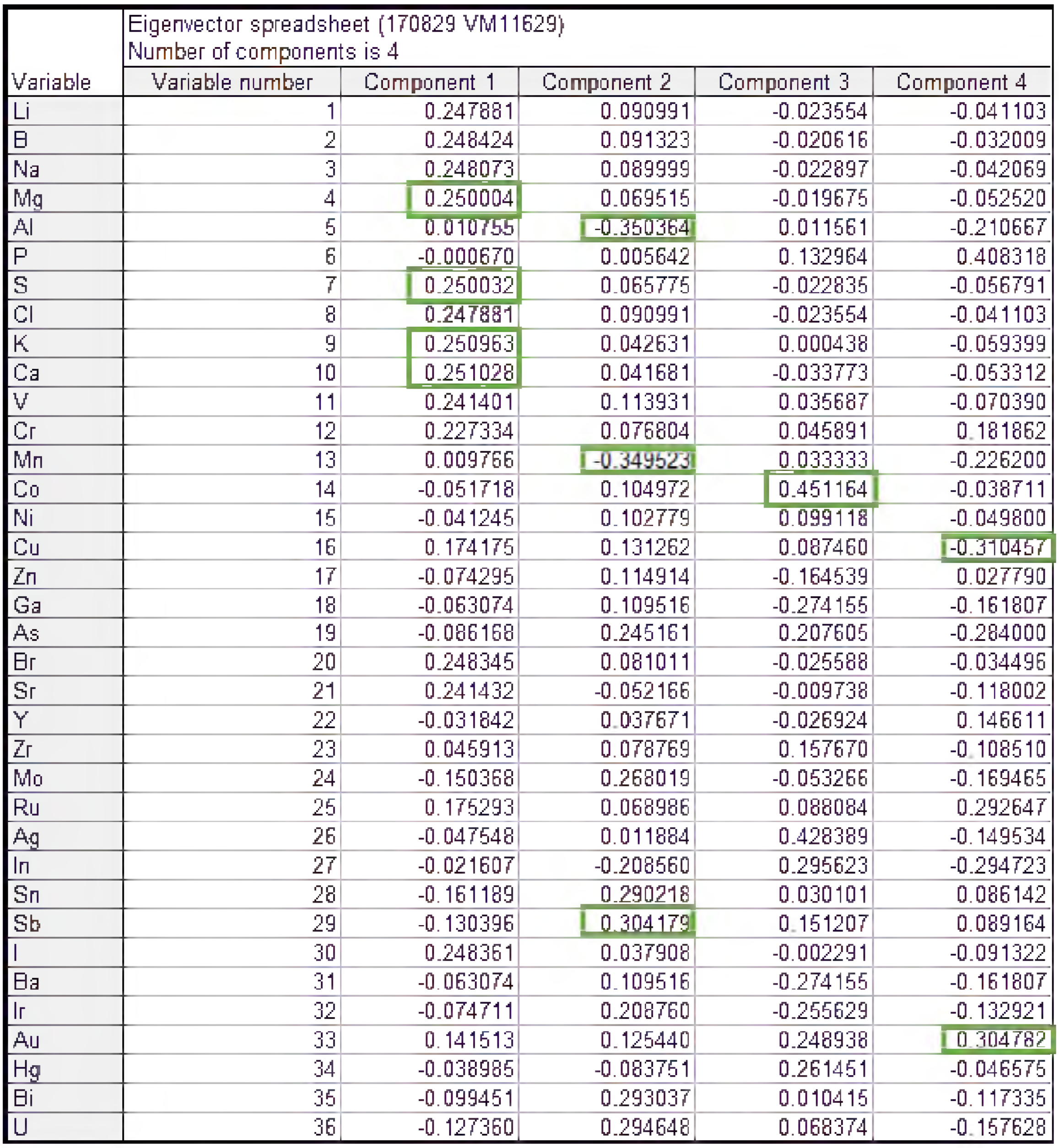

Eigenvector spreadsheet (170829 VM11629)
Number of components is 4

Variable	Variable number	Component 1	Component 2	Component 3	Component 4
Li	1	0.247881	0.090991	-0.023554	-0.041103
B	2	0.248424	0.091323	-0.020616	-0.032009
Na	3	0.248073	0.089999	-0.022897	-0.042069
Mg	4	0.250004	0.069515	-0.019675	-0.052520
Al	5	0.010755	-0.350364	0.011561	-0.210667
P	6	-0.000670	0.005642	0.132964	0.408318
S	7	0.250032	0.065775	-0.022835	-0.056791
Cl	8	0.247881	0.090991	-0.023554	-0.041103
K	9	0.250963	0.042631	0.000438	-0.059399
Ca	10	0.251028	0.041681	-0.033773	-0.053312
V	11	0.241401	0.113931	0.035687	-0.070390
Cr	12	0.227334	0.076804	0.045891	0.181862
Mn	13	0.009766	-0.349523	0.033333	-0.226200
Co	14	-0.051718	0.104972	0.451164	-0.038711
Ni	15	-0.041245	0.102779	0.099118	-0.049800
Cu	16	0.174175	0.131262	0.087460	-0.310457
Zn	17	-0.074295	0.114914	-0.164539	0.027790
Ga	18	-0.063074	0.109516	-0.274155	-0.161807
As	19	-0.086168	0.245161	0.207605	-0.284000
Br	20	0.248345	0.081011	-0.025588	-0.034496
Sr	21	0.241432	-0.052166	-0.009738	-0.118002
Y	22	-0.031842	0.037671	-0.026924	0.146611
Zr	23	0.045913	0.078769	0.157670	-0.108510
Mo	24	-0.150368	0.268019	-0.053266	-0.169465
Ru	25	0.175293	0.068986	0.088084	0.292647
Ag	26	-0.047548	0.011884	0.428389	-0.149534
In	27	-0.021607	-0.208560	0.295623	-0.294723
Sn	28	-0.161189	0.290218	0.030101	0.086142
Sb	29	-0.130396	0.304179	0.151207	0.089164
I	30	0.248361	0.037908	-0.002291	-0.091322
Ba	31	-0.063074	0.109516	-0.274155	-0.161807
Ir	32	-0.074711	0.208760	-0.255629	-0.132921
Au	33	0.141513	0.125440	0.248938	0.304782
Hg	34	-0.038985	-0.083751	0.261451	-0.046575
Bi	35	-0.099451	0.293037	0.010415	-0.117335
U	36	-0.127360	0.294648	0.068374	-0.157628

7.5.2 pH and electrical conductivity

All of the samples analysed were acidic (pH<7) (Table 7.5.4) with the least acidic being that of Valterkulten (J12) (6.19 mol/L) and the most acidic being Flårjuven (JF1/2) (4.42 mol/L). The average pH for all the samples was 5.05 mol/L with the highest average per sample site being that of Valterkulten (6.06 mol/L), while Flårjuven (4.46 mol/L) was the lowest average per sample site. Lakes or streams in catchments which acidify contain the products of leached chemical components, typically a result of hydrologic and geologic characteristics of the environment (Giovanoli *et al.*, 1988; Astrom & Bjorklund, 1995). According to Giovanoli *et. al.* (1988), this occurs as "chemical weathering is unable to supply sufficient denudation products from rock forming minerals to neutralise incipient acid deposition and protons, which are supplied by other chemical processes". Solute trends are thus influenced by the dissolution of salts and carbonates in bulk sediments (Marra *et al.*, 2017). pH cannot be analysed in isolation as it is typically related to the electrical conductivity (E.C.) of the sample, whereby as pH values increase so do the electrical conductivity readings (Meiklejohn & Hall, 1997). For example, Valterkulten sample J12 (Table 7.5.4) displayed the highest pH value 6.19 mol/L, and also displayed the highest E.C. value (797 µs) these readings were possibly a result of increased alkalinity in this sample, resultant from augmented calcium and magnesium ion concentrations (Meiklejohn & Hall, 1997). When comparing the calcium and magnesium ion concentrations between this site and the nine others (Table 7.5.4) it became clear that this site, had the highest calcium and magnesium concentrations. Since this site was also a meltwater pool, it was possible for augmentation of calcium and magnesium to occur on the pool bottom. Although to test this argument, meltwater pool coring samples needed to be examined.

E.C. and total dissolved solids (T.D.S.) have a direct relationship to one another, through T.D.S. measuring the concentration of solutes (ppm) and E.C. measuring the relative conductivity of these solutes in the water (µs). Essentially as one value increases the other increases proportionally. The sample with the highest T.D.S. value (Table 7.5.4) was Valterkulten, J12 (510 ppm) while the lowest T.D.S. value was Grunehogna (JGrun1) with 3.05 ppm. The remainder of the samples were confined to a range of 4-17 ppm, except for Grunehogna (JG01) that displayed a T.D.S. value of 23.4 ppm. From the above interpretation it is safe to say that Valterkulten the site with the highest T.D.S. values and Grunehogna follows second, while the lowest T.D.S values were those of Vesleskarvet (J02 and J04).

Two arguments were put forward to explain T.D.S. values, one by Gibbs (1970) and another by Stallard and Edmund (1983), which contradict one another. Gibbs (1970) argued that the dissolved load (T.D.S.) in rivers is controlled by atmospheric precipitation, evaporation/mineral precipitation and rock weathering (Walther, 2005). While Stallard and Edmund (1983) argued that river solute concentrations were influenced by bedrock geology and extent of erosion. The main difference between these two suggestions was the argument about the influence of geology/atmosphere and the importance of previously weathered material contributing to $Na^{+}/(Na^{+} + Ca^{2+})$ values (Fig. 9.3).

Table 7.5.4: pH, electrical conductivity and total dissolved solids of selected samples at 13 sites

Sample Number	Name	Type of sample	pH (mol/L)	pH temp (°C)	E.C (µs)	E.C temp (°C)	TDS (ppm)
1	JGrun1	Control snow	4.47	17.1	4.76	17.3	3.05
2	JG01	Ice sample	5.93	16.8	36.6	17.2	23.4
3	J12	Lake sample	6.19	17.1	797	17.2	510
4	VC1	Control snow	5.92	17.4	15.92	17.7	10.2
5	001J	Snow sample	4.53	17.2	19.26	17.5	12.3
6	002J	Snow sample	4.53	17.4	19.55	17.6	12.5
7	JF1/2	Snow sample	4.42	17.2	12.28	17.5	7.86
8	JF4	Snow sample	4.49	17	11.99	17.3	7.67
9	J02	Snow sample	5.38	17	8.31	17.2	5.32
10	J04	Control snow	4.75	17	6.7	17.2	4.29
11	JenVes01	Snow sample	4.92	17.3	26.1	17.4	16.7
12	JenVes02	Snow sample	4.95	17.1	8.58	17.3	5.49
13	JP2	Snow sample	5.24	17.4	19.91	17.5	12.7

The chemistry of Slettfjell (002J) displayed the greatest influence of atmospheric precipitation dominance (Fig. 7.5.3) with the sodium to calcium ratios being the highest for this sample. JG01 (Grunehogna) was classified in this section of graph as being atmospheric precipitation dominant, although at a lower $Na^{+}/(Na^{+} + Ca^{2+})$ ratio and with increased T.D.S. and thus, a higher conductivity. When interpreting T.D.S. values Gibbs (1970) argued that samples with low T.D.S value were precipitation dominant and had a high $Na^{+}/(Na^{+} + Ca^{2+})$ ratio while, rock weathering increased the T.D.S. and decreased the $Na^{+}/(Na^{+} + Ca^{2+})$ ratio in river water (Walther, 2005). With the evaporation of river water T.D.S. hence, increases further and calcite precipitates, subsequently increasing the $Na^{+}/(Na^{+} + Ca^{2+})$ ratio in the water (Gibbs, 1970; Walther, 2005). The positioning of these two samples within this Gibbs plot suggests the possible importance of upper air circulation patterns and deposition and the possible influence of marine aerosols (Green *et al.*, 1988). An argument against the possibility of marine aerosol deposition for these two sites, however, is the extreme distance from the coast and that the two sites experience prevailing winds that are easterly (*i.e.* Slettfjell and Grunehogna respectively). Slettfjell was the furthest sample site and hence, the furthest from marine inputs. If marine aerosols were the main source of these sodium concentrations one would expect to see much higher concentrations (Stumpf *et al.*, 2012). This site, however, is highly influenced by wind originating from the Antarctic Plateau, perhaps these minerals are from the region that has yet to be studied and is merely being deposited on this nunatak. Slettfjell, however, is not isolated from chemical weathering as there was evidence of salt weathering on rocks found on top of this nunatak (Fig. 7.2.13). These precipitates were relatively small and characteristically white, an indication of possible calcium deposition. This is more than likely where the calcium in the Slettfjell 002J (Fig. 7.2.12) sample has come from and not through aerosol deposition. Similar results were noted in a study in Taylor Valley, Antarctica, where carbonates were the more likely source of high sodium/calcium ratios (such as 002J) where clasts were commonly coated in carbonate (Stumpf *et al.*, 2012).

The Grunehogna sample, however, possibly displays these values due to the overlying rock from where the sample occurred. Stallard & Edmond (1983) argued that bedrock geology and the extent of erosion were the main factors controlling the input of river solute concentrations (Walther, 2005). Subsequently, rivers with low T.D.S. values and $Na^{+}/(Na^{+} + Ca^{2+})$ ratios were a result of weathering from relatively unreactive siliceous igneous and metamorphic rocks which had already undergone weathering (Walther, 2005). High T.D.S. values and high $Na^{+}/(Na^{+} + Ca^{2+})$ ratios such as Grunehogna (JG01) (Table 7.5.4) thus, resulted from evaporite weathering (they already have high Na:Ca ratios) even when exposed in a small percentage of the area (Walther, 2005). High $Na^{+}/(Na^{+} + Ca^{2+})$ and $SO_4 : Na$ ratios together, suggest carbonate and sulphide dissolution rates were enhanced in this sample (Torres *et al.*, 2017). These results suggest that weathering reactions have been shifted towards the release of carbon dioxide, rather than it's consumption (Torres *et al.*, 2017).

The Grunehogna (JG01) sample was wedged underneath a section of intrusive dyke, which had obvious depositions of gypsum ($CaSO_4$) whereby sulphide has been deposited as sulphate. As such sulphide-carbonate weathering had released carbon dioxide into the ocean-atmosphere system(Torres *et al.*, 2017). Influencing global budgets of redox-sensitive elements such as iron, sulphur and oxygen, with their rates of dissolution orders of magnitude faster than those that undergo silica weathering (Torres *et al.*, 2017).

When considering the statistical clustering of samples, the majority of samples taken from the geographical location fell within the same regions on the Gibbs plot (purple circles in Fig. 7.5.3) (Green *et al.*, 1988). This clustering identified small differences between control samples and snow/ice samples from the relevant sites. For example Robertskollen (J02 and J04) with less $Na^+/(Na^+ + Ca^{2+})$ being input into the environment; possibly an indicator of little chemical weathering occurring at these sites. In the case of Robertskollen this was true as, no chemical precipitates were present on this nunatak, but larger areas of rock displayed weathering rinds, case hardening and the presence of liquid water (Fig. 7.5.2). The differences between the samples at Robertskollen J04 (control) and J02 (snow) although small, were apparent, with J02 having a higher concentration of $Na^+/(Na^+ + Ca^{2+})$ than J04 and slightly higher TDS values. Melting of snow (initial stream chemistry) at Robertskollen was apparent through the movement of flowing water, via surficial, glacial and limited subsurface melt. Large volumes of water rapidly resulted in decreasing contact times with sediments so increasing residence times (Runkel *et al.*, 1998; Nezat *et al.*, 2001; Stumpf *et al.*, 2012; Gooseff *et al.*, 2013; Hindshaw *et al.*, 2014; Marra *et al.*, 2015). Connected groundwater systems do not exist at this site, due to the presence of continual permafrost (Runkel *et al.*, 1998; Nezat *et al.*, 2001; Stumpf *et al.*, 2012; Gooseff *et al.*, 2013; Marra *et al.*, 2015). According to Marra *et. al.* (2015) however, "seasonally active layer thaw provides interconnected systems of water tracks at shallow depths beneath the soil surface, which enhances solute contributions to reactivated stream channels" (Conovitz *et al.*, 1998; Fountain *et al.*, 1999; McKnight *et al.*, 2007; Levy *et al.*, 2011). This causes an increase in residence time, likely linked to the slight increase in $Na^+/(Na^+ + Ca^{2+})$ concentrations

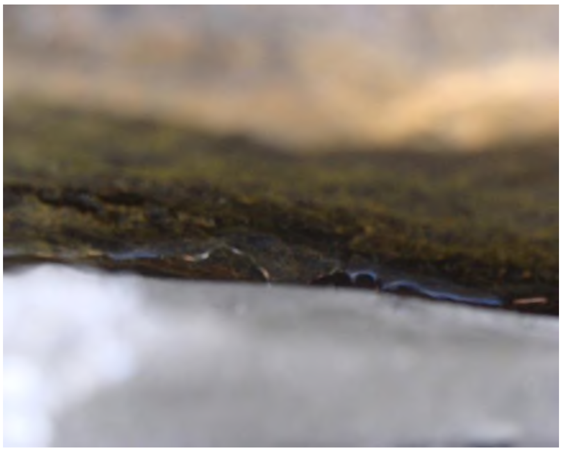

Figure 7.5.2: Liquid water running between rocks and ice at Robertskollen

noted within the Robertskollen sample (J02) as opposed to the control (J04) which, did not experience these stream like characteristics. Another possible reason behind the differences between these two major cation ratios may relate to (Stumpf *et al.*, 2012):

1. primary bedrock mineralogy underlying the streams,
2. water-soluble salts within local drift deposits,
3. dissolution of carbonates within drift deposits, or
4. differences in dust chemistry within melting glaciers.

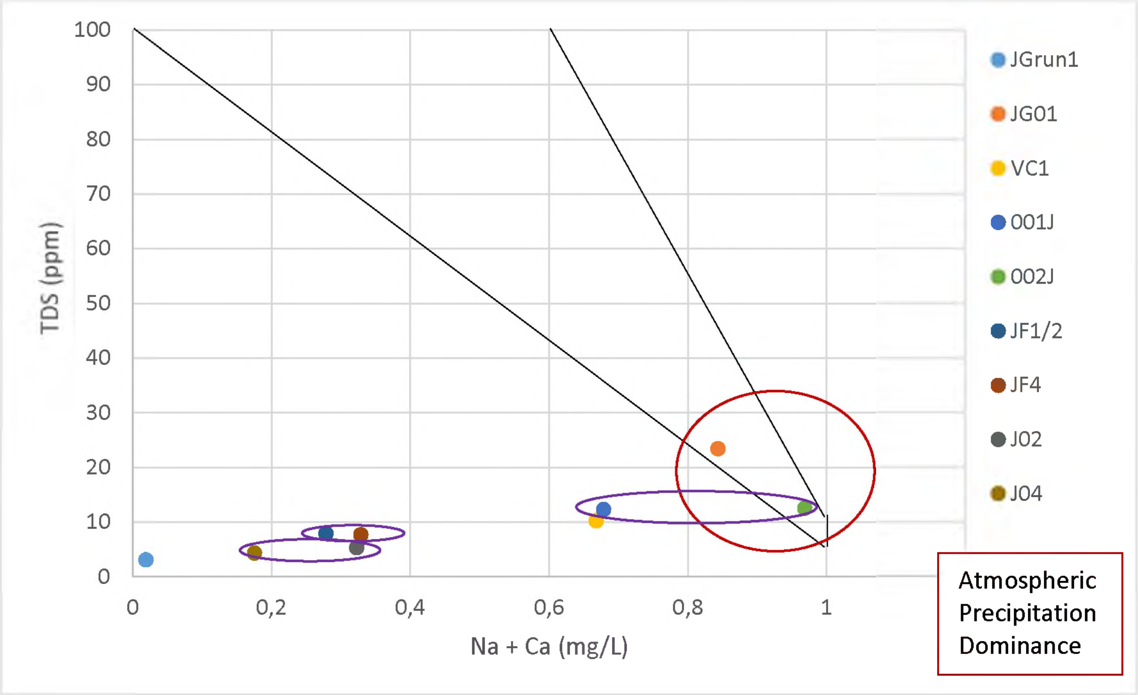

Figure 7.5.3: "Gibbs Plot" of 9 samples (excluding J12), solid line is envelope of world surface waters, Na and Na + Ca concentrations are in mg/l (adapted from Green *et al.*, 1988)

Flårjuven sites displayed a similar characteristic, in that the samples were from two different areas on the nunatak. As such, the influence of primary bedrock mineralogy at this site may differ slightly, due to the intrusive nature of previous bedrock deposition. Flårjuven sample JF1/2 was taken near both JF1 and JF2, an area with few precipitates. Demonstrated by the lower geochemistry values in comparison to JF4, possibly due to the small influence of the addition of ions to the snow in the area. Essentially linking to the influence of water-soluble salts within local drift environments. JF4 displayed a higher value of sodium and calcium; however, the total dissolved solids in both samples from this nunatak were similar. The higher $Na^{+}/(Na^{+} + Ca^{2+})$ values present in JF4 may be a contribution from the amount of precipitates, and their depth (Fig. 7.5.5) at this site. Relating directly to the dissolution of carbonates within drift deposits, and their subsequent reprecipitation upon encountering dry areas, which contain little moisture (Fig. 7.5.4).

Figure 7.5.4: Sample 002J, displaying precipitates in the region of the snow sample used for geochemical analysis

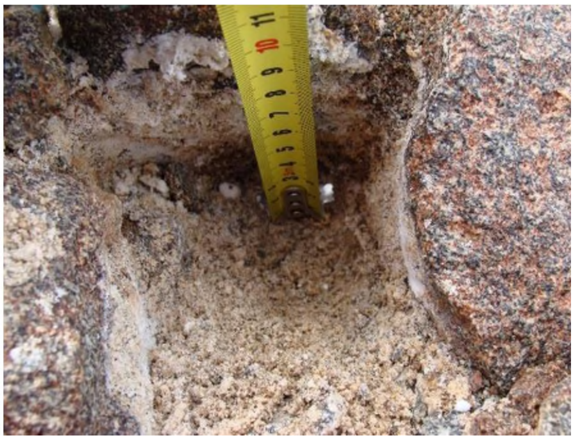

Figure 7.5.5: Depth of precipitates at JF4, a possible influence on the geochemistry of the snow

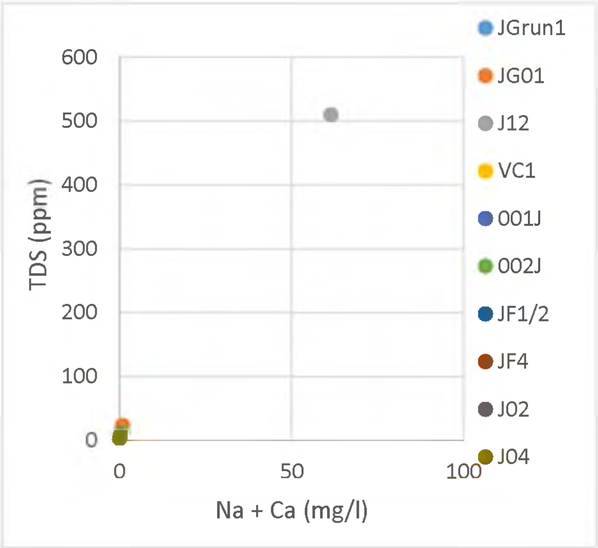

Figure 7.5.6: Gibbs Plot of all samples, displaying the outlier of J12 (Valterkulten)

Fig. 7.5.3 excluded Valterkulten (J12) and this sample represented on a new Gibbs plot (Fig. 7.5.6) as it was a large outlier in regards to the rest of the data, not displaying the relationships, present in Fig. 7.5.3. There were no clustering of samples as previously seen (Fig. 7.5.3); however, a relationship was present between the samples of each nunatak. Control samples such as Grunehogna (JGrun01) and Valterkulten (VC1) both had fewer $Na^+/(Na^+ + Ca^{2+})$ ions and lower T.D.S. than their sampled counterparts JG01 and J12 respectively (Fig. 7.5.3 and 7.5.6).

The Grunehogna samples (Fig. 7.5.3) displayed a large difference in both TDS and sodium and calcium concentrations between the control and ice sample (20.35 ppm and 0.82mg/l). While Valterkulten had similar, although elevated results between the control and lake sample for TDS and ion concentrations (499.8 ppm and 60.75 mg/l). Valterkulten (J12) elevated TDS values and ion concentrations were likely related to the meltwater pool (Fig. 7.5.7) from which the sample was taken.

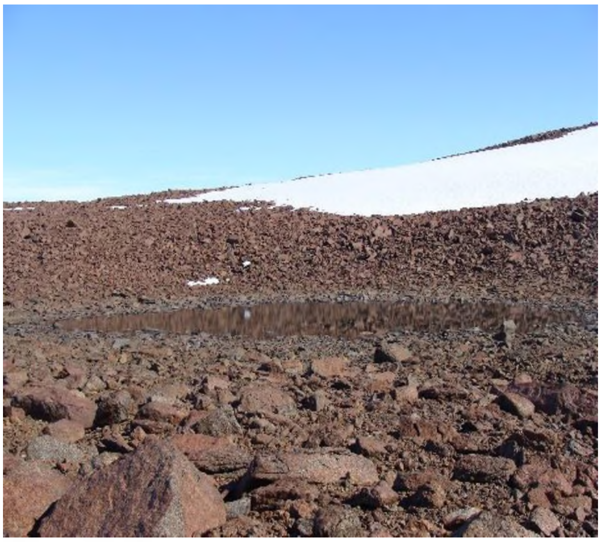
Figure 7.5.7: Valterkulten meltwater pool (24/12/2016)


Figure 7.5.8: Valterkulten meltwater pool (11/01/2017)

The reason why Valterkulten had such high values was related to the lake being a meltwater pool whereby solar warming lead to increased lake temperatures and subsequent evaporation and precipitation of calcite followed by gypsum (Green *et al.*, 1988). Under normal conditions water in the meltwater pool is maintained by the addition of ice, however, during periods of extreme cold, evaporation exceeds water input and the pool shrinks in volume, becoming more concentrated (Green *et al.*, 1988). This increase in concentration is of importance in regards to the temporal scale, as solutes can lower the freezing point (Fig. 7.5.8) such as in the Valterkulten meltwater pool and change the availability of water (Washburn, 1979). As such, temporal variation occurs, with increased water input during warmer, summer months as a result of increased snow surface melting (Hindshaw *et al.*, 2014). As water levels fall, however, lacustrine waters become more concentrated with basin wide precipitation of calcium carbonate occurring (Hall *et al.*, 2000; Whittaker *et al.*, 2008; Green & Lyons, 2009; Stumpf *et al.*, 2012). In relation to this, a study conducted by Bell (1966) found that major elements in Lake Miers, Antarctica, were predominantly calcium and bicarbonate, with the lake bottom possibly being covered in an indurated layer of calcium carbonate (although this was not cored in the study, nor was the Valterkulten meltwater pool) (Green *et al.*, 1988).

"Meltwater exchange with sediments primarily occurs within the hyporheic zone of reactivated stream channels, also known as the saturated area, underlying and adjacent to the streambed, where water can flow before encountering permafrost" (Fountain *et al.*, 1999; Gooseff *et al.*, 2002; Gooseff *et al.*, 2013; Stumpf *et al.*, 2012; Marra *et al.*, 2017: 14). Furthermore, shallow groundwater features (water tracks, snowmelt, lake and stream margins) limit water-rock interaction to the immediate hyporheic zone, mobilising solutes and providing conditions for biotic growth and biogeochemical cycling (Barrett *et al.*, 2009; Levy *et al.*, 2011; Stumpf *et al.*, 2012; Gooseff *et al.*, 2013; Mikucki *et al.*, 2015; Marra *et al.*, 2017). It is important to note, however, that both Valterkulten (J12, Fig. 7.5.7 and Fig. 7.5.8) and Robertskollen (J02, Table 7.5.1) are not sterile environments, as they contained black algae on the periphery of the pool and in the stream channels. Algal communities cause $CaCO_3$ precipitation, these organisms are known to influence the chemistry of the waters, for example through photosynthesis, respiration and nutrient uptake (McKnight *et al.*, 2004; McKnight *et al.*, 2007; Stumpf *et al.*, 2012; Marra *et al.*, 2015). Lake waters, thus, have a raised pH as a result of calcium carbonate precipitates being deposited onto the lake floor (Hall *et al.*, 2000; Stumpf *et al.*, 2012). This is noted in Table 7.5.4 where at Valterkulten (J12, lake sample) had a pH of 6.19 while VC1 (control snow) had a pH value of 5.92. The influence of the algal communities however, do not act in isolation, but rather was and additional contributing factor to the increase in pH in the meltwater pool. In the McMurdo Dry Valleys, for example, biotas that are present are generally restricted to algae, mosses and cyanobacteria (Marra *et al.*, 2017), similar to what is expected to be found in western Dronning Maud Land. McMurdo Dry Valleys have perennial algae, which grow within streams as mats, with the ability to survive long periods of desiccation (McKnight *et al.*, 1999; McKnight *et al.*, 2004; Marra *et al.*, 2017). In order to determine the types of algal communities present in the meltwater pool, samples will need to be taken and further analysis is necessary.

From the above geochemical analyses it was clear that chemical weathering processes were active in western Dronning Maud Land and that they may possibly have a significant impact on stream, meltwater pool and bedrock alteration in cold environments (Meiklejohn & Hall, 1997; Stumpf *et al.*, 2012). The wide variation in contents of the ICP analysis and T.D.S. values suggest that these values can be attributed to local conditions (such as soil, water and atmospheric aerosols) at each site (Prendez & Carrasco, 2003). Thus, high rock temperatures and meltwater flow during summer, produced an environment which was highly conductive and subsequently impacted by chemical weathering (Meiklejohn & Hall, 1997). Solutes analysed through ICP-MS were attributed to the dissolution of carbonates and salts, where weathering of silicate minerals occurred within the hyporheic soil sediments and stream channels (Lyons *et al.*, 1998; Gooseff *et al.*, 2002; Stumpf *et al.*, 2012; Marra *et al.*, 2017). An increase in pH and ion concentrations of lake waters was attributed to the influence of fluctuating water levels, algal communities and shallow groundwater features, which influenced the rock-water interaction. The prevalence of high $Na^{+}/(Na^{+} + Ca^{2+})$ and $SO_4 : Na$ ratios together, suggested enhanced carbonate and sulphide dissolution rates at the Grunehogna site (Walther, 2005). Where weathering reactions shifted towards the release of carbon dioxide, hence, sulphide-carbonate weathering influenced global budgets of redox-sensitive elements, such as iron, sulphur and oxygen, with rates of dissolution orders of magnitude faster than silica weathering (Torres *et al.*, 2017).

Overall, the majority of sites experienced silica and salt weathering, while Grunehogna was characterised by carbonate and sulphide based weathering processes, and Valterkulten displayed processes concurrent with calcium carbonate deposition on the meltwater pool floor. Flårjuven, displayed high $Na^{+}/(Na^{+} + Ca^{2+})$ values, which may be a contribution from the amount of precipitates, and their depth found at this site. These results related directly to the dissolution of carbonates, and subsequent reprecipitation upon encountering dry areas, with little moisture. Robertskollen was highly influenced by above surface water flow, as permafrost limited the movement of groundwater flow. Fast moving water channels decreased contact time between rock-water interactions, and as such, contributed a small amount to changing the pH and ion concentrations of calcium and sodium in these waters.

7.6 Microscopic and micro-chemical (EDS) analysis

Microscopic and micro-chemical analyses provided the means to identify areas of chemical weathering and weathering rind production. Quantification of the minerals found at the external surface in comparison to the internal surface, and underlying host rock provided information on the processes responsible at various sites. Differences between sites were indicative of external factors and site-specific processes.

The results of the micro-chemical analysis were here reported as element wt.% normalized to 100%. The data tables excluded oxygen and carbon, which cannot be reliably be quantified using EDS. In this investigation the main purpose was to determine the overall presence of different major element species and to identify mineral phases. The exclusion of oxygen and carbon resulted in exaggerated cation contents in carbonates, which to 44 wt.% consist of CO_2. Also in the oxidic and silicic phases the data presentation lead to exaggerated cation percentages that do not reflect mineral compositions as they were usually reported in the geological literature. However, for the purpose of determining possible element mobility as an effect of weathering, the proposed way of data reporting was adequate.

7.6.1 Robertskollen and Lorentzenpiggen

The dolerite of Robertskollen was primarily composed of apatite, augitic clinopyroxene, baddeleyite, biotite, orthopyroxene, ilmenite, potassium feldspar, plagioclase and quartz. The mineral phases contained Na (plagioclase), Ca, Al, Si, Fe, Ti (in ilmenite), and some Mg (Table 7.6.1). The typical grain size was 50µm-500µm (Fig. 7.6.1). Dolerite of Lorentzenpiggen was composed of augitic clinopyroxene (fresh and altered) and diopside. The mineral phases contained Si, Ca, Fe, Mg and small quantities of Al (Table 7.6.2). Typical grain size within this sample was 50µm-500µm.

Table 7.6.1: Wt.% composition of Robertskollen (Knox 3)

Spectrum	Na	Mg	Al	Si	S	Cl	K	Ca	Ti	Fe	Total
Apatite	0.1	0.1	0.2	2.1	0.3	2.1	0.0	94.2	0.2	0.8	100.0
Augitic Cpx	0.8	11.6	4.0	41.2	0.1	0.9	0.7	15.7	0.9	24.3	100.0
Baddeleyite	0.0	3.1	14.9	0.0	0.0	0.0	0.0	7.4	29.7	44.9	100.0
Biotite	0.2	12.4	11.0	32.5	0.0	1.1	12.7	0.2	4.1	25.7	100.0
Enstatitic Opx	0.1	18.7	0.7	44.8	0.1	0.0	0.0	2.3	0.5	32.8	100.0
Ilmenite	0.0	0.1	0.1	0.0	0.0	0.0	0.0	0.2	42.8	56.8	100.0
Ilmenite	0.0	0.1	0.0	0.2	0.0	0.0	0.0	0.1	43.6	55.9	100.0
Kfs-Pl mix	4.9	0.1	24.0	52.9	0.1	0.1	1.4	15.3	0.1	0.9	100.0
Kfs-Pl mix	4.3	0.3	22.4	52.7	0.0	0.0	5.0	13.7	0.0	1.6	100.0
Plag	4.0	0.1	24.9	50.8	0.1	0.4	0.7	17.7	0.0	1.2	100.0
Plag	4.8	0.0	24.7	51.3	0.1	0.0	0.5	17.0	0.2	1.3	100.0
Plag	6.0	0.0	23.3	55.1	0.1	0.0	1.0	13.8	0.1	0.6	100.0
Plag (unaltered)	3.5	0.0	27.0	49.0	0.1	0.1	0.2	19.4	0.1	0.7	100.0
Plag (unaltered)	4.0	0.2	24.0	52.6	0.2	0.1	0.5	17.0	0.0	1.5	100.0
Qtz	0.1	0.0	0.0	98.9	0.1	0.0	0.0	0.1	0.1	0.8	100.0
Qtz	0.1	0.0	0.1	98.4	0.1	0.1	0.0	0.1	0.4	0.7	100.0
Qtz	0.1	0.0	0.0	99.6	0.0	0.0	0.0	0.0	0.0	0.2	100.0
Qtz	0.1	0.0	0.0	99.2	0.2	0.2	0.0	0.0	0.0	0.2	100.0
Qtz	0.1	0.0	0.0	98.9	0.1	0.2	0.0	0.2	0.2	0.3	100.0

Table 7.6.2: Wt% composition for Lorentzenpiggen (Knox 4)

Spectrum	Na	Mg	Al	Si	S	Cl	K	Ca	Ti	Fe	Total
Altered Cpx	0.2	13.6	2.2	45.9	1.4	0.0	0.7	23.8	0.3	12.0	100.0
Augitic Cpx (fresh)	0.3	14.3	1.5	44.6	0.1	0.0	0.0	23.6	0.6	14.9	100.0
Augitic Cpx (fresh)	0.4	17.4	1.7	46.5	0.0	0.1	0.0	22.6	0.3	11.0	100.0
Diopside	0.3	11.0	1.5	41.3	0.2	0.0	0.0	29.4	0.8	15.5	100.0
Diopside	0.3	11.5	1.4	41.4	0.3	0.1	0.0	29.4	0.5	15.2	100.0

In transmitted light (thin section, Fig. 7.6.1) the dolerite exhibited mineral phases that were tinged by reddish hues, influencing the opacity. The discolouration was particularly evident in the margins of phases and portrayed a decreasing gradational change from the exterior to the interior. The discolouration was interpreted as a weathering rind.

Compared to the dolerite the weathering rind caused a change in colouration of minerals and the alteration of pore spaces within (Fig. 7.6.1) as seen through the alteration of colour, and thus, composition of the minerals found bordering these zones (Fig. 7.6.2). The weathering rind, occupied a zone larger than 1000µm (Fig 7.6.1) and less than 600µm (Fig. 7.6.2) thick, along the external rock surface displaying a change in colouration from reddish-brown to more opaque in the interior. This was a product of iron (Fe) deposition in the external microns of the films.

Visible alteration in Fig. 7.6.1 and Fig. 7.6.2 displayed the products of weathering. This occurred at the external rock surface and ~1000µm towards the interior of Fig. 7.6.1 and ~1500µm towards the interior of Fig. 7.6.2. The characteristics of this alteration occurred as black-reddish to dusty pigmentation at these external regions. Contrastingly, the interior, more "fresh" minerals were composed of darker hues without red colouration and less opacity (Fig. 7.6.1 and Fig. 7.6.2).

Figure 7.6.1: Opacity changes (clear to reddish-brown) at the external surface of Robertskollen (Knox 3). Arrow indicated the zonation of the discolouration

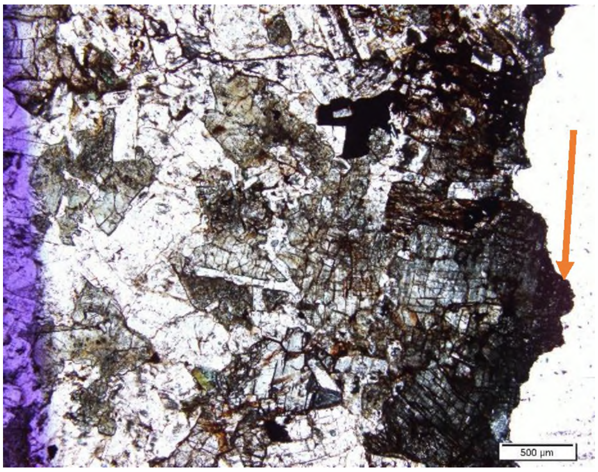

Figure 7.6.2: Changes in the external substrate were noticed within this sample, displaying the characteristic reddish-brown (dark) hues of weathering rind formation (arrow). While the interior was composed of unaltered minerals

SEM back-scattered electron (BSE) images, showed thin, short (5µm-25µm) cracks and holes within the surface topography, which were empty. There were traces of two sets of mineral cleavage planes, oriented at approximately right angles to each other (Fig. 7.6.3).

Minor, isolated, domains rich in aluminum were detected (Fig. 7.6.5). Iron was sporadically distributed, with areas of isolated high concentrations found throughout (Fig. 7.6.8). These areas of iron were in areas of relatively little to no calcium and magnesium, displaying an inverse relationship with these elements. Differences in BSE signal intensity (Fig. 7.6.8 orange circle) indicated small Fe inclusions. Extensive distributions of magnesium occurred throughout the sample, high abundance was confined to analytical artefacts. Decreased magnesium occurred along channelized features (Fig 7.6.4, grey circles) toward the external structure. Calcium, silica and magnesium concentrations were variable with the pyroxenes. Along cleavage planes which were at, a high angle to the rock surface, the concentration of these elements decreased (Fig. 7.6.7, orange arrows), which may be interpreted as leaching through channelized features (Fig. 7.6.6, grey circles) during weathering.

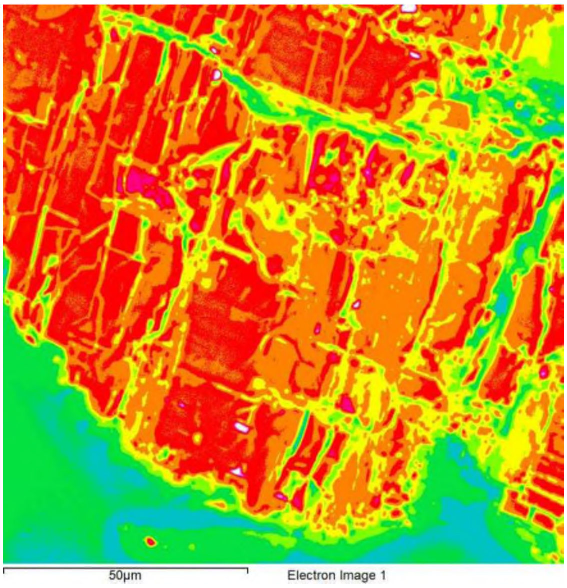

Figure 7.6.3: BSE image, Knox 4 (Lorentzenpiggen) indicating the underlying traces of mineral cleavage (yellow lines)

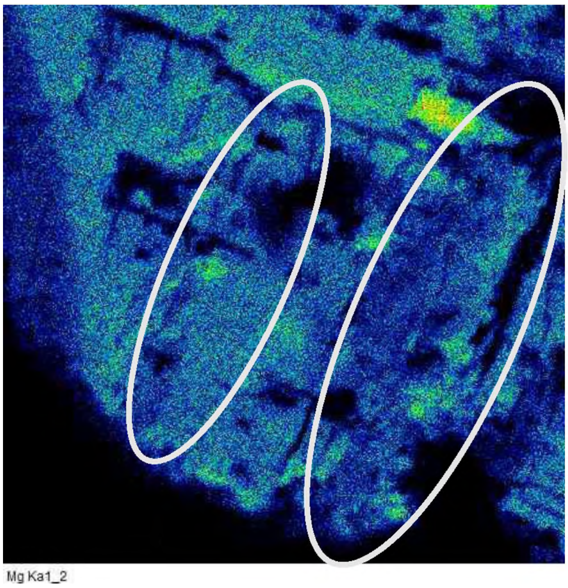

Figure 7.6.4: Magnesium had decreased concentration in areas adjacent to channelized features (grey circles) and towards the external surface

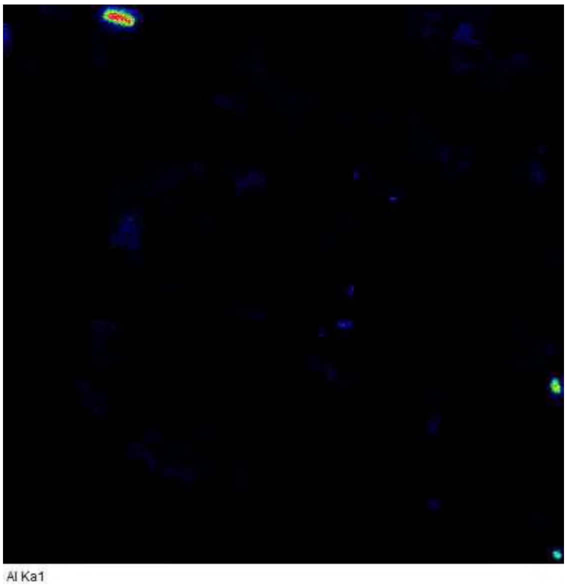

Figure 7.6.5: Aluminium maintained high concentrations in specific regions in the interior. Small flakes of elevated Al concentrations were noted towards the external surface, however, in small quantities

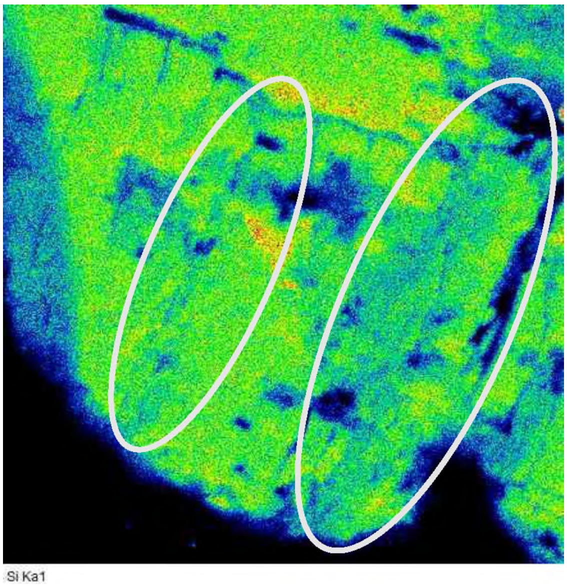

Figure 7.6.6: Even distributions of silica are found throughout the sample, however, the element is concentrated in regions close to rock pore spaces, and decreased along Mg channelized features (grey circles)

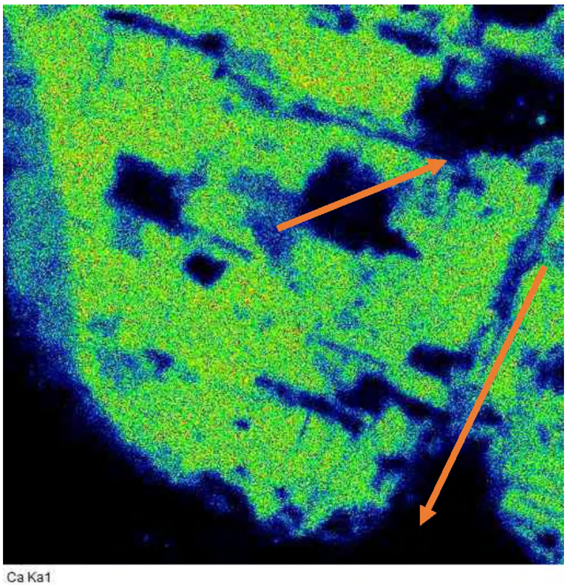

Figure 7.6.7: Concentrations of calcium decreased in areas adjacent to silica, pore spaces and magnesium. Following the same channelized features noted in Mg (orange arrows) toward the external surface

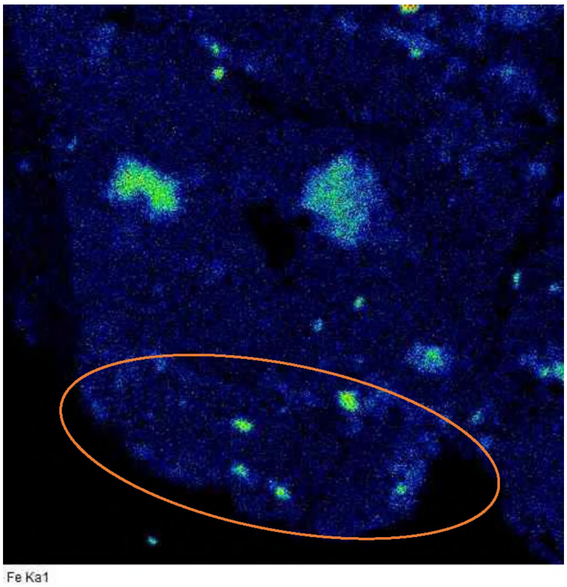

Figure 7.6.8: Iron was concentrated in regions of calcium and magnesium decrease. The distribution was sporadic within Lorentzenpiggen (Knox 4), however, a slightly more concentrated proportion of iron was found at the external rock surface (within orange circle)

In typical weathering rind samples, the elemental composition of the weathering rind differs from the elemental composition of the rock (Mergelov *et al.*, 2012). Compositions of weathering rinds and substrate differ in the following ways (Mergelov *et al.*, 2012):

a. rock coatings are depleted in Si, Al, Na and K,

b. rock coatings are enriched in Mg, Ca, S, Cl and Fe, and

c. rock coatings have a high content of C and, sometimes, N".

Correspondingly, Lorentzenpiggen and Robertskollen portrayed the same characteristics of differential weathering rind and substrate composition. Si, Al, Na and K (a) were depleted in Fig. 7.6.6, Fig. 7.6.5 and Table 7.6.1 respectively. While the enrichment of Mg, Ca, S, Cl, and Fe (b) occurred in Fig. 7.6.4, Fig. 7.6.7 and Table 7.6.2 in turn. One cannot simply assume that this was the only process which affected the apparent mineral composition, however, as iron (Fe^{2+}) had the ability to replace calcium within feldspars (Deer *et al.*, 1992). Enrichment often occurred along channelized features, indicated as circles and arrows in Fig. 7.6.4, Fig. 7.6.6 and Fig. 7.6.7 respectively. The occurrence of "channelized" features was likely the by-product of dissolution of dolerite in the region, where magnesium was transported and subsequently deposited on the rock external surface as a rock coating (Galy *et al.*, 2002). Due to the nature of EDS analysis, the carbon and nitrogen contents could not be assessed for these samples.

According to Glasby *et al.* (1981), coarse-grained dolerites display evidence of iron staining around ferromagnesian crystals in a rock matrix. This was exhibited in Lorentzenpiggen samples (Fig. 7.6.1, arrow). This suggested that water diffusion pathways, along grain boundaries in coarse-grained rocks, were shorter than in fine-grained ones (Glasby *et al.*, 1981). These ferromagnesium minerals displayed extensive oxidation on mineral grain surfaces and cleavage planes noted in Fig. 7.6.1 and Fig. 7.6.2 of Robertskollen and Lorentzenpiggen, where the external rock surfaces were stained reddish-brown from the oxidation process. Thus, dissolution occurred at a mineral grain scale once fresh bedrock experienced near-surface exposure (Dixon & Thorn, 2005).

The accumulation of Fe in the surface of the rock varnish films was linked to the continuous weathering of primary minerals in the rock, with the migration of Fe along micro-fissure networks toward the oxidation barrier on the rock surface (Mergelov *et al.*, 2012). This was exhibited in Fig. 7.6.1 and Fig. 7.6.9a, where the arrows indicated the accumulation of Fe through the discolouration at the exterior surface of the samples.

Figure 7.6.9: Weathering rind, red micro-elevations, and surfaces subject to spalling processes at Robertskollen (Knox 3)

The accumulation of Fe on the surface was also noted on surface micro-topography, where micro-elevations on the rock surface had thicker films (high degree of chemical change), whereas surfaces recently subjected to spalling had lighter colouration and are more like the underling bedrock (Dixon & Thorn, 2005; Mergelov *et al.*, 2012). Micro-elevations were visible in Fig. 7.6.9b, where the red discolouration was seen on areas that have a higher surface topography than the surrounding areas. Areas that have recently undergone spalling have exposed the underlying bedrock, such as Fig. 7.6.9c, displaying the lighter colouration of the underlying, fresh substrate.

Essentially, Robertskollen and Lorentzenpiggen displayed ferric/ferrous ratios that increased from the interior to the exterior. The increased silica and iron-rich compounds (Fig. 7.6.6 and Fig. 7.6.8) created the coloured crusts seen in Fig. 7.6.1 and Fig. 7.6.2. Produced through the movement of iron and other metals ions during dry periods; towards the exterior of the rock, where they are deposited on the surface (Bland & Rolls, 2016). As such, the process of weathering rind formation was associated with small-scale water migration, by which soluble products of chemical weathering were carried towards the rock surface and deposited during drying.

According to Glasby *et al.* (1981), the colouration of rock varnish is of importance, as the colouration influences the absorption of heat and moisture evaporation. In particular, the aspect of these rocks is of primary importance, as studies of rock varnish found on north-facing rocks demonstrated the promotion of surface weathering and that the advection of moisture from rock surfaces are increased by solar radiation (Glasby *et al.*, 1981). From the above discussion, it was clear that the abundance and availability of moisture, drives chemical weathering processes such as dissolution, and subsequent transportation of solutes (Dixon & Thorn, 2005).

7.6.2 Vesleskarvet

Dolerite of this sample consisted of augitic clinopyroxene, plagioclase and quartz (Table 7.6.3). These mineral phases essentially contained silica, magnesium, calcium, iron and some aluminum. In transmitted light (Fig. 7.6.10), the dolerite was composed of opaque to orange clasts, with a grain size of 150µm - >500µm.

A large crack passed through various minerals (Fig. 7.6.10), suggesting a young age, especially considering the intergranular nature. Fracturing was likely a product of thermal gradients. Orange – brown colouration occurred within the crack, iron mineralization was a likely cause. BSE imagery within the crack (Fig. 7.6.11) revealed small, scattered fragments and empty space. EDS results of the fragments were inconclusive.

Table 7.6.3: Wt.% of various spectra of Knox 8

Spectrum	Na	Mg	Al	Si	S	Cl	K	Ca	Ti	Fe	Total
Augitic Cpx	0.4	11.6	3.5	44.2	0.0	0.1	0.1	11.3	0.0	28.8	100.0
Augitic Cpx	0.3	12.0	1.5	43.4	0.0	0.0	0.0	25.5	0.5	16.7	100.0
Augitic Cpx	0.2	11.8	1.8	43.0	0.2	0.1	0.1	24.8	0.5	17.5	100.0
Augitic Cpx	0.2	11.4	1.5	42.9	0.0	0.0	0.1	25.1	0.7	18.0	100.0
Augitic Cpx	0.3	14.2	1.7	45.0	0.2	0.0	0.0	24.1	0.4	14.2	100.0
Contamin Cpx	0.2	12.0	1.6	43.3	0.1	0.1	0.1	25.7	0.4	16.5	100.0
Contamin Cpx	0.3	13.7	1.7	44.2	0.0	0.0	0.1	24.9	0.4	14.7	100.0
Plag	2.2	0.0	27.5	46.0	0.1	0.0	0.2	22.5	0.1	1.4	100.0
Qtz	0.9	0.2	4.0	86.9	0.1	0.0	0.1	4.9	0.3	2.6	100.0
Artefact	0.9	0.4	20.1	4.3	26.1	0.7	15.0	0.8	0.1	31.5	100.0

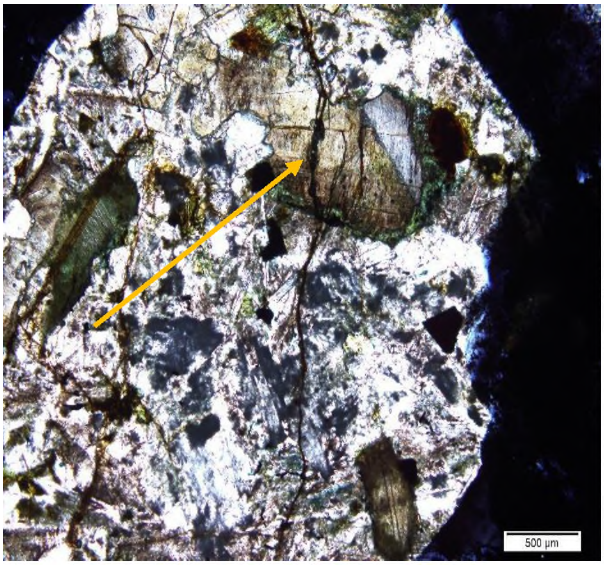

Figure 7.6.10: Homogenous mineral composition of Knox 8 (Vesleskarvet). Note the inter-granular crack (yellow arrow) within the sample.

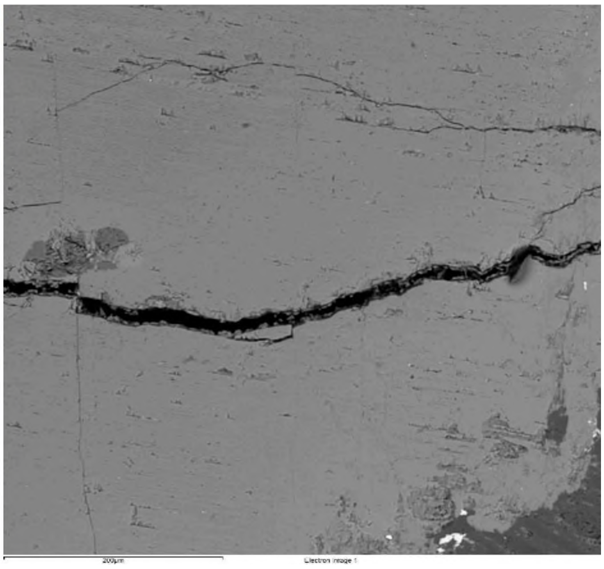

Figure 7.6.11.: Dominance of the crack in the BSE image revealed scattered, small fragments and empty space

The large intergranular crack present in Fig. 7.6.10 and Fig. 7.6.11 may be due to thermal gradients and dilation processes. This is possible as both extremes occur in an Antarctic environment, through high rock surface temperatures and low ground surface temperatures, and pressure release through the removal of weathered material or melting of ice. As such, thermal gradients have an influence on the external and internal structure of the rock, through the potential for thermal fatigue and dilation to occur.

7.6.3 Grunehogna

These samples were both taken from a dolerite outcrop at Grunehogna and are therefore described together. The dolerite consisted of plagioclase, spinel, orthopyroxene, augitic clinopyroxene and ilmenite (Fig. 7.6.17, BSE image, and Fig 7.6.12, thin section). These mineral phases contained essentially Si, Fe, Mg, Ti (in ilmenite), some calcium and sodium (plagioclase) and Al (spinel and plagioclase) (Table 7.6.4). The typical grain size in the dolerite was 50µm-200µm (Fig. 7.6.14). In transmitted light (Fig. 7.6.13), the dolerite appeared dusty, with irregular domains of reddish staining in phases that, if fresh would look clear (plagioclase, clinopyroxene). This indicated some retrograde alteration.

Along the surface of the dolerite a 100µm-200µm thick crust of homogeneous material showed carbonaceous composition. This crust was interpreted as a precipitate. The contact between the dolerite and the precipitate was irregular in topography, but sharp (Fig. 7.6.15). The irregular shapes of these layers were not uniform with the underlying rock structure, and had formed protrusions (not relict features) at the surface.

Compared to the dolerite this crust was compositionally and texturally different. It showed a thin layering visible in transmitted light (Fig. 7.6.15). Different layers had different opacity in plane polarized light, but internally they were optically homogenous. Mostly, the precipitate formed a planar surface (Fig. 7.6.16, thin section) that, however, macroscopically showed some roughness. This roughness was created by 100µm -200µm wide circular protrusions where the crust was thicker than elsewhere (Fig. 7.6.16).

The layering in the crust, indicated by opacity variations (Fig. 7.6.15), was composed of individual layers that were between 5 and 20µm thick. In the thin section analysed, there was an apparent fibrous texture, with fiber direction perpendicular to the layering. In the SEM back-scattered electron (BSE) images, the layering was seen in slight signal intensity variations (different gray scales; Fig. 7.6.17). The apparent fibrous texture could not be confirmed.

Table 7.6.4: Wt.% of Knox 9 (Fig. 7.6.13), Grunehogna

Spectrum	Na	Mg	Al	Si	S	Cl	K	Ca	Ti	Fe	Total
CC	0.5	0.2	0.0	0.2	0.1	0.1	0.0	98.7	0.0	0.2	100.0
CC	0.6	0.6	0.0	0.0	0.3	0.1	0.0	98.3	0.0	0.0	100.0
CC	0.3	0.4	0.2	0.7	0.1	0.0	0.0	97.8	0.2	0.5	100.0
CC mix	1.2	8.1	0.0	1.2	0.5	0.2	0.1	88.5	0.2	0.0	100.0
Diopsidic Augite (Cpx)	0.2	21.1	2.8	46.2	0.2	0.1	0.6	9.7	0.1	18.9	100.0
Hole	0.7	4.6	0.0	0.3	0.3	0.1	0.1	93.9	0.1	0.0	100.0
Hole CC mix	0.5	1.6	0.1	3.0	0.4	0.1	0.1	94.1	0.1	0.1	100.0
Ilmenite	0.1	1.8	0.3	0.2	0.0	0.0	0.0	0.3	40.3	57.0	100.0
Opx	0.2	19.6	7.6	42.8	0.2	0.1	0.7	2.4	0.1	26.4	100.0
Plag	4.9	0.1	23.8	51.9	0.1	0.0	0.2	16.9	0.2	2.0	100.0
Spinel	0.2	6.9	8.2	0.2	0.0	0.1	0.0	0.6	11.0	72.6	100.0

Compositionally, the precipitate consisted uniformly of calcite ($CaCO_3$). The material in different layers showed minor variations in magnesium content in the carbonate. This difference in magnesium correlated with different BSE signal intensity (Fig. 7.6.17) and with the presence of optically different layers in the crust. The magnesium content may reach up to 5 wt.%, suggesting a significant dolomite (MgCO3)-component in the carbonate solid solution. Other BSE-dark layers contained less Mg (~0.5 wt.%). The BSE-bright carbonate layers were practically Mg-free (Table 7.6.3).

Many carbonate analyses showed low Si contents (<0.8 wt.%). Si was not compatible with the carbonate crystal structure. Therefore, such Si may be related to small SiO2 precipitates (chalcedony) amongst the carbonate. Minor Fe was also regularly detected. This Fe might either be oxidic, related to small hematite flakes, or were a Fe-carbonate (siderite) endmember component in the carbonate. The latter might be more likely because no bright BSE domains suggest the presence of Fe oxides.

BSE images showed abundant, 1µm -10µm small black areas (Fig. 7.6.17), which were empty. These were interpreted as pore space in the carbonate crust.

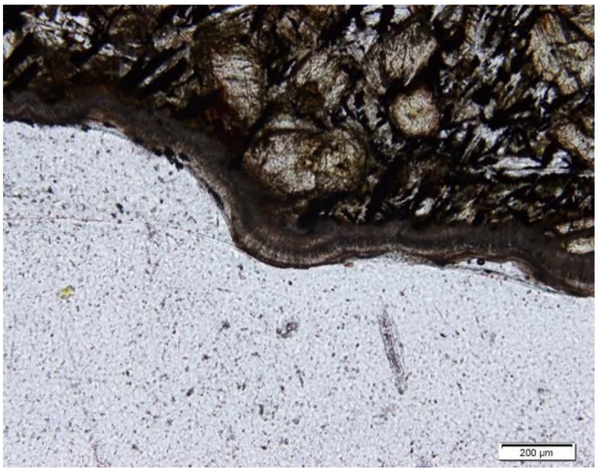

Figure 7.6.12: Knox 9, translucent layering features

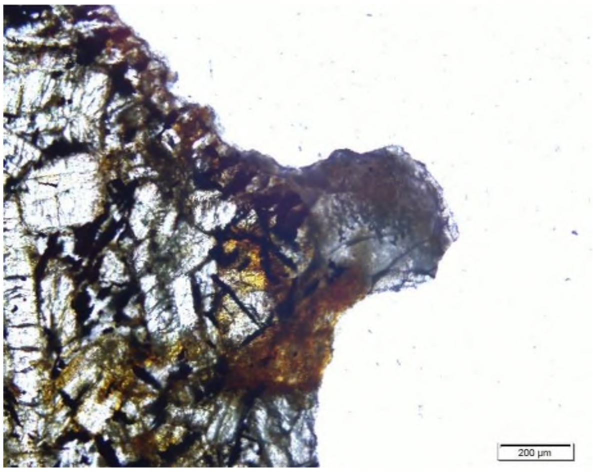

Figure 7.6.13: Knox 9, opaque reddish hues and "worm like" inclusions

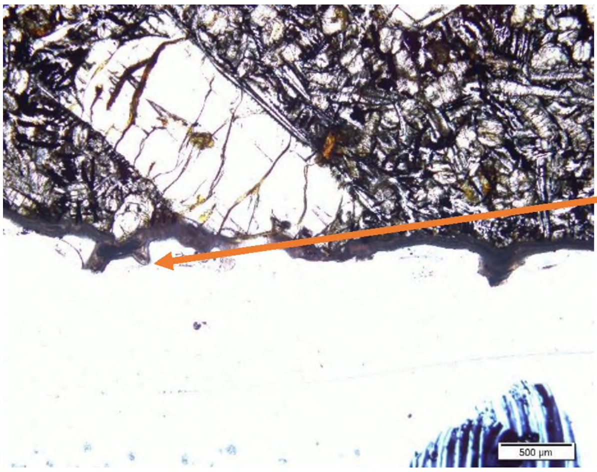

Figure 7.6.14: Knox 9, 200 µm layered features which were gradationally different from the substrate rock

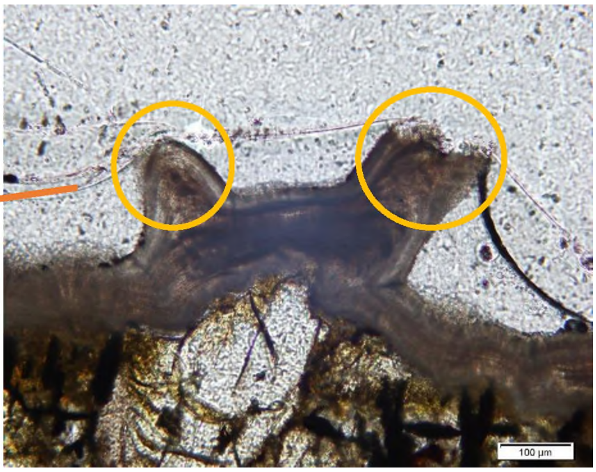

Figure 7.6.15: Knox 9, textured layered features where the arrow denotes the exact area on Fig. 7.6.14, circles indicated protrusions of over 200 µm thickness

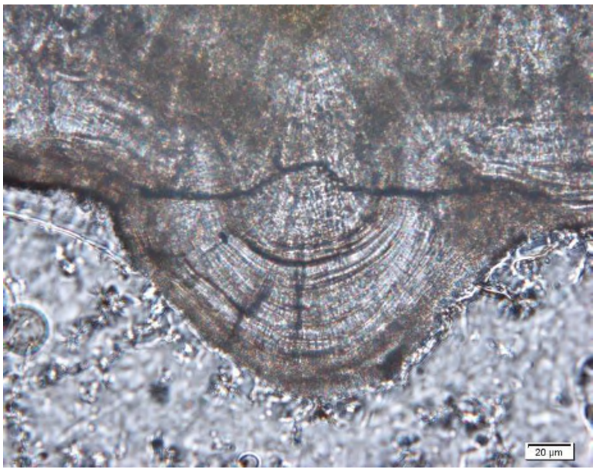

Figure 7.6.16: Knox 10, thin translucent layered features forming dark and light bands

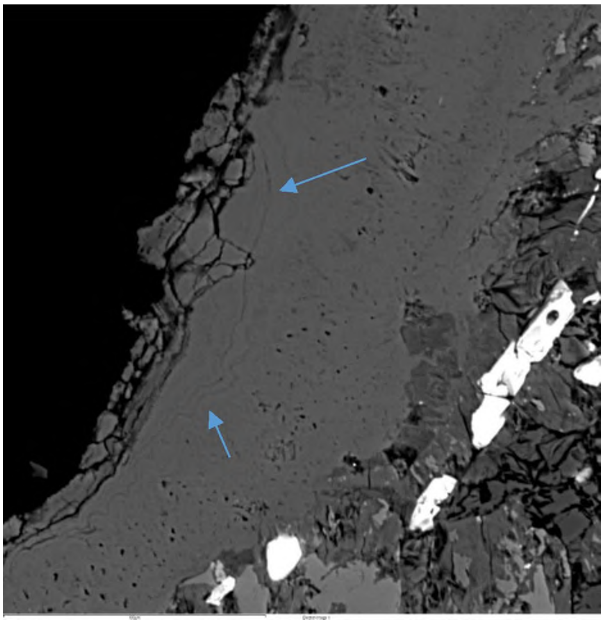

Figure 7.6.17: Knox 9 (Fig. 7.6.14), Grunehogna, BSE image with arrows indicating the layered features noted in the PPL imagery. Small holes within the precipitate were empty pore spaces.

High concentrations of calcium, iron (within the clinopyroxene) and sporadic regions of silica (clinopyroxene and plagioclase respectively) dominated the coatings (Fig. 7.6.18). Additionally, both iron and titanium occurred exclusively within the same regions of the substrate rock, particularly in the carbonaceous coatings.

Decreases in silica were noted in titanium rich areas (Fig. 7.6.26). Magnesium and silica bordered the external surface of carbonaceous coatings (Fig. 7.6.20), with the concentrations of silica (Fig. 7.6.26) higher (brighter) than those of magnesium in this region.

Textured layers (Fig. 7.6.24) were composed of dolomitic calcium carbonate (interior layers) and calcium carbonate (external layer), with small inclusions of quartz throughout. Higher concentrations of potassium were within the substrate, adjacent to the carbonaceous coatings (Fig. 7.6.23).

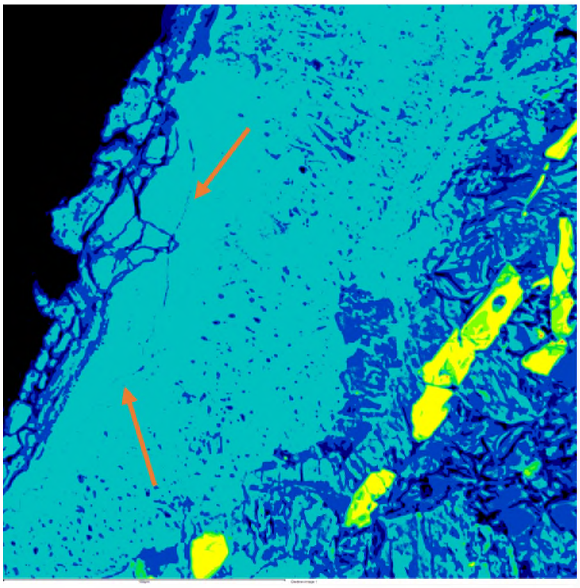

Figure 7.6.18: Knox 9 (A), BSE image showed domains with similar average element compositions. The highest signal intensity (yellow) indicated mineral phases with high average element number. Typically, these were Fe-rich phases. Note the layered features close to the external surface (arrows) and pore spaces within the carbonaceous matrix

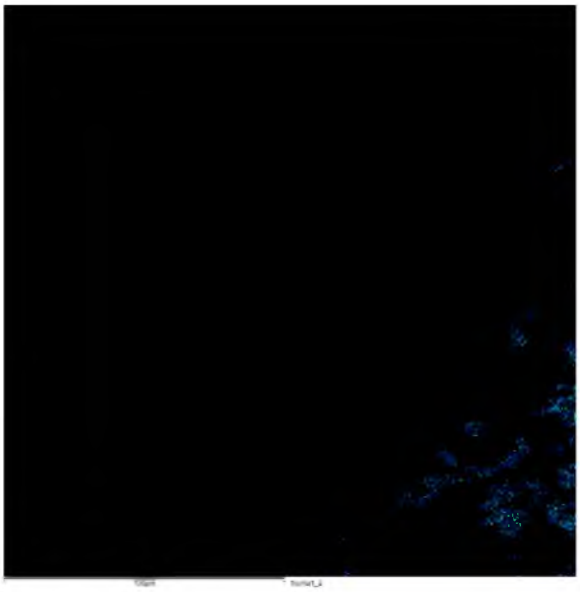

Figure 7.6.19: Distribution of sodium within Knox 9(A), confined in small domains in the host dolerite, which indicated plagioclase.

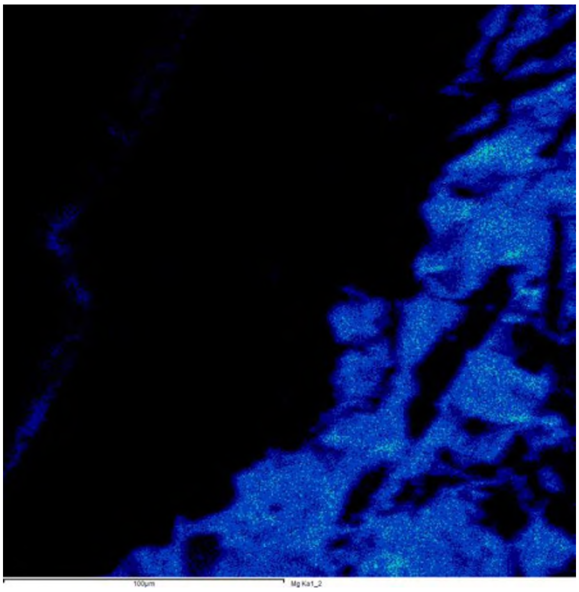

Figure 7.6.20: Magnesium was distributed in high concentration throughout the substrate of Knox 9(A), while defining the most external layer of precipitate in smaller concentrations

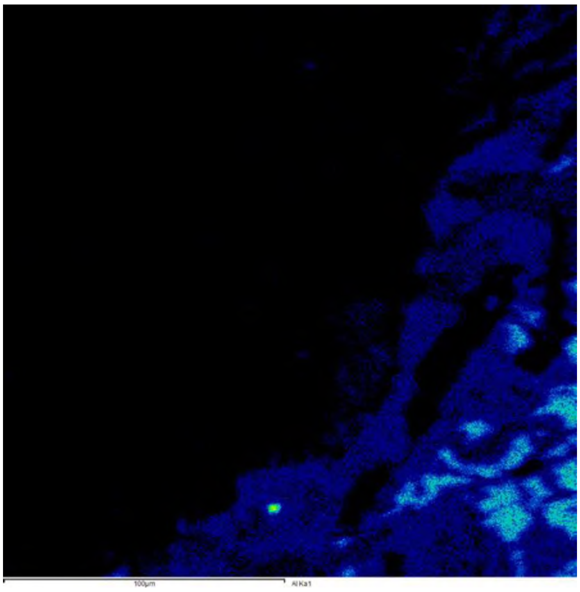

Figure 7.6.21: Aluminium was confined to specific regions of the substrate, where the concentrations were more concentrated than those at the external surface

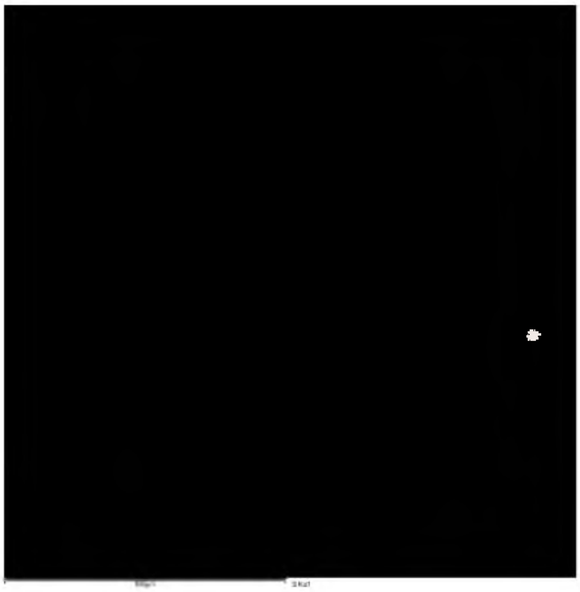

Figure 7.6.22: Sulphur played a minor role in the substrate rock of Knox 9(A), with high concentration in a sulphide inclusion.

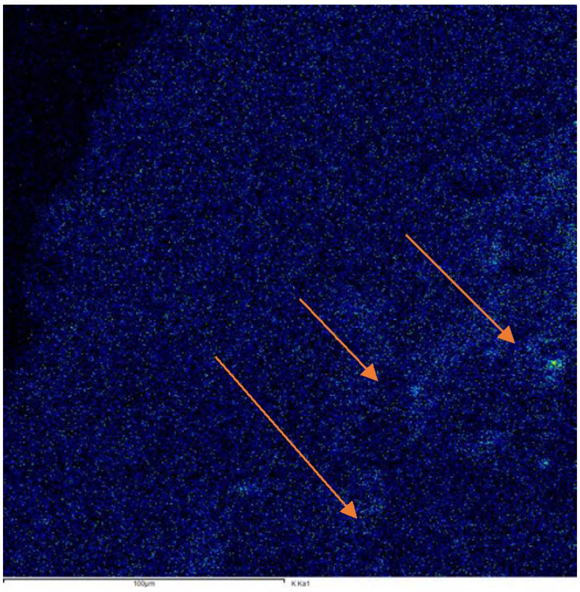

Figure 7.6.23: Potassium maintained a uniform distribution in Knox 9(A), with higher concentrations found within the substrate rock, indicated by the arrows

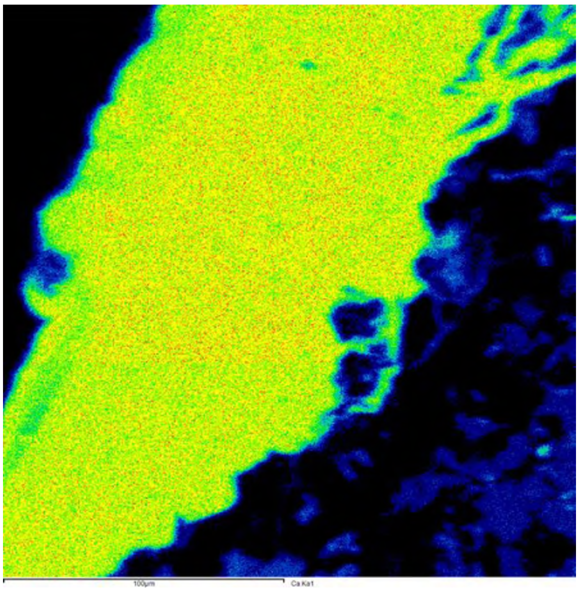

Figure 7.6.24: High calcium contents in the carbonate precipitate, with a sharp boundary to the dolerite. The dolerite showed patchy Ca patterns, with variable but, significantly lower contents than those in the precipitate.

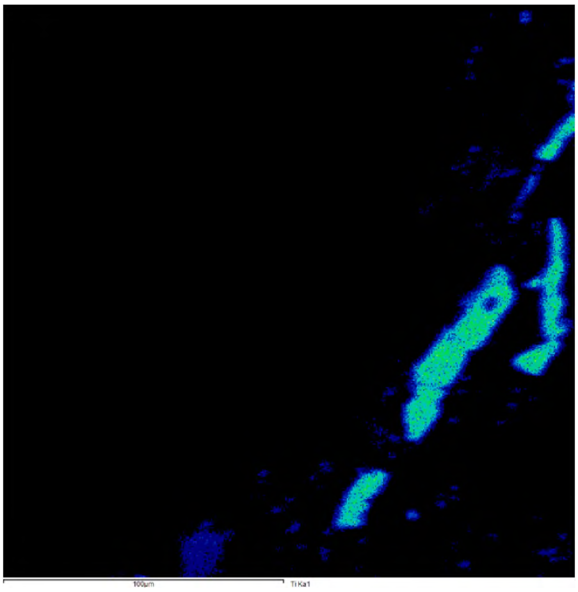

Figure 7.6.25: Titanium displayed limited distribution within the substrate (ilmenite, $FeTiO3$).

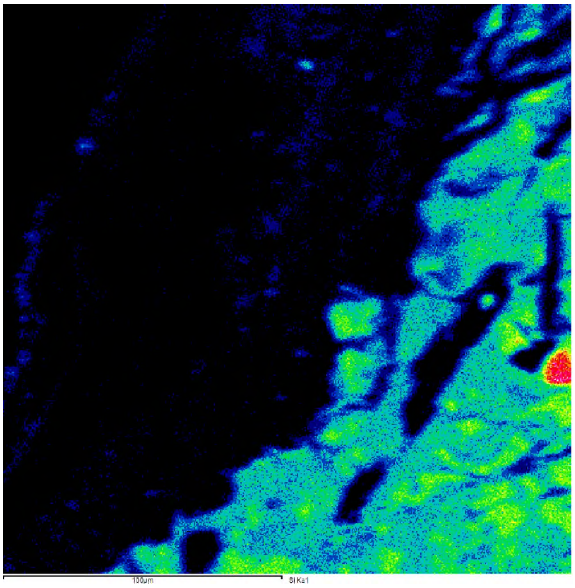

Figure 7.6.26: Highest concentrations of silica occurred within the substrate rock, maintaining a high concentration throughout. Silica was distributed sporadically within the carbonaceous matrix, while bordering the external surface of the carbonaceous layer in a flaked manner. These were likely to be chalcedony inclusions in the carbonate.

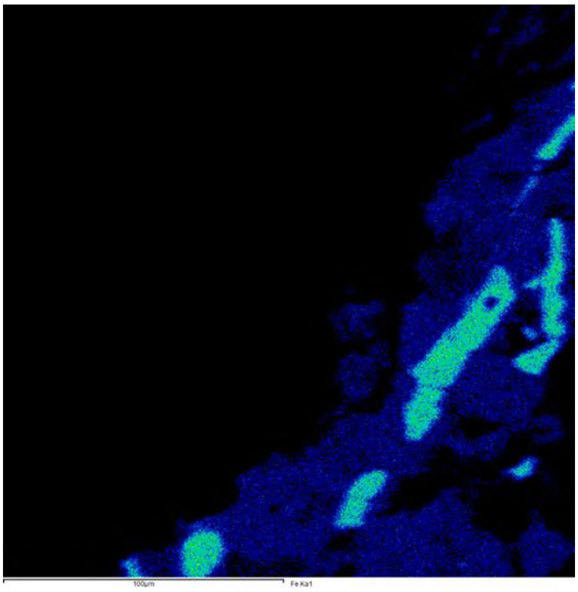

Figure 7.6.27: The carbonate crust did not contain iron. Iron was confined to areas within the host rock, with moderate concentrations in pyroxenes and high iron content in ilmenite.

Petrographic microscopy images, such as Fig. 7.6.12 – Fig. 7.6.16 displayed features common in the formation of speleothems. Namely atypically translucent layers, coloured by bands of impurities along former growth surfaces, which were effortlessly distinguishable as either a grey/white or brown in colouration (Fantidis & Ehhalt, 1970; Kendall & Broughton, 1978; Perrin *et al.*, 2014). The variation in concentration of impurities (growth layering), were the direct result of inclusions trapped by the advancing growth surface, and variations in rate of absorption or supply thereof (Kendall & Broughton, 1978). The impurities found within these bands are commonly believed to be records of cessations or periods of slow carbonate precipitation (Kendall & Broughton, 1978). The layer's aspect was often related to the orientation of different crystals, which differ from the surrounding areas (Perrin *et al.*, 2014), for example Fig. 7.6.16, where laminations were present parallel to the substrate. During the growth of these crystals, those in contact with one another met along planes, and as each crystal grew the planes enlarged (Kendall & Broughton, 1978). Their orientations were dependent on the growth rates of the crystal faces which were either growing towards or against one another, as well as the angle between them (Kendall & Broughton, 1978). The crystal morphology of the termination layer consequently depends on the mineralogy of the underlying inclusions, while the height of the crystalline termination depends on the thickness of the water film, from which they grew (Kendall & Broughton, 1978; Perrin *et al.*, 2014). Thus, "the boundaries between crystals will commonly be inclined with respect to the substrate surface because the crystal with the faster-growing (more favourably-orientated) face adjacent to the common boundary expands at the expense of the less-favoured crystal" (Kendall & Broughton, 1978: 522). Boundaries between such crystals are commonly inclined, sometimes more than 25° to the growth-layering, generating wedge-shaped crystals (Kendall & Broughton, 1978). The growth laminae of Fig. 7.6.14 and Fig. 7.6.15, which displayed these trends, were clearly visible in transmitted light. Displaying curved termination faces and pointed terminations on the external surface (Perrin *et al.*, 2014).

There are six types of growth layering which are characteristic of stalactites and stalagmites when the thin section is cut normal to the long axes (Kendall & Broughton, 1978). The growth layering seen in Fig. 7.6.12, and Fig. 7.6.14 – Fig. 7.6.16 were perceived to consist of the same type of layering and inclusion patterns of the Type 5 growth (Fig. 7.6.28, E and Fig. 7.6.28, G) put forward by Kendall & Broughton (1978). Type 5 layers are characterised by large quantities of impurities, where the crystal fabrics are partially to wholly obscured, as is commonly found separating layers of different crystal habits and the carbonate within, or adjacent to the impurity-rich layers (Fig. 7.6.28) (Kendall & Broughton, 1978).

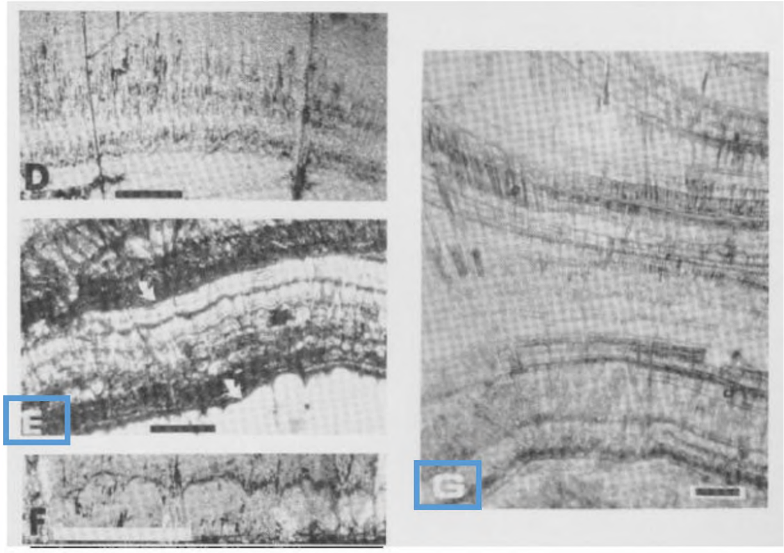

Figure 7.6.28: Inclusion patterns and growth layering in stalactites (copied directly from Kendall & Broughton, 1978: 525)

E: Growth-layering made evident by high inclusion concentrations (type 5) which terminate crystal fabrics of underlying layers (arrowed) and associated with acicular calcite. Plane polarised light: scale = 0.5mm (Kendall & Broughton, 1978: 524).
G: Layers of acicular calcite passing gradationally into columnar crystals with linear inclusions. Plane polarised light: scale =0.5mm (Kendall & Broughton, 1978: 524).

Increased concentrations of calcium content at the external surface, were likely due to the leaching of calcium from the interior, deposited as calcium carbonate on the external surface (Glasby *et al.*, 1981). This is due the concentration of compounds within water; when it exceeds the solubility of the solution, a supersaturated solution occurs (Bland & Rolls, 2016). Supersaturation commonly occurs in environments of changing conditions, such as increased evaporation or cooling (Bland & Rolls, 2016). An example of this environment would be continental Antarctica, which experiences sublimation and severely negative air temperatures. Supersaturated solutions, thus, arise due to there being a lack of suitable surfaces or particles on which crystals are able to form (Bland & Rolls, 2016). "They will crystallise very rapidly once the process of crystallisation starts and the crystals present provide centres for it to continue" (Bland & Rolls, 2016: 128). This process of crystal formation on suitable centres is called nucleation (Bland & Rolls, 2016). Nucleation leads to the deposition of the supersaturated solution, where if not rapidly evaporated, forms drip water upon the external surface, a major process of speleothem production and growth (Perrin *et al.*, 2014). Seen for example in Fig. 7.6.12 – Fig. 7.6.16, where layers of calcium carbonate occurred on the external rock surface.

Calcium carbonate deposited as layering features was a direct effect of solubility; magnesium has a higher solubility, and as such, precipitates less than calcium (Murray, 1954). The loss of carbon dioxide to the atmosphere was thus, one of the factors which influenced the precipitation of carbonates (Murray, 1954). Other factors that were likely to influence the formation of these karst features were the environmental conditions within the area. For example, increased evaporation, such as in dry environments in Antarctica, influences the upper layers of regolith, encouraging the precipitation of calcium carbonate (Bland & Rolls, 2016).

7.6.4 Valterkulten and Flårjuven

Typical uniform grain size and texture within the interior of the dolerite (50 µm – >500 µm) occurred, with fragmentation close to the rock surface (Fig. 7.6.29 and Fig. 7.6.31). Fragments were isolated from the substrate and consisted of planar, fibrous textures under transmitted light, forming part of the precipitate (Fig. 7.6.30).

The dolerite of Valterkulten consisted of albite, plagioclase, orthopyroxene and potassium feldspars (Table 7.6.5). Composition of minerals changed at the exterior, with baddelyite, zircon and quartz occurring most frequently where mineral disintegration was apparent (Table 7.6.5). These mineral phases contained essentially Si, and Al, limited Mg and Fe (in orthopyroxene) (Table 7.6.5).

The thickness of the fragmented zone along the dolerite surface varied from 1500 µm – 2000 µm (Fig. 7.6.29). The fragmented zone of Flårjuven was substantially greater than of Valterkulten, varying between 2000 µm – 6000 µm (Fig. 7.6.31). Clast concentration and size were greater in Flårjuven (Fig. 7.6.33).

A crack in the interior of the dolerite displayed orange – reddish colouration, along previous intergranular crack surfaces (Fig. 7.6.31). Minerals found at the exterior of the thin section, such as altered plagioclase were more dispersed and fragmented and less opaque than those of the interior (Fig. 7.6.30).

This dolerite (Valterkulten, Knox 15B) consisted primarily of alkali feldspar and vesuvianite (Table 7.6.5). Mineral phases contained S and Ca, and small quantities of Fe (in vesuvianite) and Al (in alkali feldspar). Fragmented minerals at the external surface (precipitate crust) were identified as gypsum (Table 7.6.5), minerals at the interface of the gypsum were altered albite, silicates and pyroxenes.

Table 7.6.5: Wt.% of Valterkulten (Knox 11)

Spectrum	Na	Mg	Al	Si	S	Cl	K	Ca	Ti	Fe	Total
Albite Plag	10.0	0.0	18.9	67.3	0.1	0.1	0.3	2.9	0.1	0.2	100.0
Biotite	0.2	6.7	13.5	21.1	0.0	0.0	2.2	0.0	9.0	47.3	100.0
Kfs	0.9	0.0	15.2	57.2	0.0	0.1	25.9	0.1	0.3	0.4	100.0
Opx	0.2	6.6	15.1	24.6	0.1	0.0	0.1	0.1	0.1	53.0	100.0
Plag	10.6	0.0	18.6	68.1	0.0	0.2	0.2	2.1	0.0	0.1	100.0
Qtz	0.0	0.0	0.0	99.4	0.2	0.1	0.0	0.0	0.0	0.2	100.0
Qtz	0.1	0.1	0.2	98.2	0.3	0.0	0.0	0.1	0.0	1.0	100.0

Table 7.6.6: Wt.% of Knox 15B (Flårjuven)

Spectrum	Na	Mg	Al	Si	S	Cl	K	Ca	Ti	Fe	Total
Alkali Feldspar	5.2	0.6	24.0	55.3	0.0	0.1	11.7	1.0	0.1	1.9	100.0
Gypsum	0.0	0.0	0.0	0.2	44.2	0.2	0.0	55.1	0.0	0.2	100.0
Gypsum	0.1	0.0	0.0	0.1	44.8	0.4	0.0	54.5	0.0	0.0	100.0
Vesuvianite	0.2	6.0	4.8	28.2	0.5	0.1	0.3	33.9	0.2	25.9	100.0

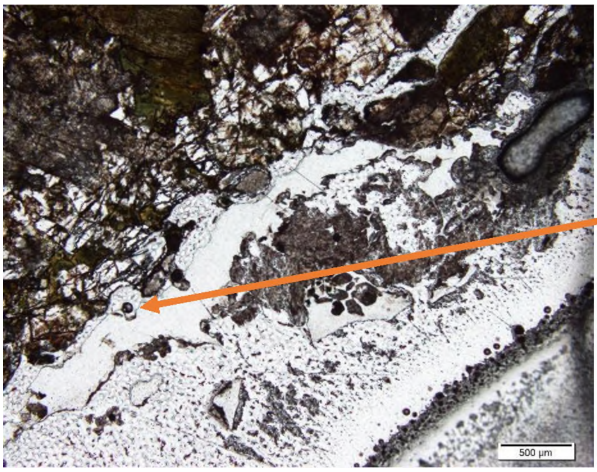

Figure 7.6.29: Fragmented minerals at the external surface of Knox 11 (Valterkulten). Note the disintegrated nature in comparison to the interior substrate

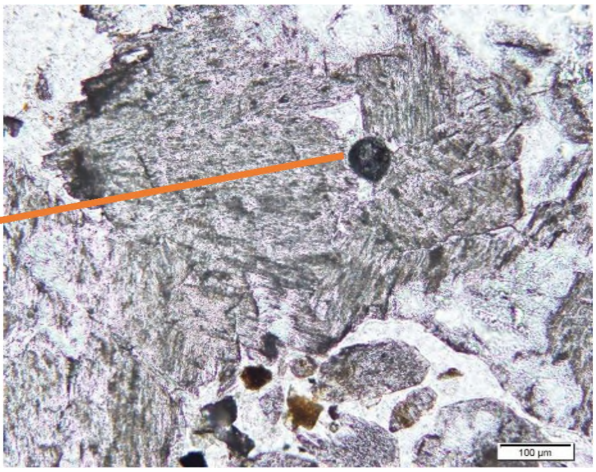

Figure 7.6.30: Fibrous, planar textured phases, at the most external surface of Knox 11, forming part of the precipitate

Figure 7.6.31: Precipitate disintegration and pore space enlargement of Flårjuven (Knox 15B). Note the reddish colouration within the crack the extent

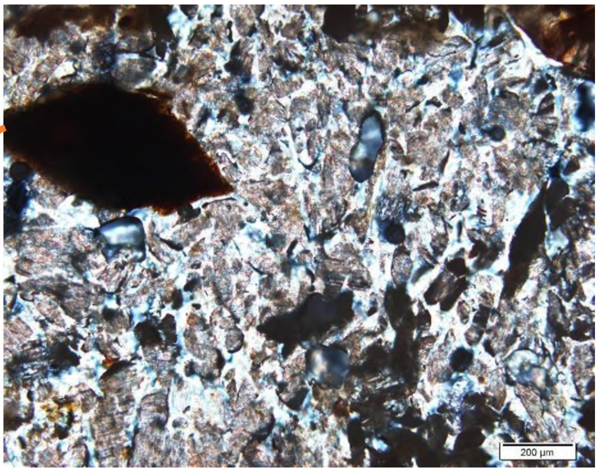

Figure 7.6.32: Effect of precipitation on minerals at the external surface of Knox 15B. Mixture of fibrous, planar textured phases and intact domains

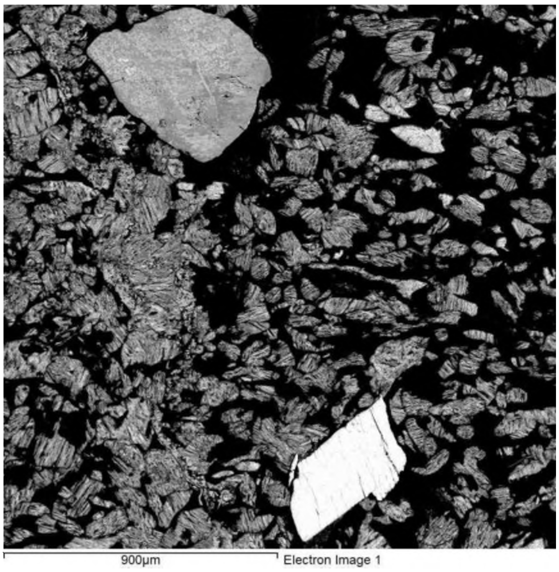

Figure 7.6.33: Gypsum flakes were more concentrated at the interior. Large clasts found within the gypsum matrix were alkali feldspar and vesuvianite (bright in BSE imagery). Sample: Knox 15B (Flårjuven)

Aluminium was found in small quantities within the gypsum flakes, closest to the internal surface (Fig. 7.6.35). Silica varied within the substrate rock (quartz, orthopyroxene) with the highest concentrations confined to the interior, small flakes occurred towards the exterior surface of the rock in a string-like manner, while being isolated by their composition (Fig. 7.6.36). Iron and magnesium precipitates were confined to the edge of the external substrate surface (Fig. 7.6.39 and Fig. 7.6.40).

The high Ca and S content suggested that the precipitate on the dolerite surface consisted of gypsum ($CaSO_4$). Calcium depleted areas adjacent to the flakes, suggested that secondary leaching (Fig. 7.6.38, arrows) may have created the domain's pore space. Silica was depleted, followed by calcium, flaking off with the gypsum clasts (Fig. 7.6.36). Colouration comparisons for sulphur increased towards the exterior surface, where there were abundant gypsum flakes (Fig. 7.6.37).

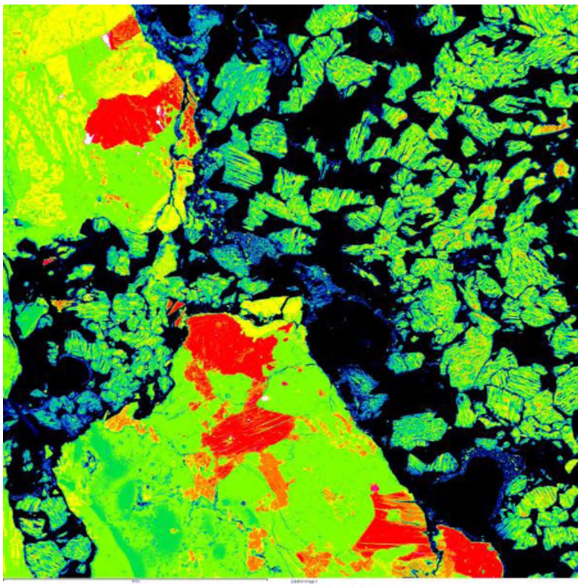

Figure 7.6.34: BSE image of Flårjuven (Knox 15B), gypsum flakes occurred at the right corners and within the central pore space. Substrate rock is pictured at the corners on the left hand side.

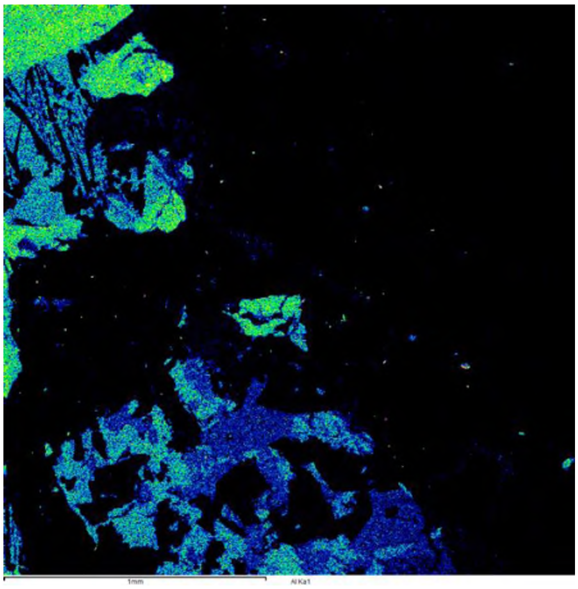

Figure 7.6.35: Highest concentration of aluminium distribution was at the most external substrate surface (margins of the pore space)

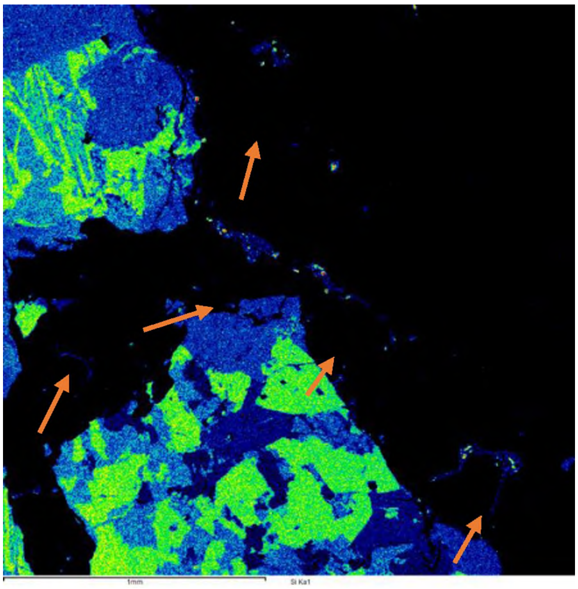

Figure 7.6.36: The primary constituent was silica. Small inclusions moved towards the external surface in a string-like manner, indicated by the orange arrows

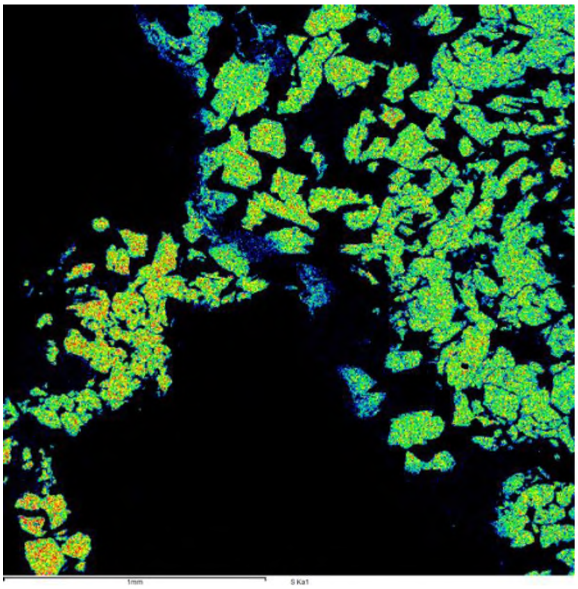

Figure 7.6.37: Gypsum flakes were primarily sulphur rich, while the substrate rock lacks this elemental composition

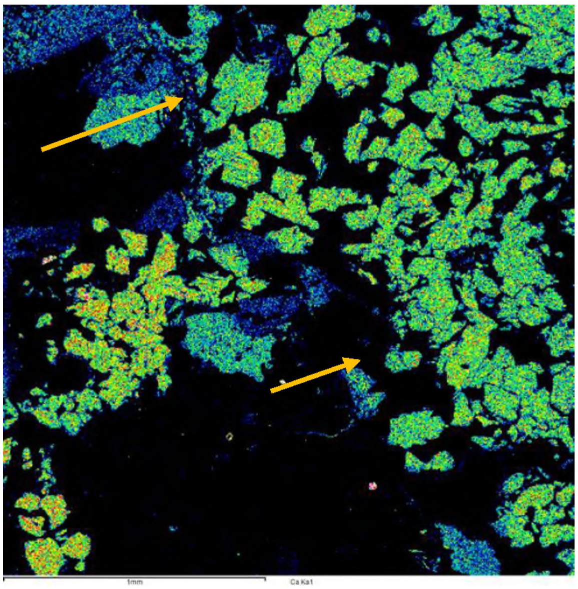

Figure 7.6.38: Highest concentrations of calcium were within the gypsum flakes at the external surface. Calcium was depleted in areas adjacent to the gypsum flakes, with the arrow indicated the leaching towards the exterior

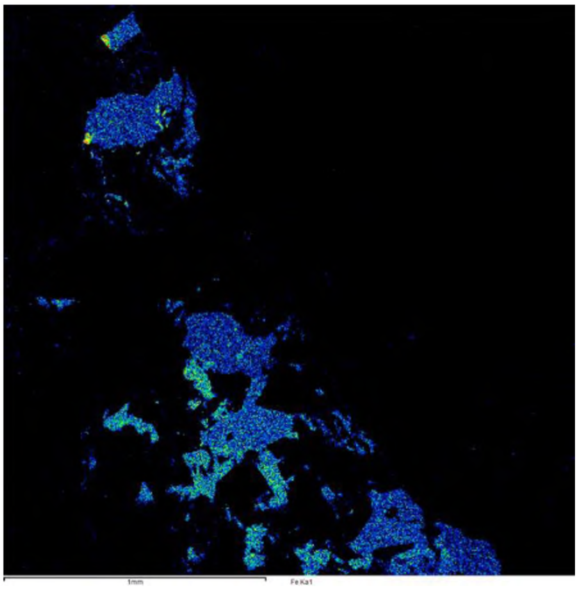

Figure 7.6.39: Iron distribution occurred along the edge of the external surface, concentrated at the interior

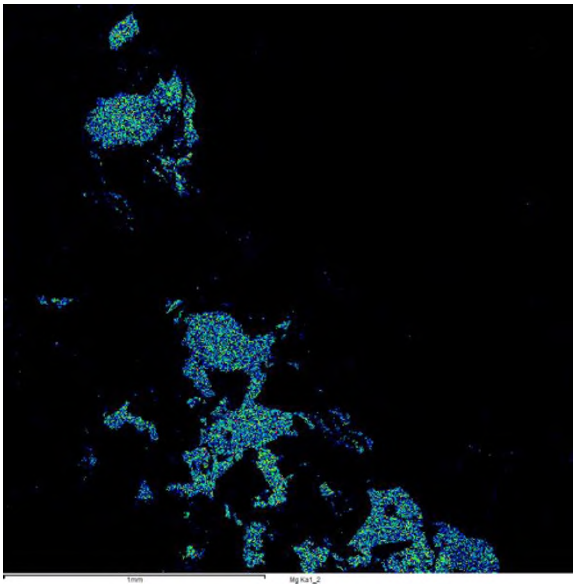

Figure 7.6.40: Uniform concentration and distributions of magnesium occurred within the substrate rock. Although, primarily at the external surface's margin

According to results produced by Gibson *et al.* (1983), halite was the dominant evaporite at one of their study sites in Wright Valley, Antarctica, with it comprising of nearly 50% of the soil volume. In terms of their study however, the halite was of marine origin, which is not the case in western Dronning Maud Land, Antarctica, as these nunataks are too far inland. The quantity of halite in this study were found to decrease in the soil profile, from the salt layer downwards, while the evaporite concentrations were greatest at the 2-4cm depth (Gibson *et al.*, 1983). In relation to this, calcite abundance was found to increase with depth, while gypsum and thenardite abundances were variable (Gibson *et al.*, 1983). This was similar to results from Flårjuven (Fig. 7.6.37 and Fig. .7.638.) where gypsum salt accumulation occurred at the most external surface of the rock. Similarly, at the Flårjuven site, salt accumulation beneath the rock decreased as the depth of the soil profile increased.

Typically, gypsum accumulates in environments where groundwater flow is limited, allowing for the accumulation of gypsum/sulphates produced from sulphuric acid reactions (Davis, 2000). Upon dissolution, gypsum produces pitting effects, essentially causing undermining at the contact with moist, underlying rock, triggering the rock to calve from the lower edge (Davis, 2000). The abundance of several centimetres of gypsum overlaid on these rocks and subsequent accumulation below the ground surface, thus, indicated that sulphuric acid development was an active process at this site (Davis, 2000). From the above interpretations it was clear that calcium sulphate (gypsum) salts, were associated with the weathering of fine- to medium grained dolerites (Glasby *et al.*, 1981). Chemical weathering processes, are thus, essential in decomposing bedrock, and serve as preconditioning functions for the transportation of materials (Dixon & Thorn, 2005).

Were mechanical processes faster than chemical ones, weathering rinds, polygonal cracking and solution features on silicate rocks would be uncommon in the landscape, however, this is not the case and the existence of these landforms implies that chemical weathering occurs faster than mechanical weathering (Pope *et al.*, 1995). As such, chemically weathered features were only able to grow and deposit onto surfaces where this process dominates, for example speleothem growth. As such, it is important to note that various processes are involved in the development of the speleothem, while others are related to the modification of pre-existing structures (Perrin *et al.*, 2014). For example, the dissolution of calcite in speleothems; through which dissolution occurs preferentially in elongated voids, and along the boundaries between neighbouring crystals (Perrin *et al.*, 2014). Secondary voids are thus, further enlarged, eventually connecting to one another, forming micro-channels (Perrin *et al.*, 2014). The events, processes and products which interact in speleothem growth are thus, essential to distinguish from one another, especially in terms of speleothem development, and the modification of existing karst features (Perrin *et al.*, 2014).

Local environmental conditions are key in incorporating colloidal particles or aerosols into the stalagmite surface, through the advancing growth surface (Perrin *et al.*, 2014). As such, the drip rates of the supersaturated solutions influence the amount of aerosol/colloidal particles incorporated into the upper surfaces of growing stalagmites (Perrin *et al.*, 2014). Inclusion horizons are, thus, related to events favouring the input of colloidal/aerosol particles into the system, such as through transportation by drip waters or air circulation (Perrin *et al.*, 2014). Local conditions, however, have the ability to stunt stalagmite growth as well, such as through the change in drip water supply or chemistry (Kendall & Broughton, 1978; Perrin *et al.*, 2014). The rate of water supply is hence, of importance, for example, a slower rate relative to surface area allows evaporation to play a greater role in the precipitation of dissolved materials (Murray, 1954). Slow drip rates and subsequent precipitation of carbonates indicates arid conditions in speleothems, where incongruent dissolution and prolonged water/rock interactions occur (Riechelmann *et al.*, 2014).

Drip water chemistry changes, such as increased magnesium concentrations, results in mineralogical changes in speleothems, related to climatic changes towards aridity (Perrin *et al.*, 2014). As such, seasonality influences the precipitation of calcite, for example, less arid conditions are typical of spring and summer in Antarctica, effectively altering the drip water chemistry through lowered magnesium/calcium saturation (Riechelmann *et al.*, 2014). Effectively altering the concentration gradients for dissolved ions and carbon dioxide, directly interfering with the emission of carbon dioxide and precipitation of calcium carbonate at the surface interface of the stalagmite (Murray, 1954; Fantidis & Ehhalt, 1970).

This has a direct influence on the Antarctic environment, especially when climate models predict increased moisture availability in these traditionally dry regions. Increased moisture creates conditions that favour chemical weathering through dissolution processes. The direct results of this being both an increase in weathering rind development and depth, and a greater accumulation of salts upon the ground surface. Speleothem growth is likely to be altered, with greater concentrations of carbon dioxide being released to the atmosphere through increased calcium carbonate precipitation. Gypsum coatings, however, are likely to decrease in these conditions, as increased water availability and groundwater flow allows the salts to be transported.

8. Conclusion

This investigation provided a baseline study and documentation of chemical weathering processes in western Dronning Maud Land, Antarctica. The documentation of these weathering processes is of importance for future studies into weathering processes in desert environments. The collection of these data allows further processes, to be studied, such as the historical interactions between ice and solid earth. This is of importance, as understanding how environments have reacted in the past to changing climates allows for the understanding of future environmental changes, and the hazards or implications thereof.

The present investigation focused on four overarching objectives:

a. To undertake a chemical analysis of rock composition at different depths beneath the surface.

b. Determine the chemical composition of the input and outputs of chemical weathering.

c. Document and compare chemical weathering processes and forms at different sites.

d. To determine the type and extent of rock coatings and weathering rinds.

a). Robertskollen maintained a primary composition of apatite, augitic clinopyroxene, baddeleyite, biotite, orthopyroxene, ilmenite, potassium feldspar, plagioclase and quartz, on par with dolerite lithology. The mineral phases contained Na (plagioclase), Ca, Al, Si, Fe, Ti (in ilmenite), and some Mg. Dolerite of Lorentzenpiggen was composed of augitic clinopyroxene (fresh and altered) and diopside. The mineral phases were found to contain Si, Ca, Fe, Mg, small quantities of Al.

Vesleskarvet consisted of augitic clinopyroxene, plagioclase and quartz, with mineral phases essentially containing Si, Mg, Ca, Fe and some Al. Grunehogna consisted of plagioclase, spinel, orthopyroxene, augitic clinopyroxene and ilmenite. With the mineral phases containing essentially Si, Fe, Mg, Ti (in ilmenite), some Ca, Na (plagioclase) and Al (spinel and plagioclase).

The dolerite of Valterkulten consisted of albite, plagioclase, orthopyroxene and potassium feldspars. Composition of minerals changed at the exterior, with baddelyite, zircon and quartz occurring most frequently where mineral disintegration was apparent. The mineral phases within this sample were Si, and Al, limited Mg and Fe (in orthopyroxene). Flårjuven on the other hand, contained S and Ca, and small quantities of Fe (in vesuvianite) and Al (in alkali feldspar). Fragmented minerals at the external surface (precipitate crust) were identified as gypsum, while the minerals at the interface of the gypsum were found to be altered albite, silicates and pyroxenes.

b). Chemical compositions of the inputs and outputs of weathering were determined using ICP-MS analysis and EDS analysis. The results indicated the dissolution of carbonates and salts, from the weathering of silicate minerals. Increases in pH and ion concentrations are attributed to fluctuating water levels, prevalence of algal communities and shallow groundwater features, which influence the rock-water interaction. At the Grunehogna site, high $Na^+/(Na^+ + Ca^{2+})$ and $SO_4 : Na$ ratios suggest enhanced sulphide and carbonate dissolution rates, while Valterkulten displayed calcium carbonate deposition on the meltwater pool floor. Flårjuven was found to have high $Na^+/(Na^+ + Ca^{2+})$ values, a contribution from the amount of precipitates, and their depth found at this site. Robertskollen was highly influenced by above surface water flow as permafrost limits the movement of groundwater flow.

Overall, the prevalence of high $Na^+/(Na^+ + Ca^{2+})$ and $SO_4 : Na$ ratios, related directly to the dissolution of carbonates, and subsequent reprecipitation upon encountering moisture limiting regions. Fast moving water channels were found to decrease the contact time between rock-water interactions, and as such, contribute to changing the pH and ion concentrations of calcium and sodium.

c). Chemical weathering processes were found to differ between sites, namely between sites with visible weathering rinds and those which were composed of precipitate accumulations. Weathering rind samples displayed discolouration in the margins of phases and portrayed a decreasing gradational change from the exterior to the interior. The discolouration was interpreted as a weathering rind. The characteristics of this alteration occurred as black-reddish to dusty pigmentation at external regions, portraying the stereotypical hues of iron oxidation. Dissolution of these weathering rinds occurred at a mineral grain scale, once fresh bedrock experienced near-surface exposure (Dixon & Thorn, 2005). This allowed for channelized features to form through which the migration of ions such as magnesium occur.

Precipitate accumulation samples displayed a variability between carbonaceous and sulphate weathering. Carbonaceous coatings were identified at Grunehogna, with a 100-200µm thick crust of homogeneous material along the external surface of uniform calcite composition ($CaCO_3$), this was interpreted as a precipitate. The contact between the dolerite and the precipitate was irregular in topography, but sharp. The layering in the crust, was indicated by opacity variations, was composed of individual layers between 5µm and 20µm thick. The translucent layers, displayed coloured by bands of impurities along former growth surfaces, effortlessly distinguishable as either a grey/white or brown in colouration (Fantidis & Ehhalt, 1970; Kendall & Broughton, 1978; Perrin *et al.*, 2014). These karst features were interpreted as speleothem growth surfaces where calcite precipitated out of a super saturated solution. Since the underlying host geology does not support the external migration of calcite, it is expected that this carbonaceous formation was externally sourced.

Sulphate weathering was identified at the Flårjuven study site, where the high Ca and S contents suggested that the precipitate on the dolerite surface consisted of gypsum ($CaSO_4$). Calcium was depleted in areas adjacent to the flakes, a result of secondary leaching processes. The abundance of several centimetres of gypsum overlaying these rocks and accumulating below the ground surface, thus, indicated that sulphuric acid development was an active process at this site (Davis, 2000).

d). The type and extent of rock coatings were related to the underlying lithology between sites and on the prevalence of water availability at these sites. Coatings at Robertskollen and Lorentzenpiggen were found to contain iron (Fe) deposition at the external microns of the rock. Typical grain size within the samples of dolerite were 50µm-500µm with small inclusions of iron found throughout. The weathering rinds occupied a zone larger than 1000µm (Robertskollen) and less than 600µm (Lorentzenpiggen) thick. Carbonaceous coatings were identified at Grunehogna, with a 100µm -200µm thick crust of calcite ($CaCO_3$), with individual layers being between 5µm and 20 µm thick. Fragmented minerals at the external surface (precipitate crust) of Flårjuven were identified as gypsum coatings approximately 1500µm – 2000µm thick. Overall the greatest concentration of coatings was that of the gypsum coatings, followed by weathering rinds (ferric and siliceous) and finally calcite coatings.

This thesis only provides an initial analysis of chemical weathering in western Dronning Maud Land, Antarctica, and was predominately qualitative in nature. To understand these processes in periglacial environments, high-resolution quantitative analysis needs to be conducted. Since this study is currently the first of its kind in this region of Antarctica, the majority of the results were either entirely new or, have been linked to processes found in other environments, such as the formation of speleothems to explain karst features at the Grunehogna site.

In conclusion, this study into chemical weathering, and the processes which influence lithospheric and planetary evolution have been investigated; further knowledge into the forces that modulate planetary ice, heat, water and chemical budgets has been supplemented (Kennicutt *et al.*, 2016). Future considerations into expanding the current understanding of chemical weathering have been provided in the following section, with focuses on terminology, macro- and micro- scale disconnect, and technical advances and applications being of primary importance.

8.1 Future considerations

There is a disconnect between natural weathering and laboratory studies, and as such, one needs to question the establishment of boundaries among processes (Hall *et al.*, 2012). For example, is the compartmentalisation of research into natural and laboratory conditions limiting the study of weathering processes? How does one integrate these two juxtaposed methods of research, and does the representation of one category of research, lead to the production of knowledge that does not accurately reflect the system as a whole?

The term “weathering” itself is under debate, with the more favourable term “rock decay” being suggested as its replacement. This would solve various arguments about the zonation of weathering and erosion, for example, when does one become the other? At what point does weathering become erosional, and is there not a step in-between? I feel that this is where the suggested term of rock decay would clear the line between the two.

Looking towards the future, technological advances have the ability to increase the current knowledge system at micro- and macro- scales. New designs, sensor technologies, instrumentation and non-contaminated sample retrieval systems are likely to become more valued and widely used by scientists to probe challenging environments and answer increasingly difficult questions (Kennicutt *et al.*, 2016). This is particularly important in terms of pristine sample recovery, with the elimination of artefacts which occur during transportation, handling and storage being of high importance (Kennicutt *et al.*, 2016).

In addition, new battery technologies are able to increase the amount of time, which autonomous technologies can function, increasing long-term, sustained monitoring, and enhanced communications (Kennicutt *et al.*, 2016). This links directly to the increased need for a wide variety of sample collections and subsequent measurements over various time scales, in a variety of diverse and often difficult to reach locations (Kennicutt *et al.*, 2016).

As such, the critical understanding of the Earth System, can only be advanced through holistic studies of Antarctica and its inherent role in planetary processes (Kennicutt *et al.*, 2016). Further studies into chemical weathering in periglacial regions are likely to enhance the current knowledge on soils formation processes and the interactions of solid earth and atmospheric processes, such as greenhouse warming. The study of the window into past rock and sediment records, will hence influence the prediction of future planetary changes, through enhancing model accuracy and predictions (Kennicutt *et al.*, 2016).

9. Appendix A

Table 9.1: Summary of the thin sections of dolerite samples, including sample number, nunatak name and the area identified as the area of study

 Knox 3 J02 Robertskollen, Ice Axe Peak	 Knox 4 JP2 Lorentzenpiggen	 Knox 8 VES02 Vesleskarvet, Northern Buttress
 Knox 9 JG01 Grunehogna	 Knox 11 JV123 Valterkulten	 Knox 15B JF4 Flårjuven

10. Reference List

ACR Systems Inc. 2016. SmartReader plus 8. http://www.acrsystems.com/products/accessories/et-004-gp/ 28 March 2017.

Anderson, R.S. & Anderson, S.P. 2010. *Geomorphology: The mechanics and chemistry of landscapes*. 1st ed. Anderson. R.S. & S. P. Anderson, eds. Cambridge: Cambridge University Press.

André, M.F., Hall, K.J. & Comte, V. 2004. Optical rock properties and weathering processes in polar environments (with special reference to Antarctica). *Polar Geography*, 28(1): 43–62.

Aoki, H. & Matsukura, Y. 2007. A new technique for non-destructive field measurement of rock-suface strength: an application of the Equotip hardness tester to weathering studies. *Earth Surface Processes and Landforms*, 32: 1759–1769.

Astrom, M. & Bjorklund, A. 1995. Impact of acid sulphate soils on stream water geochemistry in western Finland. *Journal of Geochemical Exploration*, (55): 163–170.

Atkins, C.B. 2014. Geomorphological evidence of cold-based glacier activity in South Victoria Land, Antarctica. *Geological Society, London, Special Publications*, (381): 299–318.

Ayers, G.A. 2017. *Biogeomorphic aspects of lichen colonisation in part of western Dronning Maud Land, Antarctica*. Rhodes University. MSc Thesis.

Bardin, V.I., Dundo, O.P. & Konovalov, G. V. 1964. Brief geomorphological description of the mountains of Queen Maud Land. *Soviet Antarctic Expedition*, (3): 354–357.

Barrett, J.E., Gooseff, M.N. & Takacs-Vesbach, C. 2009. Spatial variation in soil active-layer geochemistry across hydrologic margins in polar desert ecosystems. *Hydrology and Earth System Sciences*, (13): 2349–2358.

Barsch, D. 1993. Periglacial geomorphology in the 21st century. *Geomorphology*, 7(1–3): 141–163.

Bell, R.A.I. 1966. Lake Miers, South Victoria Land, Antarctica. *New Zealand Journal of Geology and Geophysics*, 10(2): 540–556.

Blackhurst, R.L., Verchovsky, A., Jarvis, K. & Grady, M.M. 2003. Cryptoendolith communities in Antarctic Dry Valley region sandstones: potential analogues of Martian life-forms. *Lunar and Planetary Science XXXIV*, 978: 1–2.

Bland, W. & Rolls, D. 2016. *Weathering: an introduction to the scientific principles*. 2nd ed. W. Bland & D. Rolls, eds. New York: Routledge.

Bluth, G.J.S. & Kump, L.R. 1994. Lithologic and climatologic controls of river chemistry. *Geochimica et Cosmochimica Acta*, 58(10): 2341–2359.

Bockheim, J.G. & Hall, K.J. 2002. Permafrost, active-layer dynamics and periglacial environments of continental Antarctica. *South African Journal of Science*, 98(1–2): 82–90.

Boelhouwers, J. 2004. New perspectives on autochthonous blockfield development. *Polar Geography*, 28: 120–146.

Boelhouwers, J. & Jonsson, M. 2013. Critical assessment of the 2°C min −1 threshold for thermal stress weathering. *Geografiska Annaler Series A, Physical Geography*, 95(4): 285–293.

Borsato, A., Frisia, S., Jones, B. & Van Der Borg, K. 2000. Calcite moonmik: Crystal morphology and environment of formation in caves in the Italian Alps. *Journal of Sedimentary Research*, 70(5): 1179–1190.

Brady, N.C. 1974. Soil water: characteristics and behaviour. In H. O. Buckman, eds. *The nature and properties of soils*. New York: Macmillan Publishing Co. Inc.: 164–199.

Briggs, D.J. 1977a. Hyrological properties. In M. A. Morgan & D. J. Briggs, eds. *Soils. Sources and Methods in Geography*. Durban: Butterworth & Co. Ltd: 66–104.

Briggs, D.J. 1977b. Particle size analysis. In M. A. Morgan & D. J. Briggs, eds. *Sediments. Sources and Methods in Geography*. London: Butterworth & Co Ltd: 55–77.

Von Brunn, V. 1962. *Scientific studies in western Dronning Maud Land*. University of Cape Town. MSc Thesis.

Budel, B., Weber, B., Kuhl, M., Pfanz, H., Sultemeyer, D. & Wessels, D. 2004. Reshaping of sandstone surfaces by cryptoendolithic cyanobacteria: Bioalkalization causes chemical weathering in arid landscapes. *Geobiology*, 2(4): 261–268.

Chinn, T.J. 1994. Glacier disequilibrium in the Convoy Range, Transantarctic Mountains, Antarctica. *Annals of Glaciology*, (20): 296–276.

Chiu, C.F. & Ng, C.W.W. 2014. Relationships between chemical weathering indices and physical and mechanical properties of decomposed granite. *Engineering Geology*, 179: 76–89.

Claridge, G.G.C. 1965. The clay minerology and chemistry of some soils from the Ross Dependency, Antarctica. *New Zealand Journal of Geology & Geophysics*, (8): 165–220.

Claridge, G.G.C. & Campbell, I.B. 1985. Physical Geography - Soils. In W. N. Bonner & D. W. H. Walton, eds. *Key Environments - Antarctica*. Oxford: Pergamon Press: 62–70.

Conovitz, P.A., McKnight, D.M., MacDonald, L.H., Fountain, A.G. & House, H.R. 1998. Hydrologic processes influencing streamflow variation in Fryxell Basin, Antarctica. In J. C. Priscu, ed. *Ecosystem dynamics in a polar desert. The McMurdo Dry Valleys, Antarctica*. American Geophysical Union: 93–108.

Convey, P., Bindschadler, R., Di Prisco, G., Fahrbach, E., Gutt, J., Hodgson, D.A., Mayewski, P.A., Summerhayes, C.P., Turner, J. & Consortium, A. 2009. Antarctic climate change and the environment. *International Journal of Climatology*, 21(6): 541.

Davis, D.G. 2000. Extraordinary features of Lechuguilla Cave, Guadalupe Mountains, New Mexico. *Journal of Cave and Karst Studies*, 62(2): 147–157.

Deer, W.A., Howie, R.A. & Zussman, J. 1992. *An introduction to the rock-forming minerals*. 2nd ed. W. A. Deer, R. A. Howie, & J. Zussman, eds. Harlow, England: Pearson Education Ltd.

Dixon, J.C. & Thorn, C.E. 2005. Chemical weathering and landscape development in mid-latitude alpine environments. *Geomorphology*, 67: 127–145.

Dixon, J.C. 2013. Chemical weathering in cold climates. In J. Shroder & G. A. Pope, eds. *Treatise on Geomorphology*. San Diego, CA: Academic Press: 245–257.

Dorn, R.I. 2013. Rock coatings. In J. Shroder & G. A. Pope, eds. *Treatise on Geomorphology*. San Diego, CA: Academic Press: 70–97.

Dwight, R.A. 2015. *Geomorphic and ambient environmental impacts on lichen distribution on two inland nunataks in western Dronning Maud Land, Antarctica*. Rhodes University.

Etienne, S. 2002. The role of biological weathering in periglacial areas: A study of weathering rinds in south Ireland. *Geomorphology*, 47(1): 75–86.

Fantidis, J. & Ehhalt, D.H. 1970. Variations of the carbon and oxygen isotopic composition in stalagmites and stalactites: Evidence of non-equilibrium isotopic fractionation. *Earth and Planetary Science Letters*, 10: 136–144.

FLIR Systems Inc. 2017. FLIR E8 specifications. http://www.flir.eu/instruments/e8/ 28 March 2017.

Forstner, U. 1986. Chemical forms and environmental effects of critical elements in solid-waste materials: combustion residues. In M. Bernhard, F. E. Brinckman, & P. J. Sadler, eds. *The Importance of Chemical 'Speciation' in Environmental Processes, Dahlem Konferenzen*. Berlin: Springer: 465–491.

Fortner, S.K., Lyons, W.B. & Munk, L. 2013. Diel stream geochemistry, Taylor Valley, Antarctica. *Hydrological Processes*, (27): 394–404.

Fountain, A.G., Lyons, W.B., Burkins, M.B., Dana, G.L., Doran, P.T., Lewis, K.J., McKnight, D.M., Moorehead, D.L., Parsons, A.N., Priscu, J.C., Wall, D.H., Wharton, R.A. & Virginia, R.A. 1999. Physical controls on the Taylor Valley ecosystem, Antarctica. *Bioscience*, (49): 961–971.

French, H.M. 2011. Periglacial environments. In A. S. Goudie & K. J. Gregory, eds. *The Sage Handbook of Geomorpology*. London: SAGE Publications Ltd: 393–411.

Friedmann, E.I. 1982. Endolithic microorganisms in the Antarctic cold desert. *Science*, (215): 1045–1053.

Friedmann, E.I., McKay, C.P. & Nienow, J.A. 1987. The cryptolithic microbial environment in the Ross Desert of Antarctica: Satellite transmitted continuous nanoclimate data, 1984 to 1986. *Polar Biology*, (7): 273–287.

Galy, A., Bar-Matthews, M., Halicz, L. & O'Nions, R.K. 2002. Mg isotopic composition of carbonate: Insight from speleothem formation. *Earth and Planetary Science Letters*, 201: 105–115.

Gardner, J.S. 1992. The zonation of freeze–thaw temperatures at a glacier headwall, Dome Glacier, Canadian Rockies. In J. C. Dixon & A. D. Abrahams, eds. *Periglacial Geomorphology: Proceedings of the 22nd Annual Binghamtpon Symposium in Geomorphology, The Binghampton Symposia in Geomorphology*. New York: Wiley: 89–102.

Geiger, R. 1965. *The climate near the ground*. Cambridge, Massachusetts: Harvard University Press.

Gibbs, R.J. 1970. Mechanisms controlling world water chemistry. *Science*, 170: 1088–1090.

Gibson, E.K., Wentworth, S.J. & McKay, D.S. 1983. Chemical weathering and diagenesis of a cold desert soil from Wright Valley, Antarctica: An analog of Martian weathering processes. In *Proceedings of the 13th Lunar and Planetary Science Conference*. Journal of Geophysical Research: A912–A928.

Giovanoli, R., Schnoor, J.L., Sigg, L., Stumm, W. & Zorbrist, J. 1988. Chemical weathering of crystalline rocks in the catchment area of acidic Ticino lakes, Switzerland. *Clays and Clay Minerals*, 36(6): 521–529.

Glasby, G.P., McPherson, J.G., Kohn, B.P., Johnston, J.H., Keys, J.R., Freeman, A.G. & Tricker, M.J. 1981. Desert varnish in southern Victoria Land, Antarctica. *New Zealand Journal of Geology & Geophysics*, 24: 389–397.

Gold, L.W. & Lachenbruch, A.H. 1973. Thermal conditions in permafrost: a Review of North American literature. In *North American Contribution to the Second International Conference on Permafrost*. Washington D.C.: National Academy of Sciences, Publ.: 17–18.

Gooseff, M.N., McKnight, D.M., Lyons, W.B. & Blum, A.E. 2002. Weathering reactions and hypoheric exchange controls on stream water chemistry in a glacial meltwater stream in the McMurdo Dry Valleys. *Water Resources Research*, (38): 1279.

Gooseff, M.N., Barrett, J.E. & Levy, J.S. 2013. Shallow groundwater systems in a polar desert, McMurdo Dry Valleys, Antarctica. *Hydrogeology Journal*, 21(1): 171–183.

Goudie, A. 1990. Material Properties. In J. Lewin, K. Richards, M. Anderson, T. Burt, B. Whalley, & P. Worsley, eds. *Geomorphological Techniques*. London: Unwin Hyman Ltd: 112–191.

Green, W.J., Angle, M.P. & Chave, K.E. 1988. The geochemistry of Antarctic streams and their role in the evolution of four lakes of the McMurdo Dry Valleys. *Geochimica et Cosmochimica Acta*, 52(5): 1265–1274.

Green, W.J. & Lyons, W.B. 2009. The saline lakes of the McMurdo Dry Valleys, Antarctica. *Aquatic Geochemistry*, (15): 321–348.

Guglielmin, M., Cannone, N., Strini, A. & Lewkowicz, A.G. 2005. Biotic and abiotic processes on granite weathering landforms in a cryotic environment, Northern Victoria Land, Antarctica. *Permafrost and Periglacial Processes*, 16(1): 69–85.

Guglielmin, M., Dalle Fratte, M. & Cannone, N. 2014. Permafrost warming and vegetation changes in continental Antarctica. *Environmental Research Letters*, 9(4): 1–14.

Hall, K.J. 1992. Mechanical weathering in the Antarctic: a maritime perspective. In J. C. Dixon & A. D. Abrahams, eds. *Periglacial Geomorphology: Proceedings of the 22nd Annual Binghamtpon Symposium in Geomorphology, The Binghampton Symposia in Geomorphology*. New York: Wiley: 103–123.

Hall, B.L., Denton, G.H. & Hendy, C.H. 2000. Evidence from Taylor Valleyfor a grounded ice sheet in the Ross Sea, Antarctica. *Geografiska Annaler Series*, (82): 275–303.

Hall, K.J. & André, M.F. 2001. New insights into rock weathering from high-frequency rock temperature data: An Antarctic study of weathering by thermal stress. *Geomorphology*, 41(1): 23–35.

Hall, K.J., Thorn, C.E., Matsuoka, N. & Prick, A. 2002. Weathering in cold regions: Some thoughts and perspectives. *Progress in Physical Geography*, 26(4): 577–603.

Hall, K.J. 2003. Micro-transducers and high-frequency rock temperature data: Changing our perspectives on rock weathering in cold regions. In M. Phillips, S. M. Springman, & L. U. Arenson, eds. *Proceedings of the 8th International Conference on Permafrost*. Lisse: Swets: 349–354.

Hall, K.J. & André, M.F. 2003. Rock thermal data at the grain scale: Applicability to granular disintegration in cold environments. *Earth Surface Processes and Landforms*, 28(8): 823–836.

Hall, K.J. & Thorn, C.E. 2011. The historical legacy of spatial scales in freeze-thaw weathering: Misrepresentation and resulting misdirection. *Geomorphology*, 130(1–2): 83–90.

Hall, K.J., Thorn, C.E. & Sumner, P.D. 2012. On the persistence of 'weathering'. *Geomorphology*, 149–150: 1–10.

Hall, K.J. 2013. Mechanical weathering in cold regions. In J. Shroder & G. A. Pope, eds. *Treatise on Geomorphology*. San Diego, CA: Academic Press: 258–276.

Hannell, F.G. 1973. The thickness of the active layer on some of Canada's arctic slopes. *Geografiska Annaler Series A, Physical Geography*, 55(3/4): 177–184.

Hansen, C.D., Meiklejohn, K.I., Nel, W., Loubser, M.J. & Van Der Merwe, B.J. 2013. Aspect-controlled weathering observed on a blockfield in Dronning Maud Land, Antarctica. *Geografiska Annaler, Series A: Physical Geography*, 95(4): 305–313.

Hedding, D.W. 2008. Spatial inventory of landforms in the recently exposed Central Highland of Sub-Antarctic Marion Island. *South African Geographical Journal*, 90(1): 11–21.

Hindshaw, R.S., Rickli, J., Leuthold, J., Wadham, J. & Bourdon, B. 2014. Identifying weathering sources and processes in an outlet glacier of the Greenland Ice Sheet using Ca and Sr isotope ratios. *Geochimica et Cosmochimica Acta*, 145: 50–71.

Jonsson, S. 1985. In O. Orheim, ed. Report of the Norwegian Antarctic Research Expedition (NARE) 1984/85. Geomorphological and glaciological observations in Vestfjella, Dronning Maud Land. *Norsk Polarinstitutt Rapportserie*, 22: 83–88.

Kappen, L., Friedmann, E.I. & Garty, J. 1981. Ecophysiology of lichens in Dry Valleys of southern Victoria Land, Antarctica I. Microclimate of the cryptoendolithic lichen habitat. *Flora*, 171(3): 216–235.

Kendall, A.C. & Broughton, P.L. 1978. Origin of fabrics in speleothems composed of columnar calcite crystals. *Journal of Sedimentary Petrology*, 48(2): 519–538.

Kennicutt, M.C., Chown, S.L. & Cassano, J.J. 2014. Six priorities for Antarctic science. *Nature*, 512: 23–25.

Kennicutt, M.C., Chown, S.L., Cassano, J.J., Liggett, D., Peck, L.S., Massom, R., Rintoul, S.R., Storey, J., Vaughan, D.G., Wilson, T.J., Allison, I., Ayton, J., Badhe, R., Baeseman, J., Barrett, P.J., Bell, R.E., Bertler, N., Bo, S., Brandt, A., Bromwich, D., Cary, S.C., Clark, M.S., Convey, P., Costa, E.S., Cowan, D., Deconto, R., Dunbar, R., Elfring, C., Escutia, C., Francis, J., Fricker, H.A., Fukuchi, M., Gilbert, N., Gutt, J., Havermans, C., Hik, D., Hosie, G., Jones, C., Kim, Y.D., Le Maho, Y., Lee, S.H., Leppe, M., Leitchenkov, G., Li, X., Lipenkov, V., Lochte, K., López-Martínez, J., Lüdecke, C., Lyons, W.B., Marenssi, S., Miller, H., Morozova, P., Naish, T., Nayak, S., Ravindra, R., Retamales, J., Ricci, C.A., Rogan-Finnemore, M., Ropert-Coudert, Y., Samah, A.A., Sanson, L., Scambos, T., Schloss, I.R., Shiraishi, K., Siegert, M.J., Simões, J.C., Storey, B., Sparrow, M.D., Wall, D.H., Walsh, J.C., Wilson, G., Winther, J.G., Xavier, J.C., Yang, H. & Sutherland, W.J. 2015. A roadmap for Antarctic and Southern Ocean science for the next two decades and beyond. *Antarctic Science*, 27(1): 3–18.

Kennicutt, M.C., Kim, Y.D., Rogan-Finnemore, M., Anandakrishnan, S., Chown, S.L., Colwell, S., Cowan, D., Escutia, C., Frenot, Y., Hall, J., Liggett, D., Mcdonald, A.J., Nixdorf, U., Siegert, M.J., Storey, J., Wåhlin, A., Weatherwax, A., Wilson, G.S., Wilson, T., Wooding, R., Ackley, S., Biebow, N., Blankenship, D., Bo, S., Baeseman, J., Cárdenas, C.A., Cassano, J., Danhong, C., Dañobeitia, J., Francis, J., Guldahl, J., Hashida, G., Corbalán, L.J., Klepikov, A., Lee, J., Leppe, M., Lijun, F., López-Martinez, J., Memolli, M., Motoyoshi, Y., Bueno, R.M., Negrete, J., Cárdenes, M.A.O., Silva, M.P., Ramos-Garcia, S., Sala, H., Shin, H., Shijie, X., Shiraishi, K., Stockings, T., Trotter, S., Vaughan, D.G., De Menezes, J.V.D.U., Vlasich, V., Weijia, Q., Winther, J.G., Miller, H., Rintoul, S. & Yang, H. 2016. Delivering 21st century Antarctic and Southern Ocean science. *Antarctic Science*, 28(6): 407–423.

King, C.A.M. 1975. Sediment analysis. In *Techniques in geomorphology*. London: Edward Arnold Ltd: 273–302.

Knox, J.T. 2015. *An investigation into the effect of synoptic weather events on ground temperatures, western Dronning Maud Land, Antarctica*. Rhodes University. Honours Thesis.

Langenegger, O. 1964. Geological investigations of the Fourth South African Antarctic Expedition. *Report on the Geological Survey of South Africa*, (Unpublished).

Levy, J.S., Fountain, A.G., Gooseff, M.N., Welch, K.A. & Lyons, W.B. 2011. Water tracks and permafrost in Taylor Valley⁄ Antarctica: extensive and shallow groundwater connectivity in a cold desert ecosystem. *Geological Society of America Bulletin*, 123(11–12): 2295–2311.

Lyons, W.B., Welch, K.A., Neumann, K., Toxey, J.K., McArthur, R., Williams, C., McKnight, D.M. & Moorehead, D.L. 1998. Geochemical linkages among glaciers, streams, and lakes within the Taylor Valley, Antarctica. In J. C. Priscu, ed. *Ecosystem Dynamics in a Polar Desert: the McMurdo Dry Valleys, Antarctica*. Washington D.C.: American Geophysical Union: 77–92.

Mathys, H. 1974. Klimatische aspekte der frostverwitterung in der Hochgebirgsregion. *Mittheilungen der Naturforschenden Gesellschaft in Bern*, 31: 49-62.

Marra, K.R., Soreghan, G.S., Elwood Madden, M.E., Keiser, L.J. & Hall, B.L. 2014. Trends in grain size and BET surface area in cold-arid versus warm semi-arid fluvial systems. *Geomorphology*, (206): 483–491.

Marra, K.R., Elwood Madden, M.E., Soreghan, G.S. & Hall, B.L. 2015. BET surface area distributions in polar stream sediments: Implications for silicate weathering in a cold-arid environment. *Applied Geochemistry*, 52: 31–42.

Marra, K.R., Elwood Madden, M.E., Soreghan, G.S. & Hall, B.L. 2017. Chemical weathering trends in fine-grained ephemeral stream sediments of the McMurdo Dry Valleys, Antarctica. *Geomorphology*, 281: 13–30.

Matsuoka, N. & Moriwaki, K. 1992. Frost heave and creep in the Sør Rondane Mountains, Antarctica. *Arctic, Antarctic and Alpine Research*, 24(4): 271–280.

Matsuoka, N. 1996. Soil moisture variability in relation to diurnal frost heaving on Japanese high mountain slopes. Permafrost and Periglacial Processes, 7(2): 139–159.

Matsuoka, N., Murton, J., 2008. Frost weathering: recent advances and future decisions.

Permafrost and Periglacial Processes, 19: 195–210.

McKay, C.P. & Friedmann, E.I. 1985. The cryptoendolithic microbial environment in the Antarctic cold desert: Temperature variations in nature. Polar Biology, (4): 19–25.

McKillup, S. & Dyar, M.D. 2010. Geo*statistics Explained: An introductory guide for Earth Scientists*. 1st ed. Cambridge: Cambridge University Press.

McKnight, D.M., Niyogi, D.K., Alger, A.S., Bomblies, A., Conovitz, P.A. & Tate, C.M. 1999. Dry valley streams in Antarctica: Ecosystems waiting from water. *Bioscience*, 49(12): 985–995.

McKnight, D.M., Runkel, R.L., Tate, C.M., Duff, J.H. & Moorehead, D.L. 2004. Inorganic N and P dynamics of Antarctic glacial meltwater streams as controlled by hyporheic exchange and benthic autotrophic communities. *Journal of the North Americal Benthological Society*, (23): 171–188.

McKnight, D.M., Tate, C.M., Andrews, E.D., Niyogi, D.K., Cozezetto, K., Welch, K., Lyons, W.B. & Capone, D.G. 2007. Reactivation of a cryptobiotic stream ecosystem in the McMurdo Dry Valleys, Antarctica: A long-term geomorphological experiment. *Geomorphology*, (89): 186–204.

Meiklejohn, K.I. & Hall, K.J. 1997. Aqueous geochemistry as an indicator of chemical weathering on southeastern Alexander Island, Antarctica. *Polar Geography*, 21(2): 101–112.

Meiklejohn, K.I. & Sumner, P.D. 2008. Landscape Evolution. In R. Fox & K. Rowntree, eds. *The Geography of South Africa in a Changing World*. Cape Town: Oxford University Press South Africa: 304–326.

Meiklejohn, K.I. 2016. Imagery of western Dronning Maud Land, Antarctica. Personal Communication.

Mergelov, N.S., Goryachkin, S. V., Shorkunov, I.G., Zazovskaya, E.P. & Cherkinsky, A.E. 2012. Endolithic pedogenesis and rock varnish on massive crystalline rocks in East Antarctica. *Eurasian Soil*

Science, 45(10): 901–917.

Mikucki, J.A., Auken, E., Tulaczyk, S., Virginia, R.A., Schamper, C., Sorensen, K.I., Doran, P.T., Dugan, H. & Foley, N. 2015. Deep groundwater and potential subsurface habitats beneath an Antarctic dry valley. *Nature Communications*, 6: 6831.

Murray, J.W. 1954. The deposition of calcite and aragonite in caves. *The Journal of Geology*, 62(5): 481–492.

Murton, J. 2007. Rock weathering. *Encyclopedia of Quaternary Science*, (1988): 2249–2256.

Neethling, D.C. 1964. The geology of the 'Zukkertoppen Nunataks', Ahlmannryggen, western Dronning Maud Land. In R. J. Adie, ed. *Proceedings on the First Interntional Symposium on Antarctic Geology*. Cape Town: Antarctic Geology: 379–389.

Neethling, D.C. 1969. Geology of the Ahlmann Ridge, Western Queen Maud Land. *Antarctic Map Folio Series*, 12: Sheet 7.

Nezat, C.A., Lyons, W.B. & Welch, K.A. 2001. Chemical weathering in streams of a polar desert (Taylor Valley, Antarctica). *Geology*, 113(11): 1401–1408.

O'Kennedy, J. 2016. *Geology data of western Dronning Maud Land, Antarctica*. University of Johannesburg. Personal Communication.

Oguchi, C.T. 2013. Weathering rinds: Formation processes and weathering rates. In J. F. Shroder, ed. *Treatise on Geomorphology*. San Diego, CA: Academic Press: 98–110.

Omelon, C.R., Pollard, W.H. & Ferris, F.G. 2006. Chemical and ultrastructural characterization of high Arctic cryptoendolithic habitats. *Geomicrobiology Journal*, 23(3–4): 189–200.

Perrin, C., Prestimonaco, L., Servelle, G., Tilhac, R., Maury, M. & Cabrol, P. 2014. Aragonite-calcite speleotherms: Identifying original and diagenic features. *Journal of Sedimentary Research*, (84): 245–269.

Pope, G.A., Dorn, R.I. & Dixon, J.C. 1995. A new conceptual model for understanding geographical variations in weathering. *Annals of the Association of American Geographers*, 85(1): 38–64.

Pope, G.A. 2013. Overview of weathering and soils geomorphology. In J. Shroder & G. A. Pope, eds. *Treatise on Geomorphology*. San Diego, CA: Academic Press: 1–11.

Prendez, M. & Carrasco, M.A. 2003. Essential composition of surface waters in the Antarctic Peninsula and interactions with the environment. *Environmental Geochemistry and Health*, (25): 347–363.

Reece, A.W. 1958. Discussion following paper by L.C. King, 'Basic palaeogeography of Gondwanaland during the late Palaeozoic and Mesozoic eras'. *Quarterly Journal of the Geological Society*, 114(1–4): 75.

Reijmer, C.H. 2001. *Antarctic meteorology: A study with automatic weather stations*. Utrecht University. PhD Thesis.

Reijmer, C.H. & Oerlemans, J. 2002. Temporal and spatial variability of the surface energy balance in Dronning Maud Land, East Antarctica. *Journal of Geophysical Research: Atmospheres*, 107(D24): ACL-9.

Rhodes University. 2016a. Ethical standards for research on human and animal subjects. *Ethical standards for research on human and animal subjects*. http://www.ru.ac.za/research/research/ethics/ 26 April 2016.

Rhodes University. 2016b. Field worker safety guidelines. *Field Worker Safety Guidelines*. http://www.ru.ac.za/research/research/policiesandpractices/fieldworkersafetyguidelines/ 26 April 2016.

Riebe, C.S., Kirchner, J.W. & Finkel, R.C. 2004. Erosional and climatic effects on long-term chemical weathering rates in granitic landscapes spanning diverse climate regimes. *Earth and Planetary Science Letters*, 224(3–4): 547–562.

Riechelmann, S., Schroder-Ritzrau, A., Wassenburg, J.A., Schreuer, J., Richter, D.K., Riechelmann, D.F.C., Terente, M., Constantin, S., Mangini, A. & Immenhauser, A. 2014. Physiochemical characteristics of drip waters: Infleunce on mineralogy and crystal morphology of recent cave carbonate precipitates. *Geochimica et Cosmochimica Acta*, 145: 13–29.

Robinson, D.A. & Williams, R.B.G. 1989. Polygonal cracking of sandstone at Fontainebleau, France. *Zeitschrift für Geomorphology*, (33): 59–72.

Robinson, D.A. & Williams, R.B.G. 1992. Sandstone weathering in the High Atlas, Morocco. *Zeitschrift für Geomorphology*, (36): 413–429.

Robinson, D.A. & Moses, C.A. 2011. Rock surface and weathering: Process and form. In K. J. Gregory & A. S. Goudie, eds. *The Sage Handbook of Geomorpology*. London: SAGE Publications Ltd: 291–303.

Roots, E.F. 1969. Geology of western Queen Maud Land. *Antarctic Map Folio Series*, 12(Map Folio Series): Sheet 6.

Runkel, R.L., McKnight, D.M. & Andrews, E.D. 1998. Analysis of transient storage subject to unsteady flow: Diel flow variation in an Antarctic stream. *Journal of the North Americal Benthological Society*, (17): 143–154.

Sabacka, M., Priscu, J.C., Basagic, H., Fountain, A.G., Wall, D.H., Virginia, R.A. & Greenwood, M.C. 2012. Aeolian flux of biotic and abiotic material in Taylor Valley, Antarctica. *Geomorphology*, (155–156): 102–111.

Schmidt, D.L., Dover, J.H., Ford, A.B. & Brown, R.D. 1964. Geology of the Patuxent Mountains. In R. J. Adie, ed. *Proceedings on the First Interntional Symposium on Antarctic Geology*. Cape Town: 276–283.

Secretariat of The Antarctic Treaty. 2011. The Antarctic treaty. http://www.ats.aq/e/ats.htm 25 April 2016.

Smith, D.G. 1985. Sources of heavy metal input to the New Zealand aquatic environment. *Journal of the Royal Society New Zealand*, (15): 371–384.

Stallard, R.F. & Edmond, J.M. 1983. Geochemistry of the Amazon: 2. The influence of the geology and weathering environment on the dissolved load. *Journal of Geophysical Research: Oceans*, 88(C14): 9671–9688.

Stumpf, A.R., Elwood Madden, M.E., Soreghan, G.S., Hall, B.L., Keiser, L.J. & Marra, K.R. 2012. Glacier meltwater stream chemistry in Wright and Taylor Valleys, Antarctica. Significant roles of drift, dust, and biological processes in chemical weathering in a polar climate. *Chemical Geology*, (322–323): 79–90.

Summerfield, M.A. 1991. Weathering and Associated Landforms. In M. A. Summerfield, ed. *Global Geomorphology: an Introduction to the Study of Landforms*. New York: Longman Scientific & Technical, John Wiley and Sons: 129–160.

Sumner, P.D. & Nel, W. 2002. The effect of rock moisture on Schmidt hammer rebound: Tests on rock samples from Marion Island and South Africa. *Earth Surface Processes and Landforms*, 27(10): 1137–1142.

Sumner, P.D., Nel, W., Holness, S. & Boelhouwers, J. 2002. Rock weathering characteristics as relative-age indicators for glacial and post-glacial landforms on Marion Island. *South African Geographical Journal*, (84): 153–157.

Sumner, P.D., Meiklejohn, K.I., Nel, W. & Hedding, D.W. 2004. Thermal attributes of rock weathering: Zonal or azonal? A comparison of rock temperatures in different environments. *Polar Geography*, 28(2): 79–92.

Terauds, A., Chown, S.L., Morgan, F., Peat, H.J., Watts, D.J., Keys, H., Convey, P. & Bergstrom, D.M. 2012. Conservation biogeography of the Antarctic. *Diversity and Distributions*, 18(7): 726–741.

Todd, T. P. 1973. *Effect of cracks on elastic properties of low porosity rocks*. Massachusetts Institute of Technology. PhD Thesis.

Torres, M.A., Moosdorf, N., Hartmann, J., Adkins, J.F. & West, A.J. 2017. Glacial weathering, sulphide oxidation, and global carbon cycle feedbacks. *Proceedings of the National Academy of Sciences of the United States of America*, 113(33): 8716–8721.

Torri, T., Nakaya, S., Matsubaya, O., Matsumoto, G.I., Masuda, N., Kawano, T. & Murayama, H. 1989. Chemical characteristics of pond waters in the Labyrinth of southern Victoria Land, Antarctica. *Hydrobiologica*, (172): 255–264.

Trudgill, S. 1985. *Limestone Geomorphology*. 1st ed. K. M. Clayton, ed. London: Longman Scientific & Technical; John Wiley and Sons.

Verwaal, W. & Mulder, A. 1993. Estimating rock strength with the equotip hardness tester. *International Journal of Rock Mechanics and Mining Sciences*, 30(6): 659–662.

Viles, H.A. 2013. Synergistic weathering processes. In J. Shroder & G. A. Pope, eds. *Treatise on Geomorphology*. San Diego, CA: Academic Press: 12–26.

Walther, J. V. 2005. Chemistry of natural waters. In J. C. Walther, ed. *Essentials of geochemistry*. Sudbury: Jones and Bartlett Publishers: 221–254.

Washburn, A.L. 1979. Environmental factors. In A. L. Washburn, ed. *Geocryology*. New York: Edward Arnold Ltd: 10–17.

Whittaker, T.E., Hall, B.L., Hendy, C.H. & Spaulding, S.A. 2008. Holocene depositional environments and surface-level changes at Lake Fryxell, Antarctica. *Holocene*, 18(5): 775–786.